

Organizational Results Research Report

February 2009
OR09.017

Early Permeability Test for Asphalt Acceptance

Prepared by Center for
Transportation Research and
Education, Iowa State
University and Missouri
Department of Transportation

FINAL REPORT
RI07-053

Early Permeability Test for Asphalt Acceptance

Prepared for
Missouri Department of Transportation

by
R. Christopher Williams, Associate Professor
Department of Civil, Construction and Environmental Engineering
Iowa State University



IOWA STATE
UNIVERSITY

Center for Transportation Research and Education Iowa State University

2711 South Loop Drive
Suite 4700 Ames
IA 50010-8664
Phone 515-294-8103
Fax 515-294-0467
www.ctre.iastate.edu

February 2009

The opinions, findings, and conclusions expressed in this publication are those of the principal investigators and the Missouri Department of Transportation. They are not necessarily those of the U.S. Department of Transportation, Federal Highway Administration. This report does not constitute a standard or regulation.

TECHNICAL REPORT DOCUMENTATION PAGE.

1. Report No.: OR09-017	2. Government Accession No.:	3. Recipient's Catalog No.:	
4. Title and Subtitle: Early Permeability Test for Asphalt Acceptance		5. Report Date: February 2009	
		6. Performing Organization Code: RI07-053	
7. Author(s): R. Christopher Williams		8. Performing Organization Report No.:	
9. Performing Organization Name and Address: Center for Transportation Research and Education Iowa State University 2711 South Loop Drive Suite 4700 Ames IA 50010-8664		10. Work Unit No.:	
		11. Contract or Grant No.:	
12. Sponsoring Agency Name and Address: Missouri Department of Transportation Organizational Results Division PO BOX 270, JEFFERSON CITY MO 65102		13. Type of Report and Period Covered: Final Report.	
		14. Sponsoring Agency Code:	
15. Supplementary Notes: The investigation was conducted in cooperation with the U. S. Department of Transportation, Federal Highway Administration.			
16. Abstract: One of the primary assumptions in structural pavement design for conventional pavements is that a flexible (hot mix asphalt) pavement be impermeable. The basis for this design approach is to minimize moisture infiltration and thus maintain adequate support from the underlying unbound materials. In recent years, with the implementation of the Superpave mix design system, hot mix asphalt (HMA) pavements have been produced with coarser gradations than previously with the Marshall mix design method. A non-destructive method, such as permeability testing, also has the potential to partially characterize the HMA quality more timely than destructive methods, and not leave imperfections in a newly constructed pavement. This study identified the nominal maximum aggregate size, the theoretical maximum specific gravity of the mixture (Gmm), and thickness of the pavement or core as statistically important factors influencing permeability and air voids. Three methods of permeability testing were identified as viable: the Kentucky Air Permeameter, the Karol-Warner Permeameter, and the NCAT Permeameter. This report recommends utilizing an NCAT Permeameter for field testing as part of the quality assurance/quality control process.			
17. Key Words: hot mix asphalt, permeability, quality assurance/quality control		18. Distribution Statement: No restrictions. This document is available to the public through National Technical Information Center, Springfield, Virginia 22161.	
19. Security Classification (of this report): Unclassified.	20. Security Classification (of this page): Unclassified.	21. No of Pages: 122	22. Price:

EXECUTIVE SUMMARY

One of the primary assumptions in structural pavement design for conventional pavements is that a flexible (hot mix asphalt) pavement be impermeable. The basis for this design approach is to minimize moisture infiltration and thus maintain adequate support from the underlying unbound materials. In recent years, with the implementation of the Superpave mix design system, hot mix asphalt (HMA) pavements have been produced with coarser gradations than previously with the Marshall mix design method. A non-destructive method, such as permeability testing, also has the potential to partially characterize the HMA quality more timely than destructive methods, and not leave imperfections in a newly constructed pavement.

The study identified the nominal maximum aggregate size (NMAS), the theoretical maximum specific gravity of the mixture (G_{mm}), and thickness of the pavement or core as statistically important factors influencing permeability and air voids. Generally, larger NMAS mixtures have an influence of lower permeability and lower air voids than smaller NMAS mixtures. Higher G_{mm} mixtures generally produced mixtures with higher permeability and higher air void values. Although statistically significant, the influence of thickness varied from one method/technology to another.

Beneficial findings from this research study identified the CoreLok as a viable method for determining the density and corresponding air voids of field samples and was comparable to AASHTO T166. The CoreLok method did in general yield lower density values and thus higher air void values than AASHTO T166. The research study also found the PaveTracker did not have a strong relationship to neither AASHTO T166 nor the CoreLok methods for measuring density as well as the four methods of permeability testing conducted in this study.

Three methods of permeability testing were identified as viable: the Kentucky Air Permeameter, the Karol-Warner Permeameter, and the NCAT Permeameter. This report recommends utilizing an NCAT Permeameter for field testing as part of the quality assurance/quality control process. The specific criteria for using an NCAT Permeameter as part of a percent within limit specification is 1560×10^{-5} cm/sec for the upper specification limit and 0 cm/sec for the lower specification limit. Although the literature did not identify criteria for the NCAT Permeameter, 125×10^{-5} cm/sec average permeability criteria for the Karol-Warner device has been identified by Maupin at the Virginia Transportation Research Council as a criteria. The study identified the viability of using a Karol-Warner Permeameter as part of the mix design as it has a strong relationship to the NCAT Permeameter, which is not capable of testing gyratory compacted samples. A corresponding Karol-Warner Permeability criteria identified in this study is an upper specification limit of 530×10^{-5} cm/sec and 0 cm/sec for the lower specification criteria and results in an average permeability value of 265×10^{-5} cm/sec.

The research for this project generated a number of deliverables and are as follows:

1. A draft specification for permeability testing using an NCAT Permeameter as part of the Missouri Department of Transportation' construction quality control quality assurance testing utilizing percent within limit specifications;
2. A draft test criteria/method for permeability using a Karol-Warner Permeameter as part of the mix design evaluation process;
3. The test equipment for conducting permeability testing utilizing, namely an NCAT Permeameter, a Karol-Warner Permeameter, and a ROMUS Air Permeameter;

4. A database in an Excel spreadsheet that contains all of the data collected as part of the project, as well as majority of calculations and figures provided in this report; and
5. A draft training module for conducting permeability testing utilizing an NCAT and a Karol-Warner Permeameter.

TABLE OF CONTENTS

EXECUTIVE SUMMARY	iii
TABLE OF CONTENTS.....	vi
LIST OF FIGURES	viii
LIST OF TABLES.....	ix
ACKNOWLEDGEMENTS.....	x
CHAPTER 1 INTRODUCTION	1
1.1 Background.....	1
1.2 Objectives	1
1.3 Report Organization.....	2
1.4 Deliverables	2
CHAPTER 2 LITERATURE REVIEW	4
2.1 Introduction.....	4
2.2 Permeability Measurements of HMA	5
2.3 HMA Density Measurement: Traditional Laboratory Methods	7
2.3.1 Saturated Surface Dry (SSD) Method.....	7
2.3.2 Paraffin and Parafilm Method.....	10
2.3.3 CoreLok.....	12
2.4 HMA Density Measurement: Nuclear Density Gauges.....	16
2.5 HMA Density Measurement: Non-Nuclear Density Gauges	20
2.6 Evaluation of PQI and PaveTracker	27
CHAPTER 3 EXPERIMENTAL PLAN	37
3.1 Introduction.....	37
3.1.1 Proposed MoDOT Mixtures for Inclusion in the Experimental Plan.....	37
3.1.2 Proposed Testing at Field Locations and on Field Acquired Samples.....	39
3.2 Testing of Field Mixtures	40
3.3 Projects/Mixtures Included in Study.....	46
CHAPTER 4 TEST RESULTS & STATISTICAL ANALYSIS	47
4.1 Introduction.....	47
4.2 Compilation of Test Results	47
4.2.1 PaveTracker Density and Resulting Air Void Determinations	47
4.2.2 CoreLok Density and Resulting Air Void Determinations.....	48
4.2.3 AASHTO T166 Density and Resulting Air Void Determinations.....	49
4.2.4 ROMUS Air Permeameter Test Results	50
4.2.5 Kentucky Air Permeameter Test Results.....	51
4.2.6 NCAT Permeameter Test Results.....	52
4.2.7 Karol-Warner Permeameter Test Results.....	53
4.3 Relationships Between Air Void Determination Methods	54
4.4 Relationships Between Permeability Methods	57
4.5 Relationships Between Permeability and Air Void Determination Methods.....	60

4.6 Statistical Analysis.....	63
4.7 Confidence Limits of Kentucky and NCAT Permeabilities	64
4.8 Permeability Criteria.....	66
4.8.1 Kentucky Air Permeameter Criteria	67
4.8.2 NCAT Permeameter Criteria	68
4.8.3 Karol-Warner Permeameter Criteria	69
CHAPTER 5 FINDINGS AND RECOMMENDATIONS	71
5.1 Introduction.....	71
5.2 Findings	71
5.3 Recommendations.....	72
5.4 Deliverables	73
LIST OF REFERENCES	75
APPENDIX A.....	81
APPENDIX B	95
APPENDIX C	99
APPENDIX D.....	102
APPENDIX E	106

LIST OF FIGURES

Figure 2.1 Blotting an HMA Specimen Dry (Indiana DOT, 2006).....	8
Figure 2.2 Parafilm Application (University of Washington, 2005)	11
Figure 2.3 CoreLok Vacuum Sealing Device (Buchanan and White, 2005).....	12
Figure 2.4 Nuclear Density Gauge Gamma Ray Technology (Muench et al., 2002).....	18
Figure 2.5 Pavement Quality Indicator	21
Figure 2.6 PaveTracker.....	22
Figure 2.7 Operational Theory Schematic of PQI and PaveTracker (NCHRP, 1999)	23
Figure 2.8 Cost Comparison between PQI and Nuclear Gauge (Glagola, 2003)	27
Figure 2.9 Regression Analysis on Measured Asphalt Pavement Density Data (TransTech, 2004)	30
Figure 3.1 Experimental Test Program.....	1
Figure 3.2 PaveTracker.....	41
Figure 3.3 Schematic and Illustration of the ROMUS Air Permeameter	1
Figure 3.4 Kentucky Air Permeameter	1
Figure 3.5 NCAT Water Permeameter	1
Figure 3.6 Cooling the Core Location with Dry Ice	1
Figure 3.7 Removal of Core.....	1
Figure 3.8 Instrotek’s Corelok Test Device.....	1
Figure 3.10 Karol-Warner Flexible Wall Permeameter.....	45
Figure 3.9 AASHTO T166 Test Configuration.....	1
Figure 4.1 Comparison of CoreLok and AASHTO T166 Air Voids.....	55
Figure 4.2 Comparison of PaveTracker and AASHTO T166 Air Voids.....	56
Figure 4.3 Comparison of PaveTracker and CoreLok Air Voids	56
Figure 4.4 Comparison of NCAT and Kentucky Permeability Values	57
Figure 4.5 Comparison of Kentucky Air and Romus Permeability Values.....	58
Figure 4.6 Comparison of NCAT and Karol-Warner Permeability Values.....	58
Figure 4.7 Comparison of Karol-Warner and Kentucky Permeability Values.....	59
Figure 4.8 Comparison of NCAT and Romus Permeability Values.....	60
Figure 4.9 Comparison of AASHTO T166 and Kentucky Permeability Values.....	61
Figure 4.10 Comparison of AASHTO T166 and NCAT Permeability Values	62
Figure 4.11 Comparison of AASHTO T166 and Karol-Warner Permeability Values.....	62
Figure 4.12 AASHTO T166 and Kentucky Permeability Values with 90 Percent Level of Confidence	65
Figure 4.13 AASHTO T166 and NCAT Permeability Values with 90 Percent Level of Confidence	65
Figure 4.14 The Influence of Permeability Upper Specification Limit for the Kentucky Air Permeameter on Percent within Limit	68
Figure 4.15 The Influence of Permeability Upper Specification Limit for the NCAT Permeameter on Percent within Limit	69
Figure 4.16 The Influence of Permeability Upper Specification Limit for the Karol-Warner Permeameter on Percent Within Limit	70

LIST OF TABLES

Table 2.1 Comparison of Air Voids Determined by Vacuum Sealing/CoreLok Method versus AASHTO T166 (Williams et al., 2007).....	15
Table 2.2 Nuclear Gauge Attributes, PQI, and PaveTracker (Wen and Bahia, 2004).....	Error!
Bookmark not defined.	
Table 2.3 Attributes of PQI Model 301 & PaveTracker Model 2701 (Schmitt, 2004)	Error!
Bookmark not defined.	
Table 2.4 Nuclear and Non-Nuclear Gauge Comparison (Schmitt, 2005)..	Error! Bookmark not defined.
defined.	
Table 3.1 Proposed Experimental Plan.....	38
Table 3.2 Projects/Mixtures Included in Study.....	46
Table 4.1 PaveTracker Density and Resulting Air Void Determinations.....	48
Table 4.2 CoreLok Density and Corresponding Air Void Determinations	49
Table 4.3 AASHTO T166 Density and Air Void Determinations.....	50
Table 4.4 Romus Air Permeameter Test Results	51
Table 4.5 Kentucky Air Permeameter Test Results.....	52
Table 4.6 NCAT Permeameter Test Results.....	53
Table 4.7 Karol-Warner Permeameter Test Results	54
Table 4.8 Statistical Summary of Full Models	63
Table 4.9 Reduced Statistical Models.....	64
Table 4.10 Summary of Percent Within Limit for AASHTO T166 Air Voids Summary	66
Table 4.11 Summary of Percent Within Limit for CoreLok Air Voids Summary	67

ACKNOWLEDGEMENTS

The author would like to thank the Missouri Department of Transportation for the financial and technical support associated with this research project. Specifically, the author appreciates the technical support provided by Joe Schroer and Denis Bryant as well as the field personnel in Jeff Joens and Scott Breeding. The author also appreciates the support that John “JD” Wenzlick provided in guiding this research project and its coordination. The author also recognizes and appreciates the asphalt paving contractors of Missouri that provided logistical support. Finally, the author would like to acknowledge Mohamed Abdel Raouf for the means testing and analysis of variance contained in the report.

CHAPTER 1 INTRODUCTION

1.1 Background

One of the primary assumptions in structural pavement design for conventional pavements is that a flexible (hot mix asphalt) pavement be impermeable. The basis for this design approach is to minimize moisture infiltration and thus maintain adequate support from the underlying unbound materials. This drainage approach also transcends geometric design of roadways in ensuring standing water is not at the surface of a pavement via crown sections for safety reasons.

In recent years, with the implementation of the Superpave mix design system, hot mix asphalt (HMA) pavements have been produced with coarser gradations than previously with the Marshall mix design method. These coarser gradations have been successful at limiting distresses such as rutting, but have resulted in other issues arising namely higher permeability values of Superpave mixes as compared to Marshall mixes. Another concern is the determination of a volumetric property of HMA, namely, bulk specific gravity. This issue has emerged because the most common method for determining the bulk specific gravity was not designed to handle open or interconnected void structures, which are present in coarser-graded HMA pavements. A third issue unrelated to mix design method is the destructive sampling of pavements via coring to characterize in part the quality of the placed HMA. A non-destructive method, such as permeability testing, has the potential to partially characterize the HMA quality more timely than destructive methods, and not leave imperfections in a newly constructed pavement.

1.2 Objectives

The objectives of this research project are to identify an alternative test method(s) to AASHTO T166 for inclusion in part of the current Missouri Department of Transportation's quality assurance/quality control (QA/QC) specifications (Section 403 *Asphaltic Concrete Pavement*).

1.3 Report Organization

The report consists of five chapters including the introductory one as the first. The second chapter provides a comprehensive literature review consisting of both permeability and density research work that has been completed. The experimental plan is described in the third chapter. The fourth chapter provides the data collected as part of the research as well as a detailed statistical analysis. Finally, the fifth chapter outlines the findings, conclusions and makes recommendations. The fifth chapter also provides a summary of the deliverables for the overall project.

1.4 Deliverables

The deliverables for the project are as follows:

1. A draft specification for permeability testing using an NCAT Permeameter as part of the Missouri Department of Transportation' construction quality control quality assurance testing utilizing percent within limit specifications;
2. A draft test criteria/method for permeability using a Karol-Warner Permeameter as part of the mix design evaluation process;
3. The test equipment for conducting permeability testing utilizing, namely an NCAT Permeameter, a Karol-Warner Permeameter, and a ROMUS Air Permeameter;
4. A database in an Excel spreadsheet that contains all of the data collected as part of the project, as well as majority of calculations and figures provided in this report; and
5. A draft training module for conducting permeability testing utilizing an NCAT and a Karol-Warner Permeameter.

CHAPTER 2 LITERATURE REVIEW

2.1 Introduction

The permeability and density of HMA is an important construction variable in the long-term durability of paved surfaces. The primary objective of measuring density is to reduce permeability and that density measurements are more reliable than permeability ones. Significant information exists regarding the important effect that in-place density (or air voids content) has on the performance of HMA pavements. Although there is some substantial research work that has been done on permeability of HMA, it has primarily been on open-graded mixtures and is not nearly as comprehensive as research on HMA density. Whether the in-place density is specified as a percent of laboratory, control strip, or maximum theoretical density, it is well known and documented that density that is either too high or too low can lead to premature pavement failure (Killingsworth, 2004). Lower percentages of in-place air voids can result in rutting and shoving, while higher percentages allow water and air to penetrate into a pavement, leading to an increased potential for water damage, oxidation, raveling, and cracking. Low in-place air voids are generally the result of a mix problem while high in-place voids are generally caused by inadequate compaction (Brown et al., 2004).

Bulk specific gravity (G_{mb}) is defined as the ratio of the mass of a given volume of material at 25°C to the mass of an equal volume of water at the same temperature. The proper measurement of G_{mb} for compacted HMA samples is a major concern for the HMA industry. This issue has become a bigger problem with the increased use of coarse gradations. The volumetric calculations used during HMA mix design, field control, and construction acceptance are based upon bulk specific gravity measurements. During mix design, volumetric properties such as air voids, voids in mineral aggregates, voids filled with asphalt, and percent theoretical

maximum density at a certain number of gyrations are used to evaluate the acceptability of mixes. All of these properties are based upon G_{mb} . An erroneous G_{mb} can lead to incorrect pay bonuses or penalties (Brown et al., 2004).

Current methods of measuring in-place density of HMA pavements have limitations. Laboratory density measurement of core samples (saturated surface dry, paraffin/parafilm coated, volumetric, and CoreLok) is time-consuming and costly. The alternative, a nuclear density gauge (which uses gamma ray technology), requires strict licensing and usage procedures and has other limitations (NCHRP, 1999). For instance, a nuclear density gauge requires proper calibration and can take several minutes to obtain a density measurement making it difficult to implement in real time on a continuous paving operation (Jaselskis et al., 1998). Recently, non-nuclear electro-magnetic density gauges have entered the market, which have the potential to replace nuclear density gauges and the process of coring. A description of each of these permeability and density measurement techniques and associated studies follow.

2.2 Permeability Measurements of HMA

Permeability, more properly hydraulic conductivity or coefficient of permeability, is the rate at which a porous material will transmit water under a hydraulic gradient (Kanitpong et al., 2001). Several apparatuses have been developed to measure the coefficient of permeability of an HMA specimen. The research below outlines some of the more significant studies. Permeability is an important property of an HMA since it has been linked to a pavement's durability, providing a measure of how accessible a pavement's void structure is to its environment (air and water).

The Virginia Department of Transportation (VDOT) has conducted numerous studies on the permeability of HMA utilizing a falling head permeameter (Maupin, 2000, 2001, and 2005; Prowell and Dudley, 2002). The first study considered the acceptable maximum permeability

value to be 125×10^{-5} cm/s. The main conclusions that Maupin (2001) arrived at were that the studied mixes all exhibited distinctive permeability-void relationships and implied that the acceptable permeability value had different acceptable void contents. The implication may result in required permeability testing of all mixtures to develop an acceptable air void range. Maupin (2001) noted that sawing of the specimen, if not monitored closely, could significantly reduce the measured permeability due to closing of the air voids because of the smearing of asphalt. However, the permeability test yielded rather high multi-operator variability for sawed and unsawed specimens. The study also considered multi-lab variability in the use of the falling head permeability test by comparing two laboratories' permeability-air void relationships. The results suggested that the lab specimens and the field cores had similar permeability values for like air void contents. As a result, VDOT is implementing the permeability test into the mix design as a pilot study with maximum permeability design criteria of 125×10^{-5} cm/s. Other factors that affect permeability include air void content, gradation and lift thickness (Mohammad et al., 2003). Mohammad et al. (2003) also reported no difference in permeability measurements for the various mixtures or compaction levels. It was also noted that the permeability measurement generally decreased if the thickness of the asphalt specimen was at least 6 cm in height. The study also investigated the permeability measurement's relationship with air voids and porosity, while comparing the estimated air voids from three methods (water displacement, vacuum sealing method, and gamma ray method). The researchers observed a good correlation with air voids when using either the vacuum sealing method or the SSD method. In a later study, Mohammad et al. (2005) reported that the effective porosity as measured with the CoreLok vacuum equipment has an even better correlation with the measured permeability than with the

measured air void approximation. The permeability testing was completed in this study using the standards and equipment outlined in ASTM PS 129-01 (2004).

Brown et al. (2004) at NCAT noted that coarse-graded mixtures generally exhibited higher measured permeability than fine-graded mixtures. The researchers also reported that for the 20 projects investigated, air voids were found to influence the measured permeability, although relatively high permeability measurements were still made on mixes with low air void contents. When the researchers compared the lab and field measurements of permeability a strong correlation between the two measurements were not found. Brown et al. (2004) also suggested that efforts should be made to investigate making permeability a part of the mix design process.

Russell et al. (2005) determined that an air permeameter developed by ROMUS provided comparable permeability values to the water permeameter developed by NCAT. The ROMUS was developed utilizing essentially the falling head concept, but with air as the medium rather than water and would yield more repeatable test results. Further, the ROMUS air permeameter was more time efficient with more reproducible results than the NCAT water permeameter.

2.3 HMA Density Measurement: Traditional Laboratory Methods

There are several methods that are used to determine densities of pavement specimens. The following sections outline the most popular methods currently used.

2.3.1 Saturated Surface Dry (SSD) Method

The water displacement method, or Saturated Surface Dry (SSD) method (AASHTO T166 or ASTM D2726), is the most common method used to determine bulk specific gravity of compacted hot mix asphalt. This method consists of first weighing a dry sample in air, then obtaining a submerged mass after the sample has been placed in a water bath for a specified time

interval. Upon removal from the water bath, the SSD mass is determined after patting the sample dry using a damp towel (see Figure 2.1). Based upon Archimedes' principle, the SSD method approximates the volume of a compacted asphalt specimen as the volume of water displaced when submerged under water (Tarefder et al., 2002).



Figure 2.1 Blotting an HMA Specimen Dry (Indiana DOT, 2006)

According to the AASHTO T166 and ASTM D2726 procedures, tests are only valid for specimens (cores) with water absorptions of less than two percent and no open or interconnecting voids. Also, the reliability of the water displacement method decreases with increasing depth of the surface irregularities and the presence of interconnected voids that are open to the surface of the solid (InstroTek, 2001).

In order to determine the bulk specific gravity using the water displacement method, three weights of a specimen must be obtained. First, the dry weight of a specimen must be obtained. Second, the weight of the specimen under water for four minutes must be recorded. Finally, the weight of a specimen having a saturated surface dry condition is determined. This SSD condition is very difficult to determine as it is subject to individual interpretation of when a

specimen is SSD and thus the procedure is prone to variability and error. The following expression is used to compute the bulk specific gravity using the SSD method:

$$\text{Bulk Specific Gravity at } 25^{\circ}C = \frac{A}{B - C} \quad \text{(Equation 0.1)}$$

Where A = mass of the dry specimen in air,

B = mass of the saturated surface dry specimen in air, and

C = mass of the specimen in water.

The SSD method has proven to be adequate for conventionally designed mixes, such as those designed according to the Marshall and Hveem Methods that generally utilized fine- and dense- graded aggregates. Historically, mixes were designed to have gradations passing close to or above the Superpave defined maximum density line (e.g., fine-graded). However, since the adoption of the Superpave mix design system and the increased use of Stone Matrix Asphalt (SMA), mixes are being designed with coarser gradations than in the past (Brown et al., 2004).

The potential problem in measuring the G_{mb} of mixes like coarse-graded Superpave and SMA using the SSD method comes from the internal air void structure within these mix types. These types of mixes tend to have larger internal air voids than finer conventional mixes, at similar overall air void contents. Mixes with coarser gradations have a much higher percentage of large aggregate particles. At a certain overall air void volume, which is mix specific, the large internal air voids of the coarse mixes can become interconnected. During G_{mb} testing with the SSD method, water can quickly infiltrate into the sample through these interconnected voids. However, after removing the sample from the water bath to obtain the saturated-surface dry condition the water can also drain from the sample quickly. This draining of the water from the

sample is what causes errors when using the SSD method (Brown et al., 2004) as the displaced volume is lower.

2.3.2 Paraffin and Parafilm Method

The paraffin and parafilm method as described by AASHTO T275 (Bulk Specific Gravity of Compacted Bituminous Mixtures using Paraffin Coated Specimens) and ASTM D1188, respectively, address the water absorption problems inherent in the water displacement method. AASHTO T275 should be used with samples that contain open or interconnecting voids or absorb more than two percent of water by volume or both. In this method, the mass of the HMA sample is determined before coating it with liquid paraffin wax. The sample is then weighed in air and under water.

The compacted HMA specimens are either coated with paraffin or wrapped in parafilm (see Figure 2.2). The use of paraffin or parafilm can be time consuming, awkward to perform, and messy (Buchanan, 2000). The paraffin coating also may limit the further evaluation of a specimen after the G_{mb} testing is completed, whereas the parafilm is easily removed to allow for further testing. The testing procedure is similar to that of AASHTO T166 and ASTM D2726. First, the dry uncoated weight of a sample is determined. Second, the mass of a completely coated specimen is obtained. Next, the mass of the coated sample under water is determined. Finally, the specific gravity of the coating (paraffin or parafilm) is determined as outlined in ASTM D1188. The G_{mb} of the film-coated specimen is computed using the following formula:

$$\text{Bulk Specific Gravity} = \frac{A}{\left\{ D - E - \left(\frac{D - A}{F} \right) \right\}} \quad \text{(Equation 0.2)}$$

Where A = Mass of the dry specimen in air,

D = Mass of dry coated specimen,

E = Mass of coated specimen under water, and

F = Specific Gravity of the coating as determined at 25°C.

Unfortunately, the AASHTO T275 test method used for sealing of compacted asphalt samples can have poor repeatability, high sensitivity to operator involvement and training. Furthermore, there are currently no specifications for sealing 150 mm diameter samples. Consequently, few agencies use this method (Bhattacharjee et al., 2002).



Figure 2.2 Parafilm Application (University of Washington, 2005)

For open-and coarse-graded mixes the density results obtained by both the SSD and parafilm methods are higher than the actual density of a specimen. Problems related to inaccurate specific gravity measurements can have serious and detrimental effects on design and quality control of asphalt mixtures. Inaccurate air void contents based on erroneous specific gravity can seriously affect the performance of roadways and their quality. Field cores are generally different from laboratory prepared cores in surface texture and thickness. In Superpave gyratory compactor, the mixture is confined on all surfaces. The difference in surface roughness

of these two different sampling methods in effect produces a different degree of water absorption and drainage during water the displacement tests which in effect reduces the reliability of the saturated surface dry weight of the samples. This causes the calculated densities for laboratory and field samples with the same air content, asphalt content and density, to be different when tested with water displacement method (Bhattacharjee et al., 2002).

2.3.3 CoreLok

In the past several years, vacuum-sealing technology using a CoreLok device, as shown in Figure 2.3, has been employed by a number of researchers and transportation agencies to determine an HMA G_{mb} . *ASTM D 6752* “Standard Test Method for Bulk Specific Gravity and Density of Compacted Bituminous Mixtures Using Automatic Vacuum Sealing Method” has recently been approved outlining the G_{mb} determination procedure with the CoreLok device (Buchanan and White, 2005).



Figure 2.3 CoreLok Vacuum Sealing Device (Buchanan and White, 2005)

A CoreLok device has been developed to determine the G_{mb} of coarser-graded Superpave mixtures. A CoreLok device is a vacuum sealing method that eliminates the need for the SSD condition weighing. Through the use of flexible, puncture resistant vacuum bags, a sample is sealed and remains dry during testing (InstroTek, 2003). The process of determining the bulk specific gravity with the CoreLok system is similar in nature to AASHTO T275 and ASTM D1188, which uses a paraffin wax or parafilm to prevent water infiltration from occurring during the submersion of the sample. The CoreLok device can accommodate 4-in. diameter, 6-in. diameter, and even beam specimens.

The CoreLok system requires very little involvement from the operator, which in turn means the test results may be more easily reproducible. Also, when compared to dimensional analysis and the water displacement method, the CoreLok method has the smallest multi-operator variability, as defined by a standard deviation of test results (Hall et al., 2001).

Research conducted by Buchanan (Buchanan, 2000) has concluded that the CoreLok procedure can determine G_{mb} more accurately than such conventional methods as SSD, parafilm, and dimensional analysis (e.g., mass divided by volume). Theoretically, there should be no instance where a CoreLok G_{mb} is greater than a SSD G_{mb} . As the specimen's air voids and surface texture decrease, the results of CoreLok and water-displacement procedures should approach the same value (Buchanan and White, 2005).

Crouch et al. (2002) reported that the CoreLok device had good performance with a variety of sample types and was the most widely applicable method of G_{mb} determination. Results from a round-robin study (Cooley et al., 2002b) conducted by the National Center for Asphalt Technology (NCAT) showed the CoreLok procedure to be a viable method for determining the G_{mb} of HMA mixes. The report further stated that the CoreLok procedure

provided a more accurate measure of G_{mb} , especially for mixes with high water-absorption levels during water-displacement procedures.

The CoreLok method utilizes an automatic vacuum chamber with specially designed, puncture resistant, resilient bags. Using a 1.25 hp vacuum pump, the unit automatically evacuates and seals the bag during the vacuum operation. The vacuum pump is capable of pulling up to 30-in. Hg (1 TORR). The bags are designed in two different sizes to accommodate different asphalt sample sizes. The following steps are used in determining G_{mb} using the CoreLok procedure (InstroTek, 2003):

1. Use the plastic specimen bag predetermined density, or determine the density by using a standard aluminum reference cylinder provided.
2. Place the compacted HMA specimen (either core or laboratory-compacted specimen) into the bag.
3. Place the bag and specimen inside the CoreLok vacuum chamber.
4. Close the vacuum chamber door, at which time the vacuum pump will start and evacuate the chamber to 30-in. (760-mm) Hg.
5. In approximately two minutes, the chamber door will automatically open with the specimen completely sealed within the bag and ready for water-displacement testing. The user should ensure that the bag seal is secure before proceeding to Step 6.
6. Perform water-displacement method testing of the sealed specimen according to AASHTO or ASTM standards. Correct the results for the bag density and the displaced bag volume, as suggested by *ASTM D 1188*. Use the following equation to calculate the bulk specific gravity of the sample:

$$\text{Bulk Specific Gravity} = \frac{A}{\left\{ B - E - \left(\frac{B - A}{F_T} \right) \right\}} \quad \text{(Equation 0.3)}$$

Where A= mass of dry specimen in air, (g),

B = mass of dry, sealed specimen, (g),

E = mass of sealed specimen underwater, (g),

F_T= apparent specific gravity of plastic sealing material at 25° C (77° F),
provided by the manufacturer.

Buchanan and White (2005) investigated the G_{mb} differences between water-displacement and CoreLok vacuum-sealing procedures and the resulting changes in volumetric properties and design asphalt contents for various Superpave mix designs. The results of their study showed significant G_{mb} differences between CoreLok and water-displacement procedures, with the CoreLok procedure yielding slightly lower G_{mb} values. The observed difference between CoreLok and water-displacement G_{mb} values increased as water absorption increased for coarse-graded mixes but was generally constant for fine-graded mixes. HMA gradation most significantly affected G_{mb} differences between CoreLok and water-displacement procedures. Based on their research findings, it was recommended that the use of the CoreLok device should be considered to more accurately determine specimen G_{mb}, especially for coarse-graded mixes during HMA mix design and quality control/quality assurance testing.

As part of an ongoing study on evaluation of permeability of HMA, Bhattacharjee et al. (2002) evaluated the G_{mb} values of several dense-graded mixes with coarse and fine gradations from three New England states using both the SSD method and the CoreLok vacuum seal

method. Based on their results, the vacuum seal method provides a better estimation of air voids in a compacted HMA mix for coarse- and fine-graded mixes with high air voids.

Although the CoreLok method has significant potential for use in the asphalt industry, the repeatability and reproducibility of the procedure needs to be evaluated before the device can be specified by agencies (Cooley et al., 2002a).

Williams et al (2007) found significant statistical differences at the 95 percent level of confidence (p-value less than 0.05) for air void contents of coarse-graded mixtures determined by the vacuum sealing method and AASHTO T166. However, Williams et al (2007) did not find statistical differences between the two methods for determining air voids for fine-graded mixtures. Table 2.1 below summarizes the statistical outcomes for the comparing the air voids for the vacuum sealing and AASHTO T166 test methods. It is also interesting to note that the variability/standard deviation of the determined air voids is higher for fine-graded mixes than coarser-graded ones.

Table 2.1 Comparison of Air Voids Determined by Vacuum Sealing/CoreLok Method versus AASHTO T166 (Williams et al., 2007)

Gradation	Density Method	Mean	Std. Dev.	Sample Size	Statistical Difference
Fine-Graded	CoreLok	6.73	4.22	53	No, p-value=0.950
	AASHTO T166	6.75	4.22		
Coarse-Graded	CoreLok	6.56	2.72	81	Yes, p-value=0.011
	AASHTO T166	5.95	1.77		
All Mixes	CoreLok	6.62	3.29	134	No, p-value=0.098
	AASHTO T166	6.27	2.87		

2.4 HMA Density Measurement: Nuclear Density Gauges

The most common non-destructive method for measuring in-place density of HMA involves the use of a nuclear density gauge. The general observation is that measuring density with a nuclear gauge in the field is not as accurate as measuring the density of cores in the laboratory. Many

variables are known to impact nuclear gauge readings and it is speculated that changes in technique could improve accuracy (Padlo et al., 2005).

Surface nuclear density gauges use the interaction of gamma radiation with matter to measure density through direct transmission or backscatter. The gamma ray method is simple and non-destructive. As shown in Figure 2.4, the gamma ray method for bulk specific gravity measurement is based on the scattering and adsorption properties of gamma rays with matter (Malpass and Khosla, 2002).

The gamma rays at a specific energy interact with matter through the mechanism known as Compton scattering or inelastic scattering. As gamma rays pass through a sample, collisions occur between the photons of the gamma rays and electrons in the specimen. These collisions cause the photons to lose energy and change directions as they pass through the sample. Compton scattering is a function of electronic specific gravity of the material, hence a function of the mass specific gravity of the material and with proper calibration, the photon count is directly converted to the bulk specific gravity of the specimen (Malpass and Khosla, 2002). Most nuclear gauges use Cesium-137 as the nuclear source for density measurements and once the source is released, the readings are dependent upon the duration as the count is based upon the return of the nuclear particles to the source.

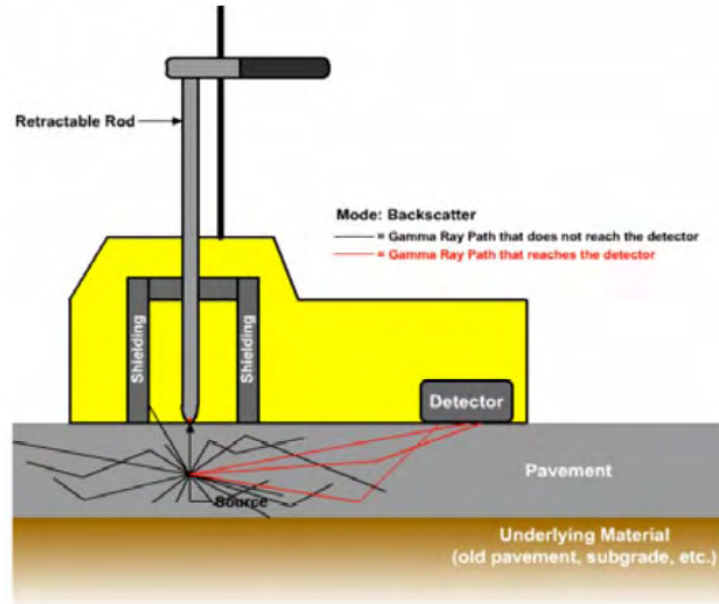


Figure 2.4 Nuclear Density Gauge Gamma Ray Technology (Muench et al., 2002)

The advantages of the gamma ray method are that it is quick and requires limited human intervention. However, because the method is relatively new more research needs to be conducted to ascertain its role for determining bulk specific gravity of compacted hot mix specimens. In addition, both accuracy and length of time for testing are important issues (Williams et. al., 1996). Furthermore, the depth of the layer to be tested is also important as 95% of the reading is obtained in the top two inches of the HMA layer with an infinite depth assumed at five inches.

The nuclear density gauge must be calibrated, preferably against actual core densities obtained from the same material it will be used to measure (Mitchell, 1984). Usually, nuclear gauges are calibrated at the factory by establishing a relationship between the counts and known density blocks (Zha, 2000). The gauge calibration will change with time due to rugged use, the rough construction industry environment, changes in the gauge's mechanical geometry, degradation of the radioactive source or the electronic drift of the gauge's components (Zha,

2000). Even with perfect calibration, the nuclear gauge can show misleading HMA density values resulting from the influence of the environment surrounding the equipment as well as variations in the material, surface texture, aggregate types, temperature, and moisture (Burati et al., 1987; Sanders et al., 1994; Mitchell, 1984). Proper field adjustments can compensate for most of these factors, but questions regarding the overall accuracy and consistency of the nuclear gauge remain (Padlo et al., 2005).

The HMA mat thickness is one factor that is considered to affect the nuclear gauge accuracy. In order to obtain nuclear density results, some gauges require a thickness value be keyed into the instrument. The value that is keyed into the instrument is the specified project thickness and does not necessarily reflect the exact thickness of the test location. Such conditions may influence the nuclear gauge readings (Parker and Hossain, 1995; Stroup-Gardiner and Newcomb, 2000).

Even if the actual thickness were known with certainty, it is possible that each nuclear gauge model measures a different depth of the pavement, which may cause variability in the resultant density measurement (Padlo et al., 2005). For example, the radioactivity may travel through two layers when the top layer is 2 inches thick and the bottom layer is 4-in. thick producing a density based upon two layers. It has been suggested that proper pre-construction surface treatments such as milling may reduce the variability in nuclear density readings caused by inconsistencies in the existing pavement layer if it is performed properly and no rip outs occur.

Finally, the surface texture of the rolled material may affect nuclear gauge density readings. The surface on which the nuclear gauge rests may have aggregates raised above the mean pavement surface thus creating higher air void content in the calculation of density. A

California study found there is no need to utilize known density material, such as rubber pads, to eliminate protrusion or irregularities on the surface of HMA. Currently, nuclear gauge operators have to pay close attention to the surface on which the nuclear gauge rests to ensure maximum surface contact between the nuclear density gauge and the pavement surface (Padlo et al., 2005).

Providing non-destructive density measurements within one to five minutes, the nuclear gauge saves time and money compared to extracting cores. However, the nuclear gauge is generally more variable than core measurements and the quality of the data obtained from a nuclear gauge is dependent on a good correlation with core data from the project. Furthermore, special training and certification is required of anyone that operates a nuclear density gauge and any inconsistencies in the manner of handling the gauge between readings can result in operator error, further affecting the variability of the measurements (Hausman and Buttlar, 2002).

Previous studies performed in California, Pennsylvania, Virginia, Nevada, Texas, Maine, and Connecticut have had similar conclusions for the use of nuclear density gauge readings. They all determined that the nuclear gauge should not be used for Quality assurance and should remain only as a Quality control tool in the field (Choubane et al., 1999; Parker and Hossain, 1995; Stroup-Gardiner and Newcomb, 2000; Padlo et al., 2005).

2.5 HMA Density Measurement: Non-Nuclear Density Gauges

Recently, non-nuclear electro-magnetic density gauges have entered the market, which have the potential to replace nuclear density gauges and the process of coring. These non-nuclear devices use electro-magnetic signals to measure in-place density. The use of electro-magnetic signals has the advantage of completely eliminating the licenses, training, specialized storage, and risks associated with devices that use a radioactive source while being nondestructive (Romero, 2002).

The first of these non-nuclear density devices, called the Pavement Quality Indicator (PQI) (Figure 2.5) was made commercially available by Trans-Tech Systems Inc. in 1998. The second of these devices, called the PaveTracker (Figure 2.6), was made commercially available by Troxler Electronics Lab. Both devices feature using non-nuclear source, thus eliminating safety concerns.



Figure 2.5 Pavement Quality Indicator

In general terms, both the PQI and PaveTracker operate on the principle of measuring changes in the electric field resulting from the introduction of a dielectric (i.e., HMA). The PQI measures bulk density or the degree of compaction by the response of an electrical sensing field to changes in electrical impedance of the material matrix, which in turn is a function of the composite resistivity and dielectric constant of the material (NCHRP, 1999).



Figure 2.6 PaveTracker

Whenever an electrical charge is applied to a conductor, an electrical field is produced. If a nonconductor, known as a dielectric, is introduced inside this electric field, the strength of the field is reduced. The amount by which this dielectric reduces the electrical field can be characterized by the dielectric constant. In order to use the dielectric constant as a measure of asphalt concrete density, the strength of an electrical field is measured. This measurement must first be taken on an asphalt concrete sample of known density. The constituents of asphalt concrete; asphalt binder, aggregates, air, and moisture, each have different dielectric constants. As the asphalt concrete is compacted (i.e., as the density increases), the ratio of the volume of air to that of the other components changes, causing a change in the dielectric constant of the system. The change in dielectric constant causes a change in the electrical signal. Since the amount and type of material remains constant (except for air), this change in the electrical signal is related to the change in density (Wen and Bahia, 2004). The operational theory schematic of the PQI is shown in Figure 2.7.

The first generation PQI machines were capacitance-based measuring systems (Patent No: US 5,900,736) while the new 301 model (Patent No: US 6,414,497) is impedance-based.

The PQI provides a sensor with a multi-configuration geometry that provides an electrical field with a controllable depth of penetration. This attribute is an innovation not previously available from devices in current use (Glagola, 2003).

As shown in Figure 2.7, the PQI system provides an electronic circuit that generates a radio frequency voltage that is applied to one sensing electrode to generate an electrical field in the paving material. A second sensing electrode measures the dielectric response of the paving material. A data processor determines the density of the paving material based on the measured complex impedance of the paving material. The data processor computes the accurate relative density corrected for moisture that may be present in or on the paving material. Corrections for influences outside of the desired measure, material density, are incorporated into the system. These automatic corrections account for: surface moisture, temperature variation, and sensor impedance. This automatic corrective action provides realistic density readings under varying conditions without having to make cumbersome manual adjustments to data (Glagola, 2003).

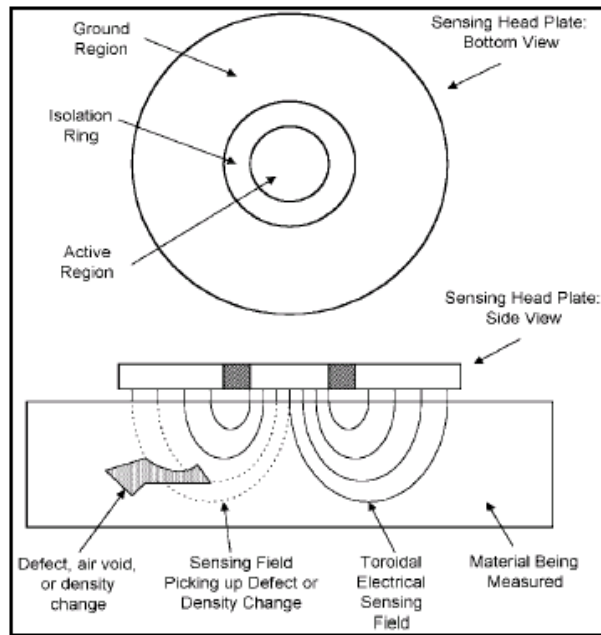


Figure 2.7 Operational Theory Schematic of PQI and PaveTracker (NCHRP, 1999)

The PQI system has been designed to be adaptable to on-site conditions. Another innovation is the ability to change the sensor configuration, under computer control, to allow for selection of the depth to be tested. This is particularly important when testing at a joint in the pavement between two different applications of asphalt. Adjustability of the sensor configuration is also advantageous to the system because the sensor configuration dictates the depth of penetration and area of electrical field and, accordingly, the volume of the field of test. For instance, operation of a smaller sized sensor allows the depth of penetration to be reduced. Being able to accurately control the depth of penetration prevents imprecise determinations when the signal penetrates through a new paving lift coat into an underlying surface that may not have the same density, which is unique. The PQI system provides a constant voltage source circuit enabling the system to detect material density with more accuracy and reliability than other devices. A precision constant voltage source provides a stable system cannot be altered by environmental factors, e.g., electro-magnetic interference (Glagola, 2003).

The examination of the underlying principles of the PQI and the PaveTracker (i.e., that of dielectric constant and permittivity) are critical in assessing the capabilities (and potentially the limitations) of the technologies. Permittivity, ϵ , describes the interaction of a material with an electric field. The dielectric constant, ϵ' , is equivalent to relative permittivity, $\epsilon_r = \epsilon/\epsilon_0$. Permittivity consists of real and imaginary components. The relationship can be described as follows:

$$\epsilon_r = \frac{\epsilon}{\epsilon_0} = \left(\frac{\epsilon_r'}{\epsilon_0} \right) - j \left(\frac{\epsilon_r''}{\epsilon_0} \right) \quad \text{(Equation 0.4)}$$

Where ϵ_r = complex relative permittivity,

ϵ_0 = permittivity of free space,

ϵ_r' = real part of permittivity,

ϵ_r'' = imaginary part of permittivity, and

j = current density.

The real part of permittivity is a measure of how much energy from an external electric field is stored in a material; it is usually greater than one for solids and liquids. The imaginary part of permittivity is also called the loss factor, and is a measure of dissipativeness of a material when exposed to an external electric field. The loss factor is always greater than zero, but is usually much smaller than the real portion. The loss factor also includes the effects of both dielectric loss and conductivity.

Many studies have compared the accuracy of nuclear density gauge measurements with those of non-nuclear measuring devices like the PQI. The accuracy and reproducibility between PQI and nuclear measuring device for determining the in-place density of compacted asphalt concrete pavements was evaluated by Sully-Miller Contracting Company (Sully-Miller, 2000). Based on their limited study, and with a correct gauge/core bias, it was reported that TransTech's PQI Model 300 is a reliable and accurate instrument to measure in-place density of compacted asphalt concrete. It was further reported that the PQI is very user friendly and being lighter causes less physical strain on the back of the technicians. It can be stored and transported anywhere and can be purchased without a Radioactive Materials license. It is fast and has good repeatability as well as having a low standard deviation between tests. Unlike the nuclear gauges, it does not require extensive and periodic calibrations either by the manufacturer or State agency.

In Pennsylvania, the State's "Innovations Council" evaluated the PQI system against a nuclear gauge. Part of the results from this study revealed data related to the cost of training and operating which is provided in Figure 2.8 (Glagola, 2003).

Both PQI and PaveTracker offer several potential advantages: (1) no threat of exposing workers to radiation; (2) they are lightweight; (3) nuclear licensing and training are not required, reducing operating costs; and (4) readings are faster than with a nuclear density gauge, almost instantaneous (Karlsson, 2002; Asphalt Contractor, 1998). It should be noted that the measurement mechanisms of the nuclear devices and non-nuclear electro-magnetic devices are different. While the nuclear density gauges measure the actual density (absolute value) of the material, the non-nuclear electro-magnetic devices indicate the density (relative value) of the material by detecting the dielectric component of the material density and relating that to a density value. As the asphalt is compacted, the air voids in the mix decrease and the dielectric properties change; therefore the non-nuclear devices report this change as an increase in the density. Cores with known density for each mix have to be available to use a PQI and PaveTracker successfully.

<u>NUCLEAR GAUGE (initial cost)</u>		
Trainer (1-day)	\$180	= \$180
Salary of Personnel for 1 day training	\$140 x 5 people	= \$700
Two Week OJT W/licensed operator	\$140 x 5 people x 5 trainers x 10 days	= \$35000
Radiation Badges	\$3.65 x 4/year x 5 people	= \$73
Annual Gauge Re-calibration	\$386 x 5 gauges	= \$1930
Storage/Transportation		Non-reportable
Total		= \$37883
<u>TRANSTECH PQI SYSTEM (initial training)</u>		
Trainer (2 hours)	\$45	= \$45
Salary of Personnel for 2 hours training	\$36 x 5 people	= \$175
Total Training Cost PQI		= \$220
TOTAL SAVINGS (initial training)	\$37883 - \$220	= \$37663
USAGE COSTS (over 5 year period)		
Final figures for operational cost savings use over a 5-year period:		= \$12655
TOTAL 5-YEAR SAVINGS (using the PQI system)		= \$50318

Figure 2.8 Cost Comparison between PQI and Nuclear Gauge (Glagola, 2003)

2.6 Evaluation of PQI and PaveTracker

A number of research studies have been conducted to evaluate the PQI and the PaveTracker, especially the PQI for in-place HMA density measurements. The most notable study was the multi-state pooled-fund study by Romero (2000, 2001). This study was led by Maryland State Highway Administration with participation from State Highway Agencies of Pennsylvania, New York, Connecticut, Oregon, Minnesota, and the Federal Highway Administration. The study consisted of two phases: lab tests and field tests. The results of lab testing were very promising in which the PQI 300 model density measurements highly correlated with the densities of HMA

slabs. However, the results of field tests in 2001 (Romero, 2001) indicated that the PQI 300 did not perform as well as the nuclear gauges.

After the calibration by the manufacturer, the test results by PQI and PaveTracker (added to the study in 2002) were improved significantly in 2002 field tests. The final report concluded that the use of the PQI for providing quality control during paving is a perfectly acceptable method and provides results at least as good as nuclear devices (Romero, 2002). The final reports of both lab and field tests are available for this study (Romero, 2000; Romero, 2001; Romero, 2002; Romero and Kuhnnow, 2002).

Other research studies involving state DOTs on the performance of non-nuclear gauges reported mixed results or findings. Henault (2001) evaluated the PQI Model 300 on ten projects in Connecticut, comparing the non-nuclear results with nuclear gauge tests and cores. The PQI Model 300 was not recommended for quality control or quality assurance testing in Connecticut. Henault (2001) believed that the poor correlations of the non-nuclear gauges may have been due to the effect of moisture. Wisconsin Department of Transportation (WSDOT) performed studies on PQI 300 with comparison to nuclear gauges and cores in 2001 and concluded that both PQI 300 and nuclear gauges tracked the core densities well (Wen and Bahia, 2004).

The results from the field projects conducted as part of NCHRP Project 9-15 (NCHRP, 2004) showed that the variation between the PQI, nuclear density gauge and core measurements were statistically the same. These results are only applicable to dense-graded HMA mixtures. Some studies have reached different conclusions; but, within the confines of this project, it has been demonstrated that the expected variability among the three different measurement methods is similar, even if the measured means are not equal in all cases.

Hausman and Buttlar (2002) conducted both laboratory and field studies to evaluate factors affecting the PQI Model 300 in Illinois. It was reported that moisture and temperature effects still needed to be considered with the Model 300. During field testing on three projects, the PQI Model 300 did not perform as well as nuclear gauges, since the PQI Model 300 had a higher standard error versus the line of equality. Based on the results from this study, the PQI Model 300 was not recommended for quality control or quality assurance testing in the State of Illinois.

Allen et al. (2003) evaluated PQI 300 in Kentucky and only one construction project was included in the study. Based on the research findings, Allen et al. (2003) recommended that since the PQI most closely approximated the data from the cores (both by comparing the means and distributions), a PQI could be used for quality control on HMA paving mats without sacrificing density or quality.

Recently, Wu (2005) evaluated the variability of air voids of plant produced HMA mixtures and compared the different methods of air void measurements by studying four rehabilitation projects in Louisiana. The PQI 301 was evaluated and the results were compared with conventional AASHTO T 166 core densities and CoreLok results. The results showed a strong correlation between air voids measured using conventional and CoreLok methods. Correlations between PQI measured air voids and other two methods (conventional and CoreLok) were reported to be fair. Note that a PQI can be set to read either percent compaction or percent air voids (PQI 301, 2002).

Recently, TransTech conducted an assessment of field asphalt density gauge data when compared with cores processed according to AASHTO T-166 method (TransTech, 2004). Factors that can affect bias, repeatability, reproducibility, and stability were carefully controlled

to determine the influence of each on the overall measurement process. Each of these parameters was evaluated in a deterministic sequence that was designed to isolate the effects of each. Defined processing of the parameters determines the effect of each on the overall measurement. The processing determines whether any of the factors prevent a gauge from meeting overall accuracy requirements when measuring a specified process, such as asphalt paving. The data acquisition procedure involved calibrating the instruments to the mat/mix by adjusting the offsets of the gauges so that the mean of a set of reference gauge and core readings are the same. The second activity involved taking the actual core and gauge data. The PQI and nuclear gauge readings were taken prior to removing each core. A linear correlation analysis was performed on the dataset to determine if a statistically significant linear relationship exists between the gauge data and the core data. The results of regression analysis conducted by TransTech are plotted in Figure 2.9.

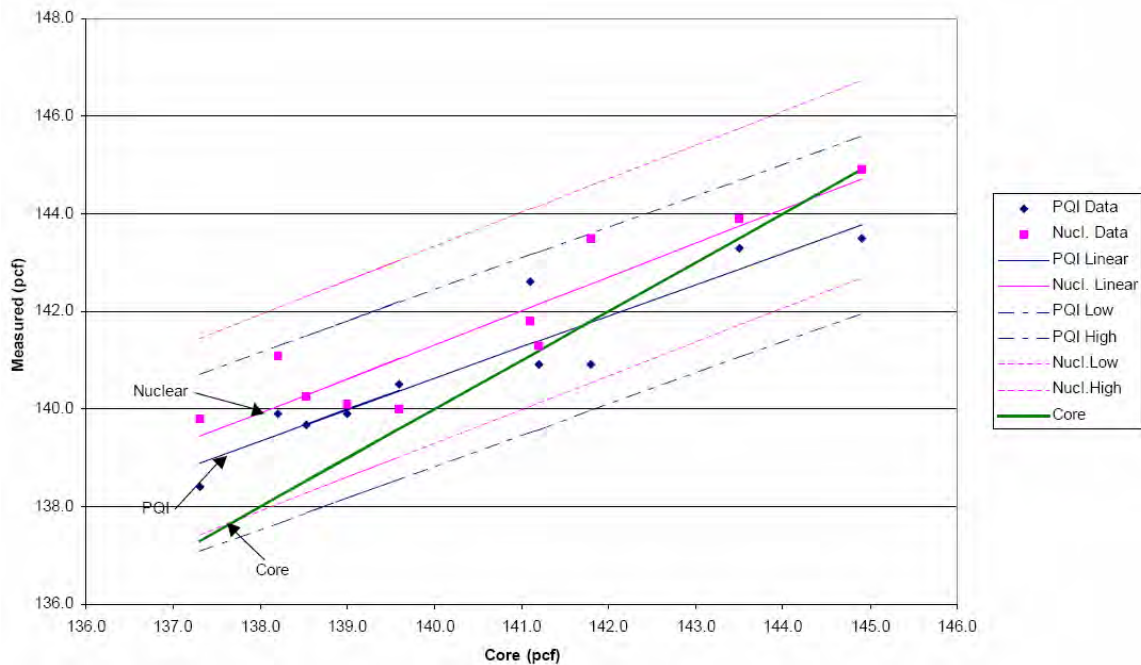


Figure 2.9 Regression Analysis on Measured Asphalt Pavement Density Data (TransTech, 2004)

Hurley et al. (2004) of the National Center for Asphalt Technology (NCAT) studied the performance of a PQI 301 and PaveTracker by comparing results to nuclear gauge readings and core densities. Even though neither the PQI Model 301, nor the PaveTracker was recommended for quality assurance testing, the paper indicated that both the PQI 301 and PaveTracker provided reasonable correlation with density measurements using cores and that the PQI 301 had improved relationships with core densities as compared to the PQI Model 300.

Improvements in the PQI 301 include its ability to compensate for surface water and the ability to measure density in a percent compaction mode as well as a percent air voids mode. There is also a segregation mode which helps the contractor find problem areas on site.

There have not been many research studies related to the PaveTracker. Scullion et al. of Texas Transportation Institute (TTI) studied the performance of a PaveTracker and indicated that good results using PaveTracker were observed on dense graded mixes and not so good results on open-graded mixes. It may be an air gap problem under the gauge with the open-graded mixes. Currently, the TTI is conducting further study on these devices, titled “New Technologies and Approaches to Controlling the Quality of Flexible Pavement Construction” (Wen and Bahia, 2004).

The manufacturers of PQI and PaveTracker propose that their devices could be potentially used for determining differences in density at and near longitudinal joints and in areas of segregation, when observed. When placing HMA, paving the full width of the pavement in a single pass is usually impossible; therefore, most HMA pavements contain longitudinal construction joints and usually differences in densities are observed at and near the longitudinal joints. Thus, these construction joints can often be inferior to the rest of the pavement and can

eventually cause an otherwise sound pavement to deteriorate more quickly (Estakhri et al., 2001).

Segregation is a major cause of early deterioration of HMA pavements. When segregation appears on the surface of the pavement, the texture of the paving mixture appears more open with larger voids in the segregated areas. The result of this differential in voids is often more infiltration of air and moisture into the pavement leading to premature raveling and potholes. Recently, the Colorado Department of Transportation conducted a research study to determine if nuclear density tests and the PQI can be used to identify segregation in asphalt pavements, but the results are not conclusive. It was indicated that additional work is needed to correlate between levels of segregation and density measurements (Shuler, 2005).

Sebesta et al. (2003) evaluated non-nuclear density gauges for assessing segregation, uniformity, and overall quality of HMA overlays. Based on the results, it was concluded that among the non-nuclear devices evaluated, the PQI provided the most reliable estimate of differential density.

Based on their initial literature review, Wen and Bahia (2004) summarized the attributes of nuclear and non-nuclear density devices for comparison (see Table 2.2). It should be noted that since the manufacturers are constantly improving the devices, this table may not include the latest attributes of their respective devices. Some specific attributes of PQI model 301 and the PaveTracker model 2701 are summarized in Table 2.3. (Schmitt, 2004).

Table 2.2 Nuclear Gauge Attributes, PQI, and Pavetracker (Wen and Bahia, 2004)

Attributes	Nuclear Density Gauge	PQI	Pavetracker
<i>Source</i>	Radioactive	Electromagnetic	Electromagnetic
<i>Density Value</i>	Absolute density value	Relative value to reference density	Relative value to reference density
<i>Calibration</i>	General Calibration	Calibration with cores is needed for each specific project	Calibration with cores is needed for each specific project
<i>Measuring Depth</i>	93% reading is affected by top 4 inches. Offer thin-layer measurement.	1-4 inches	1.75 inches
<i>Moisture Sensitivity</i>	Can read moisture content and not affected by moisture	Can read moisture index and correct internally.	Not affected by moisture
<i>Temperature Sensitivity</i>	Not affected by temperature	Can read temperature and correct internally.	Not affected by temperature
<i>Sensitive to Aggregate Source</i>	Not sensitive to aggregate source	Sensitive to aggregate source and offer internal correction.	Sensitive to aggregate source and offers internal correction.
<i>Nominal Maximum Aggregate Size</i>	Not sensitive to nominal maximum aggregate size	Sensitive to nominal maximum aggregate size and need calibration. with cores.	Sensitive to nominal maximum aggregate source and need correction
<i>Aggregate Gradation</i>	Not sensitive to aggregate gradation	Sensitive to aggregate gradation and offer internal correction.	Works well for fine-graded mixes, not good for coarse or gap graded mixes
<i>Quality Control</i>	Yes, read the density changes.	Yes, read density change	Yes, read density change
<i>Quality Assurance</i>	Yes, can read density value	Need calibration with core for each mix	Need calibration with core for each mix
<i>Core Density Measurement</i>	Can not measure the density of cores.	Can measure density of 6" diameter core	Can measure density of 6" diameter core
<i>Repeatability</i>	Fair	Excellent repeatability	+/-0.5 pcf
<i>Segregation Mode</i>	No	Yes, offer segregation mode	Yes, offer segregation mode
<i>Cost</i>	About \$6,000	About \$7,700	About \$28,000
<i>Weight</i>	~30 lbs	16 lbs	2 lbs
<i>Instant Measurement</i>	Take several minutes to read	3 seconds max.	1 second
<i>Special Training</i>	Yes	No	No

Table 2.3 Attributes of PQI Model 301 & PaveTracker Model 2701 (Schmitt, 2004)

Manufacturer	Attributes
<i>PQI Models 300 and 301</i>	<p>Measures pavement density by measuring the electrical impedance of the material.</p> <p>Must be calibrated for the mix that is currently being measured.</p> <p>Many evaluations have been made on the use of PQI, but the conclusions are not consistent.</p> <p>The latest PQI Model 301 has the ability to compensate for surface water (could possibly manage water filler used to measure coarse surface textures).</p>
<i>PaveTracker Model 2701</i>	<p>Relative reading is offset to a representative core sample.</p> <p>Uses “chemical composition per unit volume” technology by measuring dielectric properties.</p> <p>Unlike some non-nuclear, non-mounted gauges, this model needs no moisture or temperature corrections,</p> <p>Very small size (3.5 inches by 4.5 inches by 2.25 inches) allows device to be taken into the lab for calibration and placed on top of a 150mm gyratory compacted specimen.</p> <p>The latest version of the PaveTracker is Model 2701B with dimensions of 9 inches by 16 inches by 6 inches.</p>

In a recent study conducted for the Wisconsin DOT, a field evaluation was performed of selected non-nuclear density gauges to determine their effectiveness and practicality for quality control and acceptance of asphalt pavement construction; and based on the field evaluation results, recommend appropriate test protocols and systems of non-nuclear density devices as a suitable replacement of nuclear density gauges to measure in-place asphalt pavement density (Schmitt, 2005).

Preliminary data analysis was conducted for the first eight projects (out of ten). Basic statistics were computed for nuclear density gauges, non-nuclear density gauges, pavement cores, and Superpave-compacted specimens. Table 2.4 provides a comparison of average non-nuclear density readings with a research nuclear gauge (CPN MC-3 Serial #M391105379). Nuclear gauge readings were based on a 4-min. read and non-nuclear gauges used the average of 5 points within the nuclear density gauge base. The field study began using the CPN MC-3 nuclear gauge, PQI Model #301, and PaveTracker Model #2701B. A consistent finding was a bias between nuclear and non-nuclear gauges, and a change in bias within a project. PQI Model #301 consistently read 16.2 to 20.8 pcf lower than the nuclear gauge, while PQI Model #300 ranged from 9.4 to 19.9 pcf lower. PaveTracker varied from 1.8 to 13.1 pcf lower than the nuclear gauge readings (Schmitt, 2005).

Table 2.4 Nuclear and Non-Nuclear Gauge Comparison (Schmitt, 2005)

Project Index (1)	Project Name, NMAS, and Test Date (2)	Sites, n (3)	Nuclear Gauge pcf (4)	Non-Nuclear Gauges			Nuclear minus Non-nuclear		
				PQI 301 pcf (5)	PQI 300 pcf (6)	PaveTrack. pcf (7)	PQI 301 pcf (8)	PQI 300 pcf (9)	PaveTrack. pcf (10)
1	STH 142 19mm May 12	30	147.8	127.2	---	141.2	20.6	---	6.6
1	STH 142 12.5mm June7	30	144.7	---	135.3	137.5	---	9.4	7.2
1	STH 142 12.5mm June9	20	145.9	---	130.0	139.4	---	15.9	6.5
2	STH 73 19mm, May 18	30	143.4	123.1	---	130.4	20.3	---	13.1
3	STH 64 19mm, May 20	30	144.5	122.8	---	132.5	21.8	---	12.0
4	Marsh Rd 19-mm, May 23	30	146.7	125.9	---	137.8	20.8	---	8.9
5	USH 51 19mm, May 24	30	145.3	124.9	---	138.1	20.4	---	7.2
6	IH 43 19mm, June 1	30	150.3	132.1	136.6	148.2	18.2	13.8	2.1
6	IH 43 19mm, June 2	30	148.7	132.4	137.6	146.9	16.2	11.1	1.8
7	STH 59 19mm, June 3	31	145.8	---	133.7	143.5	---	12.1	2.3
8	STH 100 19mm, June 8	32	147.0	---	127.1	139.5	---	19.9	7.5
8	STH 100 12.5mm, June8	20	145.0	---	131.6	139.0	---	13.4	6.0
8	STH 100 12.5mm, June9	20	146.4	---	133.7	138.1	---	12.7	8.3

Sargand et al. (2005) provided a working review of available non-nuclear equipment for determining in-place density of asphalt based on laboratory and field studies conducted for the Ohio DOT. The objectives of laboratory study were to test the performance of the PaveTracker under a variety of factors including surface temperature, surface and internal moisture, size of

aggregate, sample area relative to device footprint, and measurement depth. In addition, a statistical analysis of the accuracy of the device was made. The field portion of the study was designed to compare the performance of the PQI Model 300 and the PaveTracker against the traditional methods at several construction sites around the state.

Based on laboratory study findings, Sargand et al. (2005) reported that the performance of the PaveTracker was not significantly influenced by HMA mix surface temperature. In general, gauge readings slightly dropped with decreasing mix temperature. The presence of surface moisture significantly affected the gauge readings. With an increase in surface moisture without internal moisture, gauge readings decreased appreciably. But with the introduction of internal moisture without the application of surface moisture, gauge readings increased. The increased amount was far larger than that of core density. It was concluded that the results given by the PaveTracker must be interpreted carefully when moisture is present. The PaveTracker performed better with fine mixtures than with coarse mixtures. The area of the specimen being measured did affect the accuracy of the PaveTracker.

Based on the field study findings, Sargand et al. (2005) found both the PQI and PaveTracker results to differ from both laboratory reported core densities and nuclear density results with statistical significance. Applying a daily mix-specific offset to gauge results as recommended by the manufacturers, hypothesis testing showed that the PaveTracker results remained statistically different from both nuclear gauge and laboratory results, but PQI results were not significantly different. Based on the results of statistical hypothesis testing, Sargand et al. (2005) recommend that use of the PQI Model 300 for both quality control and quality assurance testing provided the manufacturer's recommendation to calibrate the device daily by applying a mix-specific offset is followed.

CHAPTER 3 EXPERIMENTAL PLAN

3.1 Introduction

An experimental plan was one of the first tasks of the project and included review of the literature with respect to permeability measurements of asphalt pavements. This ensured the proposed experimental plan utilized the most recent working knowledge on permeability measurements of asphalt pavements. The experimental plan considered that a developed specification will be included in the Missouri Department of Transportation (MoDOT) percent within limit specification (Section 403 *Asphaltic Concrete Pavement*). Two components to the experimental plan are proposed herein that consider the mixtures specified by the MoDOT and the tests available to possibly replace or supplement AASHTO T166. A discussion of the two proposed components of the experimental plan is presented next.

3.1.1 Proposed MoDOT Mixtures for Inclusion in the Experimental Plan

The literature reveals that there are a number of factors that can affect permeability of compacted hot mix asphalt (HMA). These factors include characteristics of the mix including nominal maximum aggregate size, gradation, and air void content. Further, if field testing is to be performed, additional factors are lift thickness and material under the paving lift being tested (e.g. portland cement concrete, unbound granular material, etc.).

The MoDOT specifications allow for varying nominal maximum aggregate sizes (NMA), varying gradations (fine, coarse, or open-graded), and in practice a range of air voids for acceptance (90 to 96 percent of maximum theoretical specific depending upon mix type). Although the air void factor was one of primary interest, it was not within experimental control per se. In other words, the researchers were not able to specify multiple air void levels for a

particular project at field locations. The research team does believe that non-destructive technology exists that can identify locations with relative high and low density (air voids) utilizing an electro-magnetic gauge as their recent research has shown the ability of the PaveTracker manufactured by Troxler to identify low and high density (air void) locations. Thus, the two main factors that are identifiable prior to field mobilization for field testing, mix type/NMAS and gradation, are considered in the proposed experimental plan below.

Table 3.1 Proposed Experimental Plan

		Mixture Type/Nominal Maximum Aggregate Size					
		SP250	SP190	SP125	SP095	SP125xSM	SP095xSM
Gradation	Fine	If	XXX	XXX	XXX	N/A	N/A
	Coarse	Available	XXX	XXX	XXX	N/A	N/A
	Open	N/A	N/A	N/A	N/A	XXX	XXX

Based upon the research team’s experience, 25mm nominal maximum aggregate size mixtures are not used very frequently and thus it will likely not be possible to test very many of these mixtures. The SP250 mixtures were included in the experimental plan to be inclusive in the development of specifications, however the analysis of the other mixtures balanced with engineering judgment will likely need to be exercised when identifying proposed specifications for this mix type. Further, the majority of the mixtures constructed in Missouri are coarse-graded ones (gradations that are designed below the maximum density line), but a balanced experimental plan between fine (gradations that are primarily designed above the maximum density line) and coarse-graded mixtures should be pursued. The balanced experimental plan should be executed as implementation of new specifications can lead to a paradigm shift such that more fine-graded mixtures could be designed and constructed. As shown earlier in this proposal, fine-graded mixes have considerably different air void structures than coarse-graded ones. The lift thickness will be obtained via measuring the heights of cores removed during QA/QC sampling. The material under the paving lift will also be noted. These factors will be

considered in the analysis of the data using analysis of variance to understand their impacts on permeability measurements.

3.1.2 Proposed Testing at Field Locations and on Field Acquired Samples

The second important component to the experimental plan is the technology to be used in the research project and how the technology will be applied with consideration of how the technology will be implemented. The research team initially proposed that technologies be used to make field measurements at locations prior to coring that occurs in the present MoDOT QA/QC process and on QA/QC cores. Specifically, it is proposed that PaveTracker electromagnetic density and air and water permeability measurements be made at QA/QC core locations prior to coring. The MoDOT would then proceed to test the acquired cores in accordance with AASHTO T166 consistent with their current specifications. The cores would then be provided to the research team for subsequent CoreLok density and laboratory permeability testing. However it became apparent that it was more efficient and less obstructive to conduct testing at a second set of seven randomly identified locations for testing and subsequent coring. The original laboratory permeability testing proposed was to include both air and water mediums, however substantial equipment problems were encountered using the ROMUS air permeameter and this laboratory testing was not pursued. Figure 3.1 below illustrates the testing that was conducted for this research project by MoDOT. This included 17 different mixtures, 7 samples per mixture, and 8 measurements per sample/location resulting in 952 measurements.

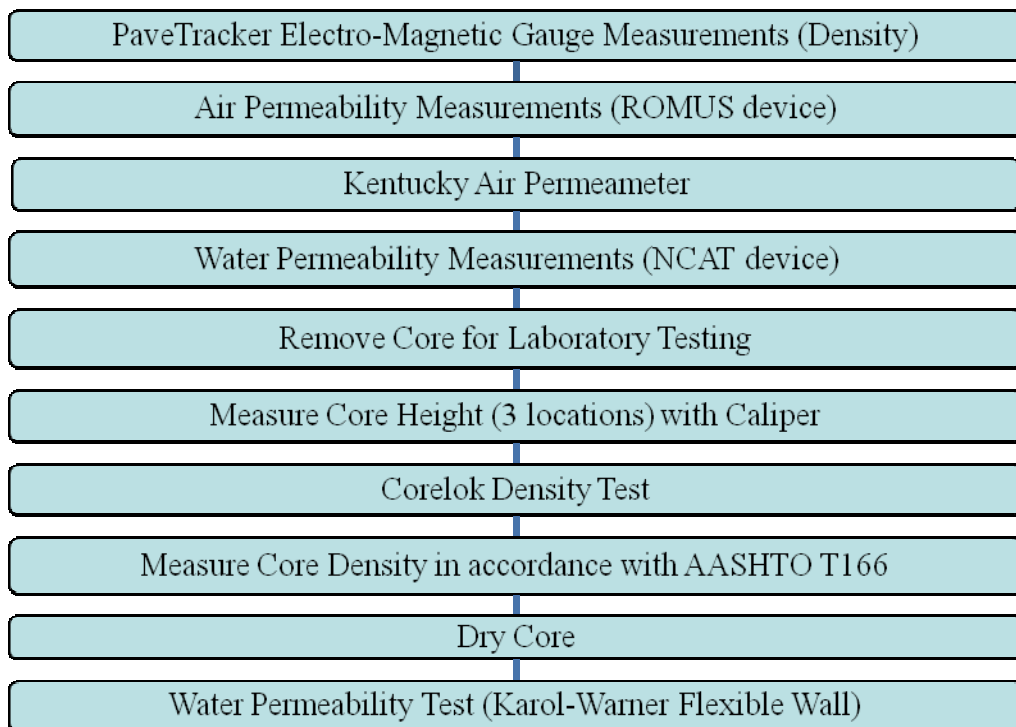


Figure 3.1 Experimental Test Program

3.2 Testing of Field Mixtures

Figure 3.1 outlines the testing of in-situ field mixes as well as on cores of the field mixtures. The field measurements were made at the random locations identified for core sampling as part of the current MoDOT QA/QC specifications (Section 403 *Asphaltic Concrete Pavement*).

PaveTracker density measurements were made once a QA/QC core location was identified. A PaveTracker takes about five seconds for a reading and one is shown in Figure 3.2 in use.

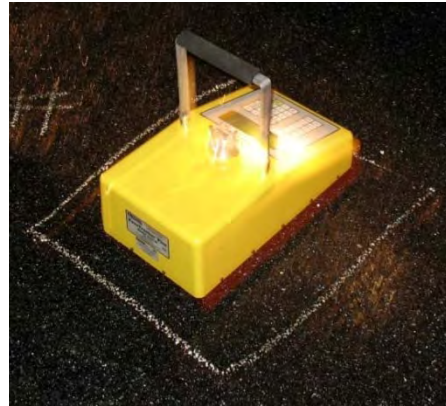


Figure 3.2 Pavetracker

Once a Pavetracker measurement was complete, air permeability measurements (ROMUS and Kentucky) were made at the same location. The ROMUS air permeameter used in this study is one made by ROMUS of Milwaukee, Wisconsin and is shown in Figure 3.3.

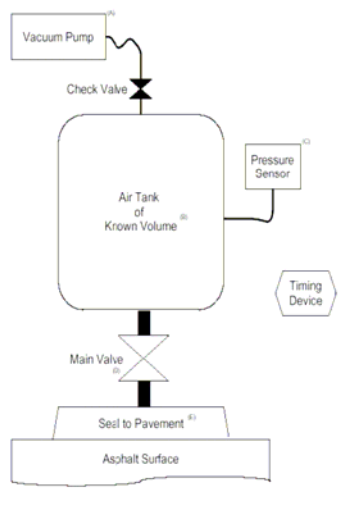


Figure 3.3 Schematic and Illustration of the ROMUS Air Permeameter

The test component of the Kentucky Air Permeameter is shown in Figure 3.4 that is attached to a compressor via an air hose.



Figure 3.4 Kentucky Air Permeameter

Once the tests utilizing non-water invasive techniques were completed, water permeability testing was done using the NCAT Water Permeameter. The NCAT Water Permeameter is shown in Figure 3.5 below.



Figure 3.5 NCAT Water Permeameter

Once the non-destructive testing was completed at a specific location, a core was removed for subsequent laboratory testing. To expedite the extraction of the core, dry ice was used to cool the core location as illustrated in Figure 3.6. Figure 3.7 shows a core just after removal using a portable Milwaukee coring machine. A 3.75-inch interior core barrel was used for obtaining the samples.



Figure 3.6 Cooling the Core Location with Dry Ice



Figure 3.7 Removal of Core

Once the cores were removed and transported to the central laboratory in Jefferson City, they were allowed to dry and then tested with a CoreLok device for density. A CoreLok device is shown in Figure 3.8 below.



Figure 3.8 Instrotek's CoreLok Test Device

Testing in accordance with AASHTO T166, also referred to as saturated surface dried bulk specific gravity, was done consistent with the current MoDOT specifications. The test configuration is shown in Figure 3.9. After AASHTO T166 testing, the samples were then tested in a Karol-Warner Flexible Wall Permeameter following ASTM PS-129 and the test device is depicted in Figure 3.10.



Figure 3.9 AASHTO T166 Test Configuration



Figure 3. 10 Karol-Warner Flexible Wall Permeameter

3.3 Projects/Mixtures Included in Study

A total of 17 projects/mixtures were tested for this study representing varying nominal maximum aggregate sizes (NMAS), traffic levels, and contractors. A summary of the sampled projects/mixtures is summarized in Table 3.2 below.

Table 3.2 Projects/Mixtures Included in Study

ID No.	Project	Route	County	JMF	NMAS, mm	Gmm
8MFO0017-1	J0P0883/J0P0969	Hwy 60	Stoddard	SP190 08-83	19.0	2.518
8MFO0018-7	J7I0841	I-44	Lawrence	SP125 08-37	12.5	2.360
8MFO0019-1	J2P0773	Hwy 63	Adair	SP125 08-24	12.5	2.451
8MFO0020-7	J8P0843C	Hwy 65	Dallas/Hickory	SP125 08-50	12.5	2.494
8MFO0021-1	J0I1253	I-55	Perry	SP125 08-61	12.5	2.441
8MFO0022-7	J3P0708	Hwy 47	Warren	SP125 08-2	12.5	2.460
8MFO0027-1	J9P0545	Hwy 63	Phelps	SP125 08-76	12.5	2.462
8MFO0028-7	J3P0727	Hwy 54	Audrain	SP190 08-80	19.0	2.503
8MFO0029-1	J4P1934	Hwy 7	Henry	SP095 08-84	9.5	2.457
8MFO0030-7	J2P0770	Hwy 63	Macon	SP190 07-72	19.0	2.456
8MFO0031-1	J1P0913	Hwy 36	Caldwell	SP125 08-97	12.5	2.466
8MFO0032-7	J7P0868	Hwy 60	Barry	SP095 08-83	9.5	2.391
8MFO0035-1	J4I1881	I-35	Clay	SP095 08-30	9.5	2.358
8MFO0036-7	J5I0971	I-70	Boone	SP125 06-60	12.5	2.394
8MFO0037-1	J5P0934	Hwy 65	Pettis	SP190 08-88	19.0	2.455
8MFO0038-7	J9P0566	Hwy 63	Howell	SP125 08-85	12.5	2.531
8MFO0048-1	J5P0590/J5P0591	Hwy 5	Camden	SP250 08-19	25.0	2.503

The sampled projects included coarse, fine and open-graded mixtures and consisted of three 9.5mm, nine 12.5mm, four 19.0mm, and one 25.0mm nominal maximum aggregate size mixtures. Unfortunately there were not an adequate number of 9.5mm and 19.0mm mixtures to complete the originally proposed factorial experimental plan. However, the number of mixtures collected is representative of the mixtures placed in Missouri and the lack of a full factorial experimental will not impact the findings and recommendations for the project.

CHAPTER 4 TEST RESULTS & STATISTICAL ANALYSIS

4.1 Introduction

Testing was conducted on 17 projects consisting of nominal maximum aggregate sizes of 9.5, 12.5, 19.0, and 25.0mm as summarized in the previous chapter. The mixes/pavements tested consisted of varying levels of traffic from 1 million to 30 million equivalent single axles over a 20-year design period. This chapter is divided into primarily two sections: the first summarizes the test results and the second provides a statistical analysis of the data.

4.2 Compilation of Test Results

The average test results for each project for each method of air void determination and permeability test method are summarized in the ensuing subsections. The standard deviation (Std. Dev.) and coefficient of variation (COV) are also summarized for each project as well as an average COV for the specific test method at the bottom of each table.

4.2.1 PaveTracker Density and Resulting Air Void Determinations

In Table 4.1 below are the summary results for each project for using the PaveTracker Density Gauge and determining the resulting air voids. Thus the density value measured by the PaveTracker was used to determine the bulk specific gravity, G_{mb} , of the test location. The maximum specific gravity value, G_{mm} , provided by MoDOT coupled with the G_{mb} was used to determine the corresponding air voids.

Table 4.1 PaveTracker Density and Resulting Air Void Determinations

ID No.	Route	NMAAS, mm	PaveTracker Air Voids, Percent		
			Mean	Std. Dev.	COV, %
8MFO0017-1	Hwy 60	19.0	7.89	3.41	43
8MFO0018-1	I-44	12.5	8.37	1.72	20
8MFO0019-1	Hwy 63	12.5	5.46	1.00	18
8MFO0020-1	Hwy 65	12.5	4.46	1.42	32
8MFO0021-1	I-55	12.5	1.40	1.79	128
8MFO0022-1	Hwy 47	12.5	9.59	2.36	25
8MFO0027-1	Hwy 63	12.5	12.64	2.20	17
8MFO0028-1	Hwy 54	19.0	8.76	2.17	25
8MFO0029-1	Hwy 7	9.5	7.06	2.22	32
8MFO0030-1	Hwy 63	19.0	4.00	2.21	55
8MFO0031-1	Hwy 36	12.5	3.87	2.26	58
8MFO0032-1	Hwy 60	9.5	11.63	1.08	9
8MFO0035-1	I-35	9.5	12.10	2.61	22
8MFO0036-1	I-70	12.5	8.66	2.16	25
8MFO0037-1	Hwy 65	19.0	3.06	1.73	56
8MFO0038-1	Hwy 63	12.5	12.19	1.60	13
8MFO0048-1	Hwy 5	25.0	16.23	2.63	16
Avg. COV					35

4.2.2 CoreLok Density and Resulting Air Void Determinations

Similar to the air void determinations made with PaveTracker density measurements, similar air void determinations were made using the Gmb test results from the CoreLok test device. The Gmm provided by MoDOT was used with the determined Gmm values to calculate the corresponding air voids for each sample for each project. The results are summarized in Table 4.2 below and are arranged in the same manner as was described in the aforementioned PaveTracker section. One observation that is readily apparent is that the average COV for the air voids for the projects using a CoreLok, 18 percent, is substantially less than that of the PaveTracker, 35 percent.

Table 4.2 CoreLok Density and Corresponding Air Void Determinations

ID No.	Route	NMAAS, mm	CoreLok Air Voids, Percent		
			Mean	Std. Dev.	COV, %
8MFO0017-1	Hwy 60	19.0	10.84	2.67	25
8MFO0018-1	I-44	12.5	6.29	1.14	18
8MFO0019-1	Hwy 63	12.5	9.29	1.04	11
8MFO0020-1	Hwy 65	12.5	10.96	1.30	12
8MFO0021-1	I-55	12.5	2.66	0.50	19
8MFO0022-1	Hwy 47	12.5	9.09	0.74	8
8MFO0027-1	Hwy 63	12.5	10.56	1.95	19
8MFO0028-1	Hwy 54	19.0	9.59	1.32	14
8MFO0029-1	Hwy 7	9.5	12.23	1.81	15
8MFO0030-1	Hwy 63	19.0	7.43	1.66	22
8MFO0031-1	Hwy 36	12.5	9.77	1.57	16
8MFO0032-1	Hwy 60	9.5	10.47	1.23	12
8MFO0035-1	I-35	9.5	3.67	1.23	33
8MFO0036-1	I-70	12.5	4.91	1.02	21
8MFO0037-1	Hwy 65	19.0	5.50	1.37	25
8MFO0038-1	Hwy 63	12.5	7.41	1.43	19
8MFO0048-1	Hwy 5	25.0	7.29	1.02	14
Avg. COV					18

4.2.3 AASHTO T166 Density and Resulting Air Void Determinations

The current standard used in part to assess HMA quality is AASHTO T166 with the associated air void determinations by MoDOT. The summary results for all of the projects are in Table 4.3 below. It is interesting to note that 11 of the 17 projects exceed an average of 8 percent air voids and thus placing the majority of projects in a less than full payment situation. It may be beneficial to examine the outcomes of quality assurance testing that was done on the same subplot for each project as this research project and to determine if differences occurred. It is also important to note that the average COV is 17 percent and is quite close to the COV for the air voids determined from CoreLok testing.

Table 4.3 AASHTO T166 Density and Air Void Determinations

ID No.	Route	NMA5, mm	AASHTO T166 Air Voids, Percent		
			Mean	Std. Dev.	COV, %
8MFO0017-1	Hwy 60	19.0	9.10	1.54	17
8MFO0018-1	I-44	12.5	5.74	1.02	18
8MFO0019-1	Hwy 63	12.5	9.33	0.97	10
8MFO0020-1	Hwy 65	12.5	9.56	0.99	10
8MFO0021-1	I-55	12.5	2.14	0.44	20
8MFO0022-1	Hwy 47	12.5	8.56	0.96	11
8MFO0027-1	Hwy 63	12.5	9.20	1.43	16
8MFO0028-1	Hwy 54	19.0	8.83	0.85	10
8MFO0029-1	Hwy 7	9.5	11.96	1.71	14
8MFO0030-1	Hwy 63	19.0	6.83	1.46	21
8MFO0031-1	Hwy 36	12.5	8.96	1.38	15
8MFO0032-1	Hwy 60	9.5	10.57	1.66	16
8MFO0035-1	I-35	9.5	3.17	1.16	37
8MFO0036-1	I-70	12.5	4.23	0.87	21
8MFO0037-1	Hwy 65	19.0	5.30	1.32	25
8MFO0038-1	Hwy 63	12.5	6.71	1.09	16
8MFO0048-1	Hwy 5	25.0	7.10	0.95	13
Avg. COV					17

4.2.4 ROMUS Air Permeameter Test Results

The summary of the Romus air permeability test results are summarized in Table 4.4.

Unfortunately technical difficulties were encountered with this technology resulting in only 8 of the 17 projects being testing. The technical difficulty encountered was the device continued to pull a vacuum and seemed unable to shut off until the battery was fully discharged. Of the three field permeability technologies, the Romus had the lowest COV with 43 percent which is less than half of the Kentucky Air Permeameter’s (89 percent) and about one third of the NCAT Permeameter’s (125 percent). Although the technology has demonstrated potential and the possibility of conducting laboratory permeability tests as well, the support service of the equipment appears to be limited.

Table 4.4 Romus Air Permeameter Test Results

ID No.	Route	NMAAS, mm	Romus Permeability, $k \times 10^{-5}$ cm/sec		
			Mean	Std. Dev.	COV, %
8MFO0017-1	Hwy 60	19.0	213	122	57
8MFO0018-1	I-44	12.5	N/T	N/T	N/T
8MFO0019-1	Hwy 63	12.5	N/T	N/T	N/T
8MFO0020-1	Hwy 65	12.5	N/T	N/T	N/T
8MFO0021-1	I-55	12.5	N/T	N/T	N/T
8MFO0022-1	Hwy 47	12.5	N/T	N/T	N/T
8MFO0027-1	Hwy 63	12.5	215	77	36
8MFO0028-1	Hwy 54	19.0	483	104	22
8MFO0029-1	Hwy 7	9.5	234	115	49
8MFO0030-1	Hwy 63	19.0	228	125	55
8MFO0031-1	Hwy 36	12.5	102	59	58
8MFO0032-1	Hwy 60	9.5	173	57	33
8MFO0035-1	I-35	9.5	N/T	N/T	N/T
8MFO0036-1	I-70	12.5	N/T	N/T	N/T
8MFO0037-1	Hwy 65	19.0	N/T	N/T	N/T
8MFO0038-1	Hwy 63	12.5	N/T	N/T	N/T
8MFO0048-1	Hwy 5	25.0	317	104	33
Avg. COV					43

4.2.5 Kentucky Air Permeameter Test Results

The summary of the Kentucky Air Permeameter test results are shown in Table 4.5. On some projects, the COV is more than 100 percent which means that the standard deviation is greater than the mean permeability. Although the COV permeability results are rather high overall, it is important to note that the variability about the maximum average air voids is less and is discussed in more detail in section 4.6.

Table 4.5 Kentucky Air Permeameter Test Results

ID No.	Route	NMAAS, mm	Kentucky Permeability, $k \times 10^{-5}$ cm/sec		
			Mean	Std. Dev.	COV, %
8MFO0017-1	Hwy 60	19.0	2837	6232	220
8MFO0018-1	I-44	12.5	22	18	85
8MFO0019-1	Hwy 63	12.5	405	315	78
8MFO0020-1	Hwy 65	12.5	2629	2313	88
8MFO0021-1	I-55	12.5	13	1	12
8MFO0022-1	Hwy 47	12.5	283	187	66
8MFO0027-1	Hwy 63	12.5	1095	1278	117
8MFO0028-1	Hwy 54	19.0	777	1064	137
8MFO0029-1	Hwy 7	9.5	970	722	74
8MFO0030-1	Hwy 63	19.0	165	233	141
8MFO0031-1	Hwy 36	12.5	110	88	80
8MFO0032-1	Hwy 60	9.5	252	154	61
8MFO0035-1	I-35	9.5	13	1	9
8MFO0036-1	I-70	12.5	27	27	100
8MFO0037-1	Hwy 65	19.0	14	5	37
8MFO0038-1	Hwy 63	12.5	53	46	88
8MFO0048-1	Hwy 5	25.0	641	781	122
Avg. COV					89

4.2.6 NCAT Permeameter Test Results

The results of the NCAT Permeameter are similar to the Kentucky Air Permeameter test results and are summarized in Table 4.6. The average COV of the NCAT Permeameter is 125 percent and is about 40 percent higher than the COV of the Kentucky Air Permeameter of 89 percent. As mentioned previously, the COV of NCAT Permeameter is much higher than that of the CoreLok's and AASHTO T166 which are 18 and 17 percent, respectively.

Table 4.6 NCAT Permeameter Test Results

ID No.	Route	NMAAS, mm	NCAT Permeability, $k \times 10^{-5}$ cm/sec		
			Mean	Std. Dev.	COV, %
8MFO0017-1	Hwy 60	19.0	3547	4627	130
8MFO0018-1	I-44	12.5	79	130	164
8MFO0019-1	Hwy 63	12.5	1091	957	88
8MFO0020-1	Hwy 65	12.5	3888	2461	63
8MFO0021-1	I-55	12.5	11	23	200
8MFO0022-1	Hwy 47	12.5	810	433	53
8MFO0027-1	Hwy 63	12.5	1866	1478	79
8MFO0028-1	Hwy 54	19.0	1511	1770	117
8MFO0029-1	Hwy 7	9.5	972	771	79
8MFO0030-1	Hwy 63	19.0	1055	1435	136
8MFO0031-1	Hwy 36	12.5	348	279	80
8MFO0032-1	Hwy 60	9.5	953	578	61
8MFO0035-1	I-35	9.5	18	45	255
8MFO0036-1	I-70	12.5	404	630	156
8MFO0037-1	Hwy 65	19.0	20	47	241
8MFO0038-1	Hwy 63	12.5	746	719	96
8MFO0048-1	Hwy 5	25.0	895	1060	119
Avg. COV					125

4.2.7 Karol-Warner Permeameter Test Results

The Karol-Warner Permeameter was used to determine the permeability of sampled field cores and was done in accordance with ASTM PS-129. The summary permeameter results are provided in Table 4.7 below. The average COV is 108 percent and is unfortunately much higher than other lab tests that were conducted in the CoreLok and AASHTO T166. For the I-55 and I-35 projects, the samples were found to be impermeable and thus the corresponding average and standard deviation values of permeability are “zero” and results in the COV being indeterminate.

Table 4.7 Karol-Warner Permeameter Test Results

ID No.	Route	NMAAS, mm	K-W Permeability, $k \times 10^{-5}$ cm/sec		
			Mean	Std. Dev.	COV, %
8MFO0017-1	Hwy 60	19.0	3830	5947	155
8MFO0018-1	I-44	12.5	86	134	156
8MFO0019-1	Hwy 63	12.5	695	298	43
8MFO0020-1	Hwy 65	12.5	3418	2268	66
8MFO0021-1	I-55	12.5	0	0	N/A
8MFO0022-1	Hwy 47	12.5	269	197	73
8MFO0027-1	Hwy 63	12.5	1459	1167	80
8MFO0028-1	Hwy 54	19.0	808	880	109
8MFO0029-1	Hwy 7	9.5	877	552	63
8MFO0030-1	Hwy 63	19.0	235	309	131
8MFO0031-1	Hwy 36	12.5	646	521	81
8MFO0032-1	Hwy 60	9.5	899	538	60
8MFO0035-1	I-35	9.5	0	0	N/A
8MFO0036-1	I-70	12.5	21	23	109
8MFO0037-1	Hwy 65	19.0	9	16	176
8MFO0038-1	Hwy 63	12.5	95	226	237
8MFO0048-1	Hwy 5	25.0	140	110	79
Avg. COV					108

4.3 Relationships Between Air Void Determination Methods

The three methods for determining or estimating the density of the pavement or bulk specific gravity (G_{mb}) of the core samples and the corresponding air voids are the PaveTracker Density, and the G_{mb} via the CoreLok and AASHTO T166 which are compared. Figure 4.1 compares the air voids calculated from the G_{mb} values of the CoreLok and AASHTO T166 and identifies a correlation coefficient of 93.8%, which is excellent. The coefficient of the independent parameter, air voids determined from the CoreLok G_{mb} , is 0.9283. This means that the estimated air voids value via the AASHTO T166 method is 0.9283 of the value of the air voids as determined from the G_{mb} of CoreLok testing. Figures 4.2 and 4.3 compare the air voids determined from the PaveTracker density values to the air voids determined from AASHTO T166 and CoreLok testing, respectively. Clearly there is substantial scatter in the relationships resulting in very poor correlation coefficients of 0.0447 and 0.0458 for the PaveTracker air voids

and the AASHTO T166 and CoreLok air voids. It can thus be concluded that the air void determination from PaveTracker density test results does not represent viable technology to pursue for quality assurance testing at this time. However, the CoreLok Gmb testing does represent viable technology to implement for quality assurance testing for air voids determination.

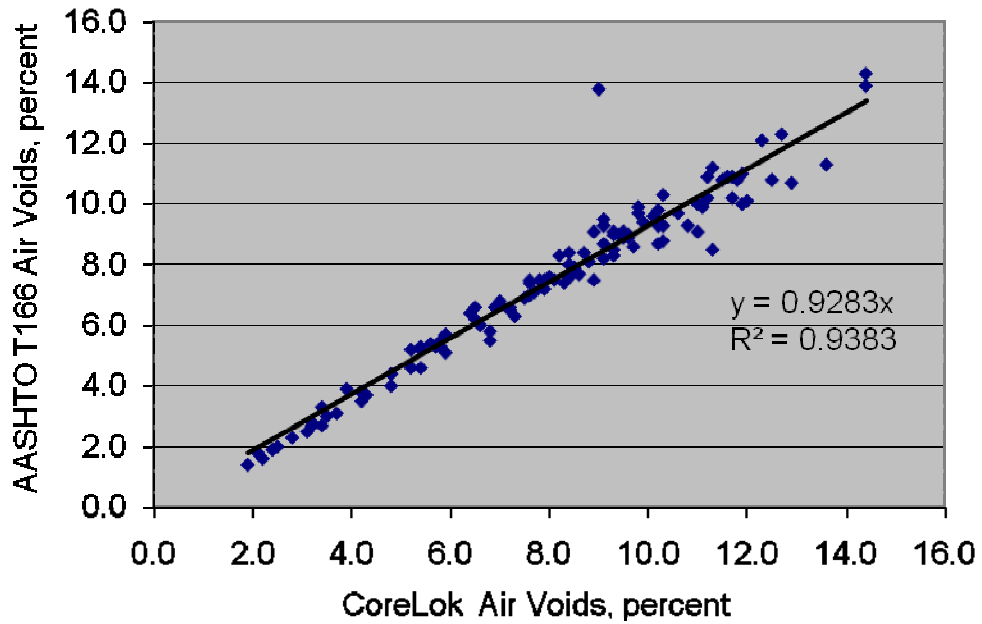


Figure 4.1 Comparison of CoreLok and AASHTO T166 Air Voids

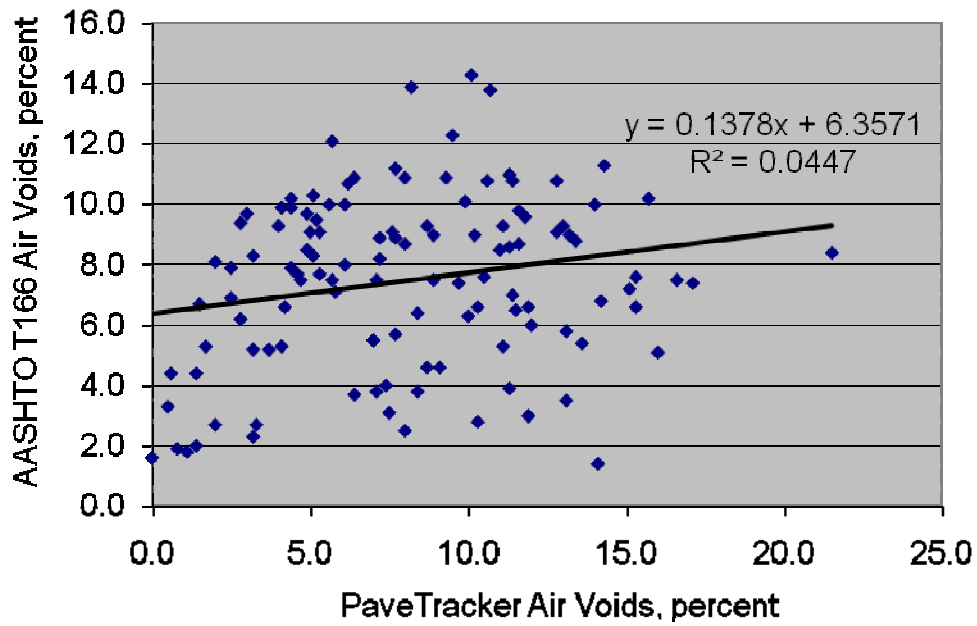


Figure 4.2 Comparison of PaveTracker and AASHTO T166 Air Voids

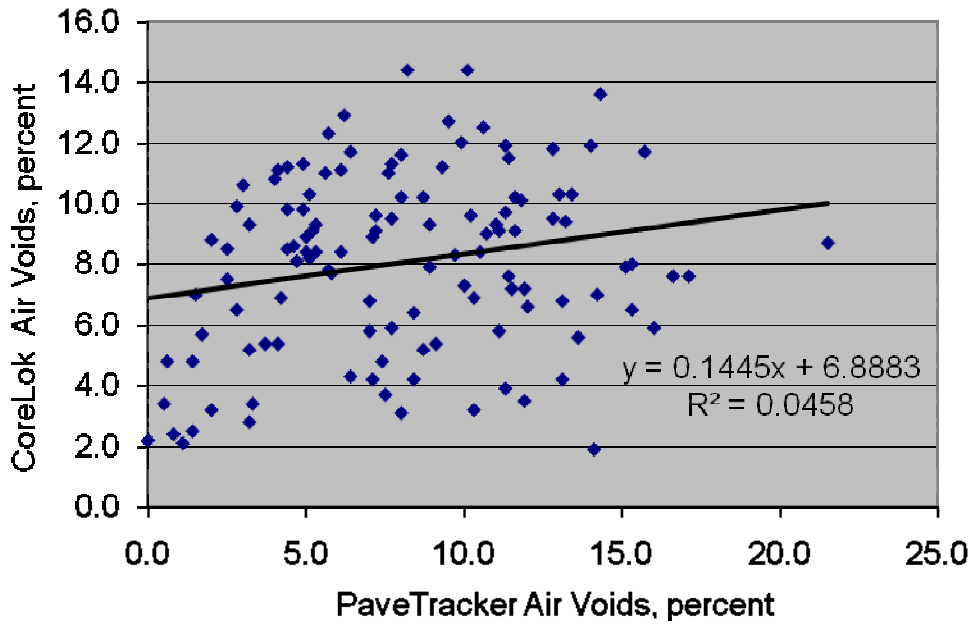


Figure 4.3 Comparison of PaveTracker and CoreLok Air Voids

4.4 Relationships Between Permeability Methods

Similar to the air voids comparisons that were made for the air voids determinations from density and Gmb testing, similar comparisons are made for the four different methods of permeability testing. Figure 4.4 compares the NCAT and Kentucky permeability values and illustrates an excellent relationship between the two test methods with a coefficient of correlation of 0.9537 for a second order model.

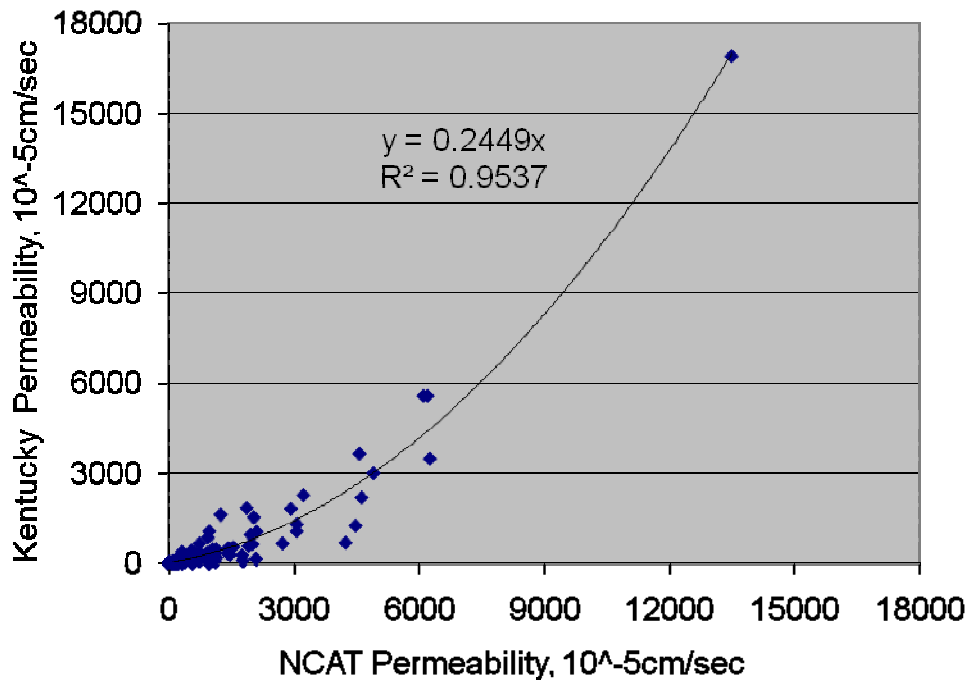


Figure 4.4 Comparison of NCAT and Kentucky Permeability Values

The permeability values for the Kentucky and Romus methods are compared in Figure 4.5 and illustrate a coefficient of correlation of -0.167, which is very poor. Figure 4.6 is a comparison between the permeability values of NCAT and Karol-Warner test methods and illustrates a very favorable coefficient of correlation of 0.9144.

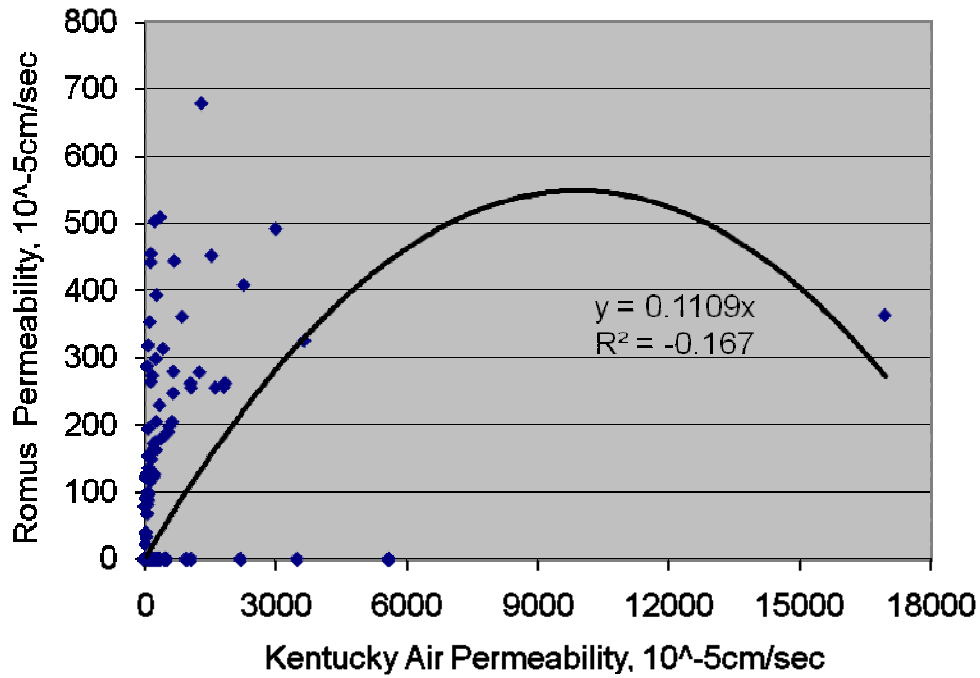


Figure 4.5 Comparison of Kentucky Air and Romus Permeability Values

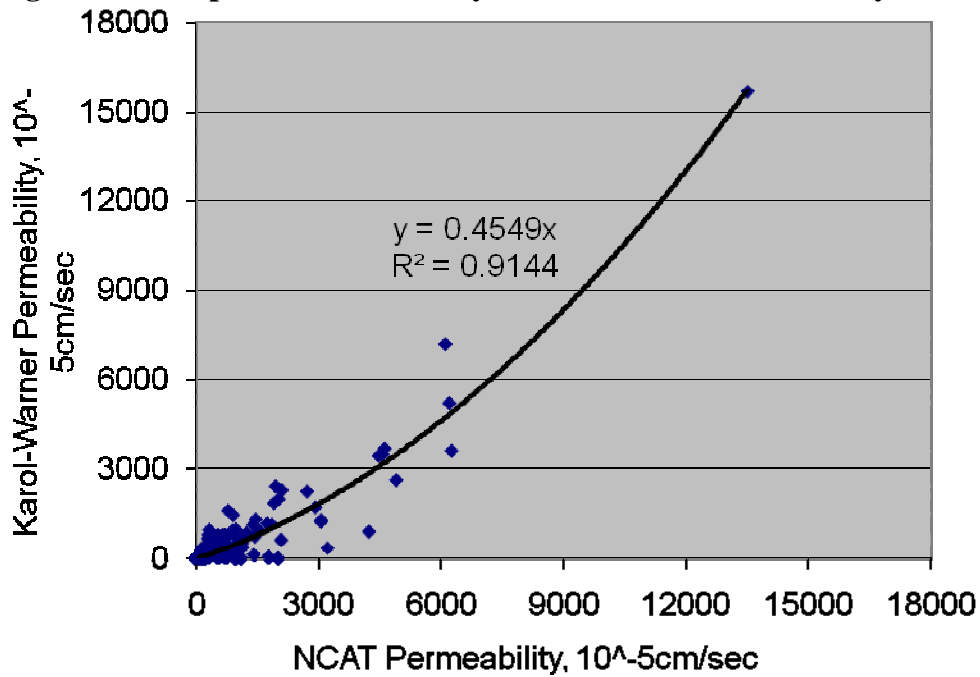


Figure 4.6 Comparison of NCAT and Karol-Warner Permeability Values

Similar to Figure 4.6, Figure 4.7 has an excellent coefficient of correlation of 0.9092 between the Karol-Warner and Kentucky permeability test values. Unfortunately, Figure 4.8 has a very poor

coefficient of correlation of 0.0258 between the NCAT and Romus permeability values and is similar to the Kentucky and Romus values.

From the comparisons illustrated in Figures 4.4 through 4.8, it is reasonable to further consider permeability values determined from the Kentucky, NCAT and Karol-Warner test methods for use in quality assurance testing.

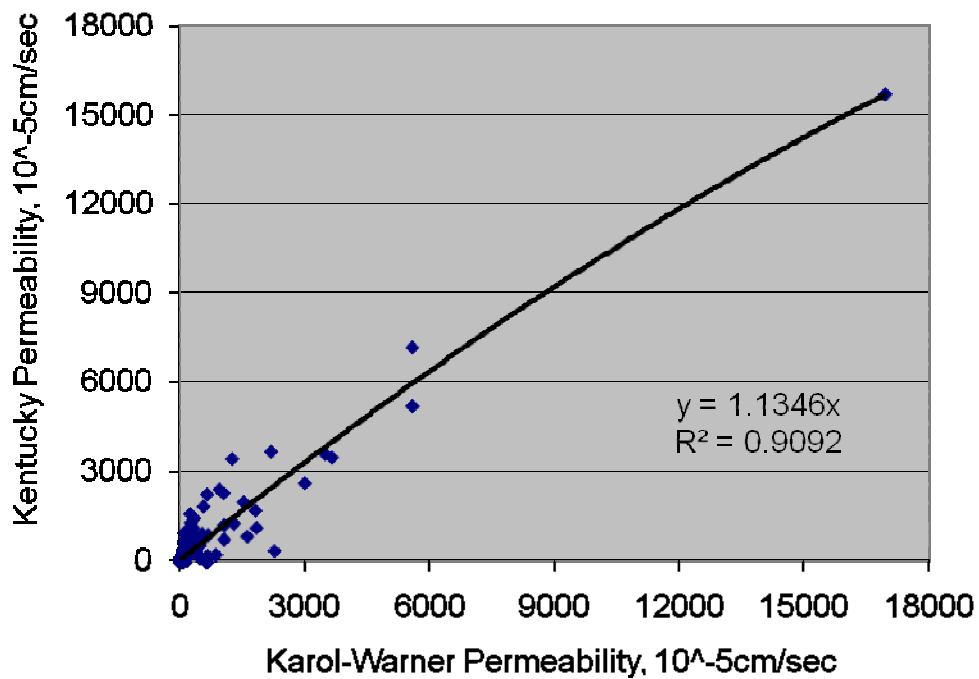


Figure 4.7 Comparison of Karol-Warner and Kentucky Permeability Values

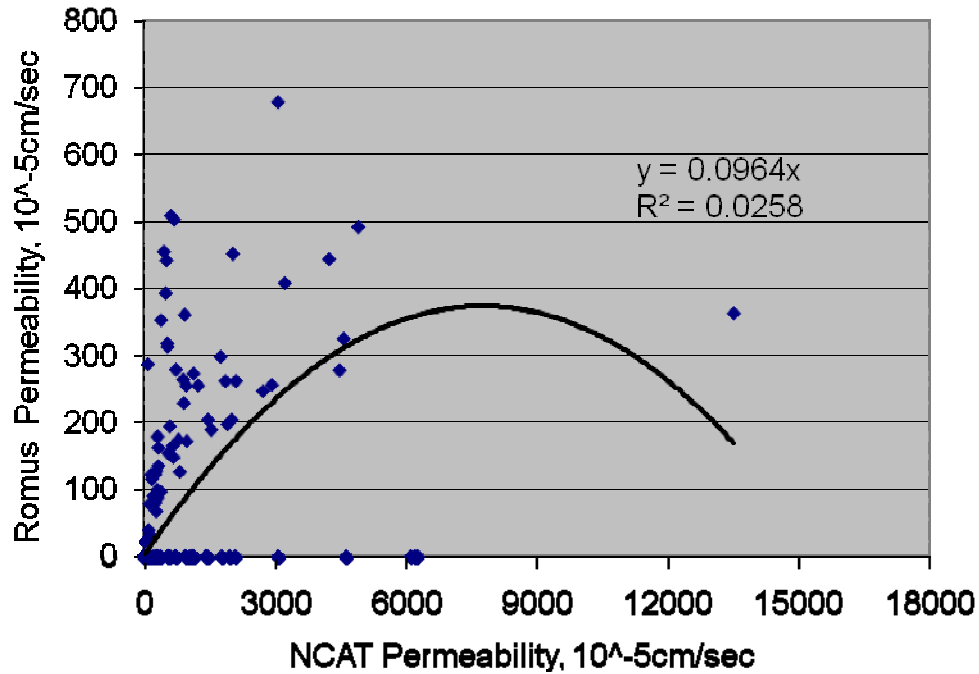


Figure 4.8 Comparison of NCAT and Romus Permeability Values

4.5 Relationships Between Permeability and Air Void Determination Methods

Figures 4.9 through 4.11 have comparisons between AASHTO T166 for determining air voids and the three viable methods for measuring permeability: the Kentucky, NCAT and Karol-Warner test methods. Figure 4.9 illustrates the comparison between AASHTO T166 and the resulting air voids with the Kentucky permeability values. At approximately 6.5 to 7.0 percent air voids, the variability and average permeability values begin increasing substantially. This is consistent with what was identified in the literature review in that specifying the upper limit of 7 to 8 percent air voids for attaining an impermeable pavement is reasonable. Although it is not intended to estimate a permeability range based upon air void contents, this could be done but a mathematical function would likely need to be applied to data to ensure adjusted uniform levels of variability in the permeability values across all values of air voids as the data appears to be heteroscedastic.

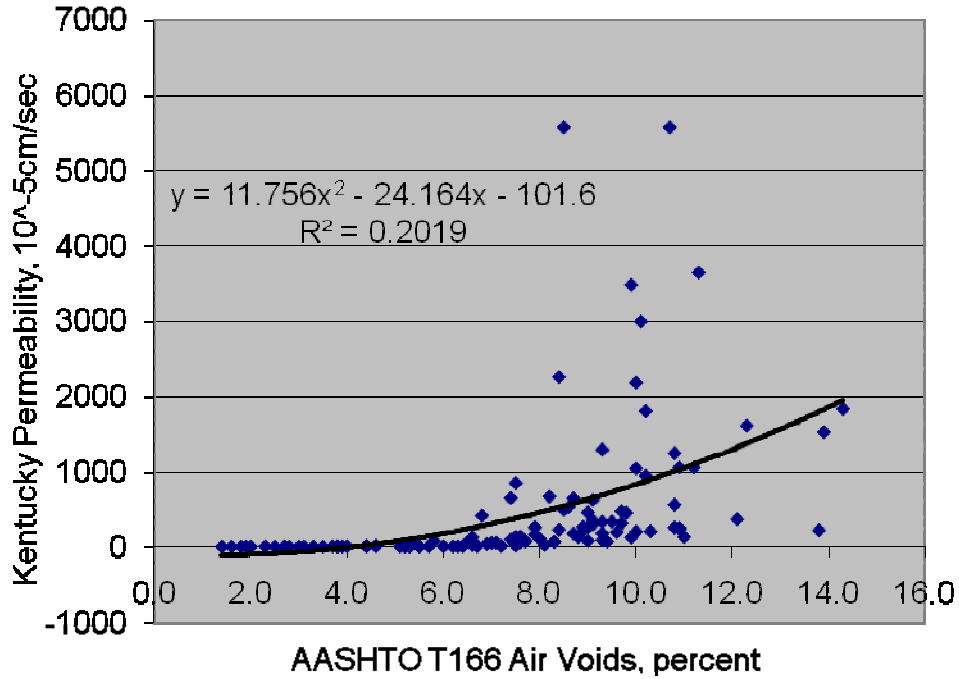


Figure 4.9 Comparison of AASHTO T166 and Kentucky Permeability Values

Figures 4.10 and 4.11 have similar outcomes as that of Figure 4.9 in that the permeability values have increasing variability and higher mean values beginning at about the 6 percent air voids levels for the NCAT and Karol-Warner Permeability test methods. For the purposes of developing a percent within limit specification criteria to be consistent with current specifications using air voids, the upper specification limit values for the three methods of determining permeability will be based upon the 8 percent air voids threshold. The development of the percent within limit criteria for permeability testing will be further discussed in section 4.8.

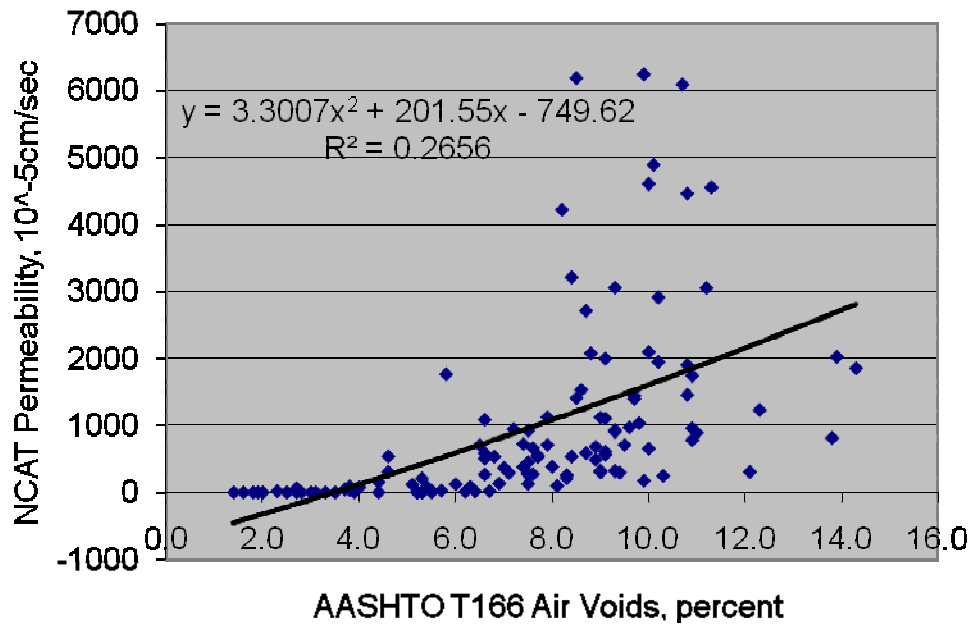


Figure 4.10 Comparison of AASHTO T166 and NCAT Permeability Values

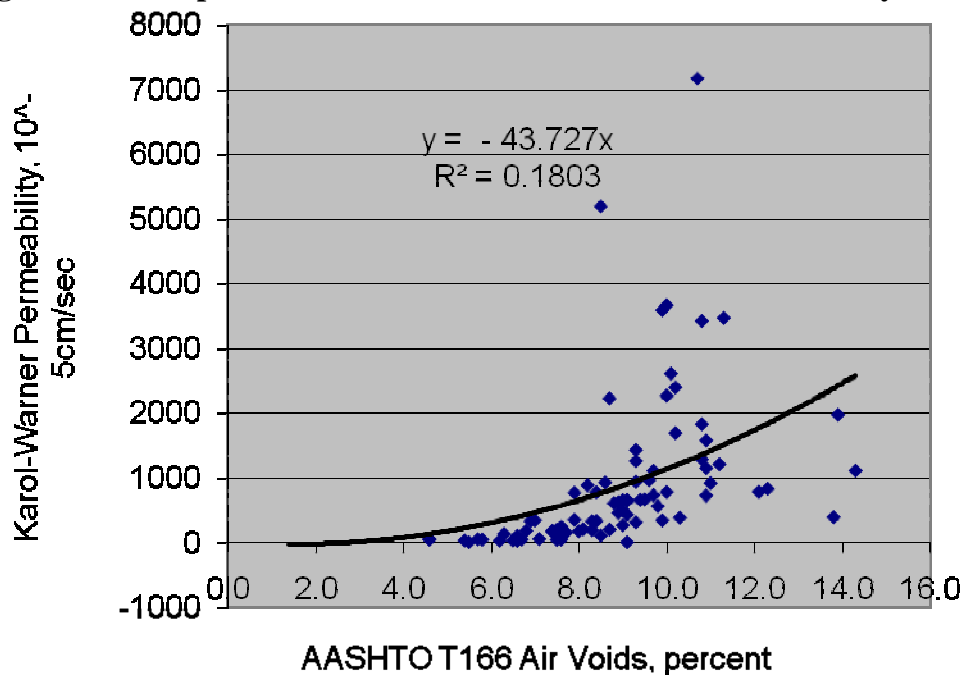


Figure 4.11 Comparison of AASHTO T166 and Karol-Warner Permeability Values

4.6 Statistical Analysis

Statistical models were developed to identify which independent variables were statistically significant at an α (alpha) level of 0.05, or statistically significant at a 95 percent level of confidence. A summary of the statistical analysis considering the main effects and all of the interactions for a second order model is provided in Table 4.8.

Table 4.8 Statistical Summary of Full Models

Parameter	Model	R ² _{adj}	F-value
NCAT	$-0.4361 - 0.0010*NMAS + 0.1809*Gmm + 0.0086*Thickness + 0.0321*NMAS*Gmm - 0.0004*NMAS*Thickness - 0.1797*Gmm*Thickness - 0.0205*NMAS*Gmm*Thickness$	0.133019	3.5863
KY	$-0.3251 - 0.0006*NMAS + 0.1368*Gmm + 0.0017*Thickness + 0.0275*NMAS*Gmm - 0.0003*NMAS*Thickness - 0.1386*Gmm*Thickness - 0.0097*NMAS*Gmm*Thickness$	0.045978	1.8124
Romus	$-0.0994 - 0.0003*NMAS + 0.0406*Gmm + 0.0030*Thickness + 0.0017*NMAS*Gmm - 0.0003*NMAS*Thickness + 0.0531*Gmm*Thickness - 0.0005*NMAS*Gmm*Thickness$	0.582028	12.1401
Karol-Warner	$-0.4460 - 0.0012*NMAS + 0.1899*Gmm + 0.0027*Thickness + 0.0445*NMAS*Gmm - 0.0009*NMAS*Thickness - 0.2574*Gmm*Thickness - 0.0129*NMAS*Gmm*Thickness$	0.081828	2.1331
PaveTracker	$-59.9448 - 0.6583*NMAS + 28.5741*Gmm + 2.7371*Thickness + 16.3521*NMAS*Gmm - 0.5415*NMAS*Thickness + 64.1968*Gmm*Thickness + 10.6592*NMAS*Gmm*Thickness$	0.417043	13.0595
AASHTO T 166	$-75.4924 - 0.3625*NMAS + 36.3697*Gmm - 0.7409*Thickness + 2.8387*NMAS*Gmm + 0.4234*NMAS*Thickness - 47.8751*Gmm*Thickness - 0.1085*NMAS*Gmm*Thickness$	0.269072	7.2055
CoreLok	$-87.7930 - 0.3904*NMAS + 41.4912*Gmm - 0.3405*Thickness + 3.9234*NMAS*Gmm + 0.3544*NMAS*Thickness - 56.1315*Gmm*Thickness - 0.6048*NMAS*Gmm*Thickness$	0.298767	8.1821

Overall, the models are relatively poor as the F-statistics and adjusted coefficient of correlation are mostly low. The adjusted coefficient of correlation is used as this accounts for the corresponding degrees of freedom and accounts for possibly over specifying the model with a large number of independent variables. The full statistical set of analyses is contained in Appendix A.

The reduced models were determined using backward stepwise regression analysis and are summarized in Table 4.9. An α value of 0.05 was used to determine the significance of the main effects (NMAAS, Gmm, and thickness). If a main effect was found not to be significant, then interactions and second order parameters were not considered in the reduced models.

Table 4.9 Reduced Statistical Models

Parameter	Model	R²_{adj}	F-value
NCAT	$-0.4058 - 0.0010 \cdot \text{NMAAS} + 0.1732 \cdot \text{Gmm} + 0.0025 \cdot \text{Thickness} + 0.0167 \cdot \text{NMAAS} \cdot \text{Gmm}$	0.109761	4.6372
KY	$-0.3102 - 0.0005 \cdot \text{NMAAS} + 0.1334 \cdot \text{Gmm} - 0.0023 \cdot \text{Thickness} + 0.0165 \cdot \text{NMAAS} \cdot \text{Gmm}$	0.04946	2.5350
Romus	$-0.0764 - 0.0002 \cdot \text{NMAAS} + 0.0312 \cdot \text{Gmm} + 0.0026 \cdot \text{Thickness} - 0.0003 \cdot \text{NMAAS} \cdot \text{Thickness} + 0.0635 \cdot \text{Gmm} \cdot \text{Thickness}$	0.586003	16.8533
Karol-Warner	$-0.4227 - 0.0009 \cdot \text{NMAAS} + 0.1840 \cdot \text{Gmm} - 0.0043 \cdot \text{Thickness} + 0.0182 \cdot \text{NMAAS} \cdot \text{Gmm}$	0.06049	2.4326
PaveTracker	$-59.9448 - 0.6583 \cdot \text{NMAAS} + 28.5741 \cdot \text{Gmm} + 2.7371 \cdot \text{Thickness} + 16.3521 \cdot \text{NMAAS} \cdot \text{Gmm} - 0.5415 \cdot \text{NMAAS} \cdot \text{Thickness} + 64.1968 \cdot \text{Gmm} \cdot \text{Thickness} + 10.6592 \cdot \text{NMAAS} \cdot \text{Gmm} \cdot \text{Thickness}$	0.417043	13.0595
AASHTO T 166	$-64.9688 - 0.2867 \cdot \text{NMAAS} + 32.0327 \cdot \text{Gmm} - 1.1381 \cdot \text{Thickness} + 0.4761 \cdot \text{NMAAS} \cdot \text{Thickness} - 38.8174 \cdot \text{Gmm} \cdot \text{Thickness}$	0.266894	9.5918
CoreLok	$-9.3123 - 0.0280 \cdot \text{NMAAS} + 4.7412 \cdot \text{Gmm} + 0.0547 \cdot \text{Thickness} - 2.2740 \cdot \text{Gmm} \cdot \text{Thickness}$	0.208914	8.7905

It is clear in the reduced models that larger NMAAS mixtures lead to a decrease in permeability as well as a decrease in air voids, whereas both higher values of Gmm and increased paving lift thickness lead to an increase in permeability and an increase in air voids. This can be shown by both examining the coefficients of the main effects in the reduced models as well as the prediction profiles (plots) shown in Appendix A.

4.7 Confidence Limits of Kentucky and NCAT Permeabilities

Figures 4.12 and 4.13 illustrate the Kentucky Air and NCAT Permeameter test results as compared to the AASHTO T166 air voids, respectively. The dashed lines in the figures show the 90 percent level of confidence limit based upon the aforementioned models in section 4.6.

Clearly the results illustrate that the variability is increased at higher air void levels, as evidence of the increase in the scatter of the test results at about 7 percent and 6 percent for the Kentucky and NCAT permeabilities, respectively as compared to lower levels of air voids.

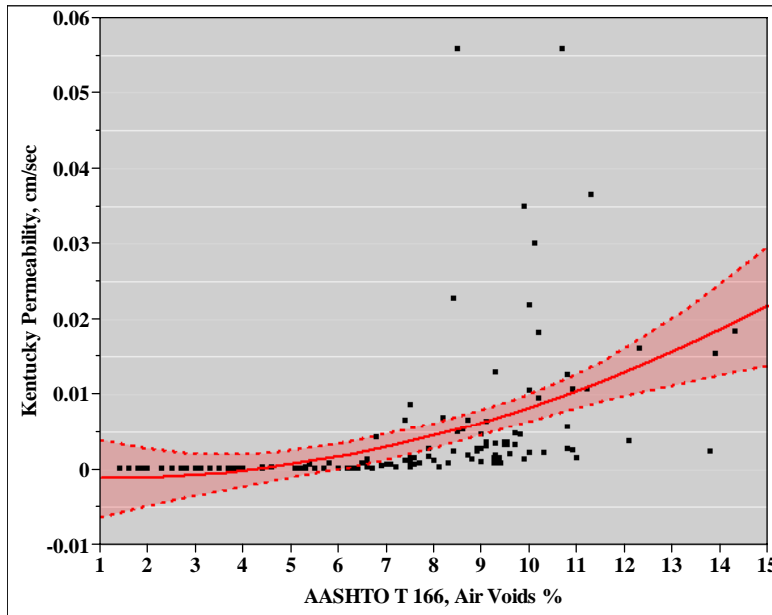


Figure 4.12 AASHTO T166 and Kentucky Permeability Values with 90 Percent Level of Confidence

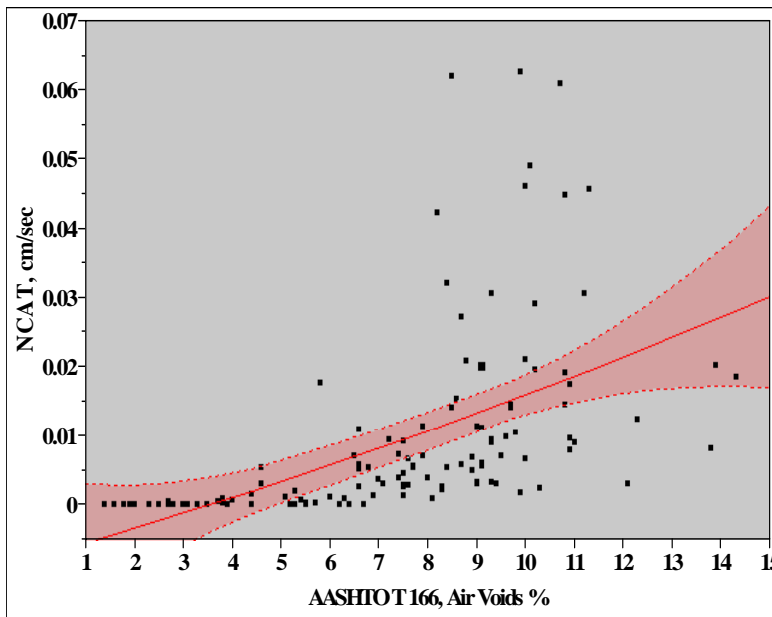


Figure 4.13 AASHTO T166 and NCAT Permeability Values with 90 Percent Level of Confidence

4.8 Permeability Criteria

The permeability criterion that is discussed in the ensuing sections is based upon the outcomes of the current MoDOT specification criteria for air voids using AASHTO T166. Namely, the criteria are 94+/-2 percent of Gmm (6+/-2 percent air voids). The percent within limit (PWLt) outcomes for each project are summarized in Table 4.10 below. The quality index values for the upper (Qu) and lower (Ql) criteria and the PWL for the corresponding upper (PWLu) and lower (PWLl) for each project are shown in the table as well. The average PWL for all projects tested is 61.09 percent. It is important to point out that the 61.09 percent within limit determination is only based upon one subplot for the particular day that sampling occurred on each project.

Table 4.10 Summary of Percent Within Limit for AASHTO T166 Air Voids Summary

ID No.	Route	Qu	Ql	PWLu	PWLl	PWLt
8MFO0017-1	Hwy 60	-0.72	3.32	50.00	100.00	50.00
8MFO0018-1	I-44	2.22	1.71	99.99	97.48	97.47
8MFO0019-1	Hwy 63	-1.36	5.47	50.00	100.00	50.00
8MFO0020-1	Hwy 65	-1.57	5.60	50.00	100.00	50.00
8MFO0021-1	I-55	13.45	-4.27	100.00	50.00	50.00
8MFO0022-1	Hwy 47	-0.58	4.74	50.00	100.00	50.00
8MFO0027-1	Hwy 63	-0.84	3.64	50.00	100.00	50.00
8MFO0028-1	Hwy 54	-0.97	5.66	50.00	100.00	50.00
8MFO0029-1	Hwy 7	-2.32	4.66	50.00	100.00	50.00
8MFO0030-1	Hwy 63	0.80	1.93	78.12	99.24	77.36
8MFO0031-1	Hwy 36	-0.69	3.59	50.00	100.00	50.00
8MFO0032-1	Hwy 60	-1.55	3.95	50.00	100.00	50.00
8MFO0035-1	I-35	4.15	-0.71	100.00	50.00	50.00
8MFO0036-1	I-70	4.34	0.26	100.00	59.67	59.67
8MFO0037-1	Hwy 65	2.04	0.98	99.71	83.35	83.06
8MFO0038-1	Hwy 63	1.18	2.48	88.43	100.00	88.43
8MFO0048-1	Hwy 5	0.95	3.26	82.52	100.00	82.52
Average						61.09

Similar to the percent within limit determination that was summarized for the AASHTO T166 testing, the same was done for the CoreLok test results. The summary of the CoreLok PWL is provided in Table 4.11 below. The average PWL for all projects is 59.60 percent for the CoreLok as compared to 61.09 for AASHTO T166. Thus implementing the CoreLok for air

voids determination would represent a more stringent specification than AASHTO T166 as this testing method yields a lower PWL which utilizes the same upper and lower specification quality of 94+/-2 percent of Gmm.

Table 4.11 Summary of Percent Within Limit for CoreLok Air Voids Summary

ID No.	Route	Qu	Ql	Qlu	Qll	PWL
8MFO0017-1	Hwy 60	-1.06	2.56	50.00	100.00	50.00
8MFO0018-1	I-44	1.51	2.01	94.87	99.60	94.47
8MFO0019-1	Hwy 63	-1.24	5.09	50.00	100.00	50.00
8MFO0020-1	Hwy 65	-2.27	5.35	50.00	100.00	50.00
8MFO0021-1	I-55	10.77	-2.71	100.00	50.00	50.00
8MFO0022-1	Hwy 47	-1.47	6.87	50.00	100.00	50.00
8MFO0027-1	Hwy 63	-1.31	3.36	50.00	100.00	50.00
8MFO0028-1	Hwy 54	-1.20	4.23	50.00	100.00	50.00
8MFO0029-1	Hwy 7	-2.34	4.56	50.00	100.00	50.00
8MFO0030-1	Hwy 63	0.35	2.07	62.94	99.79	62.73
8MFO0031-1	Hwy 36	-1.13	3.68	50.00	100.00	50.00
8MFO0032-1	Hwy 60	-2.01	5.26	50.00	100.00	50.00
8MFO0035-1	I-35	3.53	-0.27	100.00	50.00	50.00
8MFO0036-1	I-70	3.02	0.90	100.00	81.10	81.10
8MFO0037-1	Hwy 65	1.82	1.09	98.51	86.25	84.76
8MFO0038-1	Hwy 63	0.41	2.40	65.09	100.00	65.09
8MFO0048-1	Hwy 5	0.70	3.22	74.97	100.00	74.97
Average						59.60

The average PWL for the projects tested with AASHTO T166 was 61.09 percent and the upper and lower quality characteristic values for the various methods of permeability testing will be determined that yields the same 61.09 PWL. This will include conducting simulations of PWL using a range of upper quality characteristic values for permeability, whereas the lower value will be zero as this is the lower limit of permeability testing for pavements. The ensuing subsections summarize the outcomes of the simulations and corresponding criteria for the Kentucky, NCAT, and Karol-Warner Permeameters.

4.8.1 Kentucky Air Permeameter Criteria

Simulations using varying permeability values for the upper specification limit and zero for the lower specification limit yielded varying percent within limit values. A graphical representation

of the simulation is presented in Figure 4.14 below. The goodness of fit, R^2 , is very good for the data at 99.46%

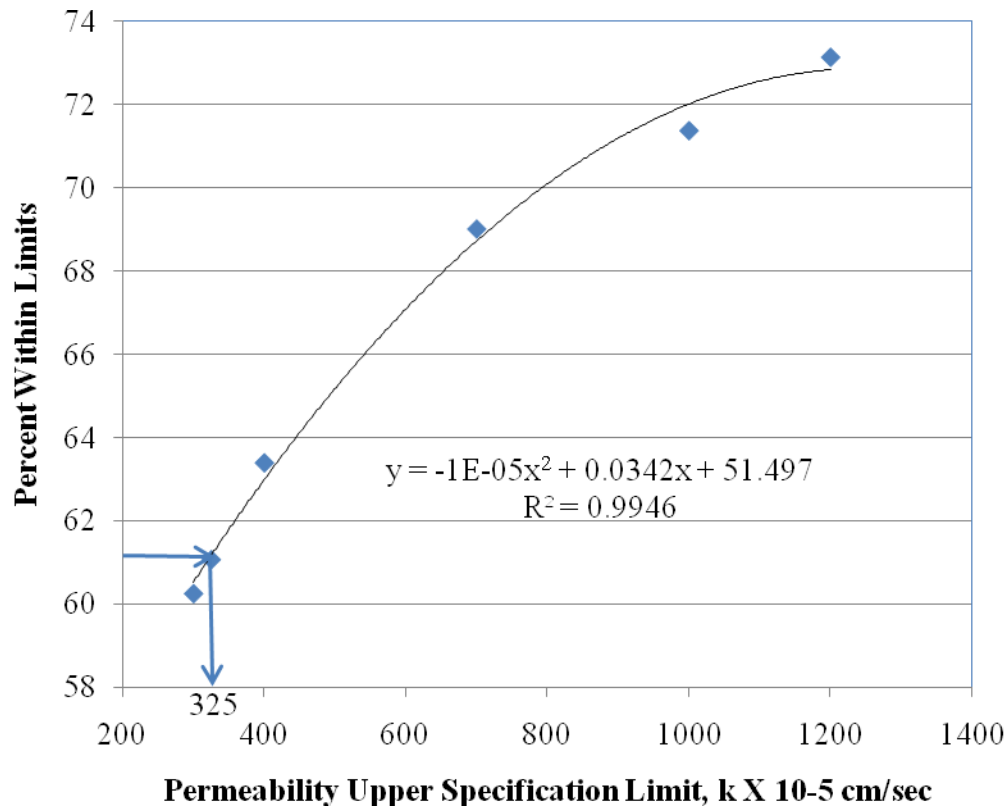


Figure 4.14 The Influence of Permeability Upper Specification Limit for the Kentucky Air Permeameter on Percent within Limit

Utilizing the previously determined 61.09 PWL outcome for the AASHTO T166 test method and applying this to determine the upper specification limit for the Kentucky Air Permeameter, a value of 325×10^{-5} cm/sec is obtained.

4.8.2 NCAT Permeameter Criteria

The same approach was used to identify the upper specification limit for the Kentucky Air Permeameter was applied to determine the corresponding value for the NCAT Permeameter.

The graphical representation of the effect of a varying upper specification limit and the effect on Percent Within Limit is presented in Figure 4.15. The corresponding upper specification criteria

for the NCAT Permeameter is 1560×10^{-5} cm/sec and would yield approximately the same 61.09 PWL as AASHTO T166. The R^2 value of 99.99 percent is excellent as shown in Figure 4.15.

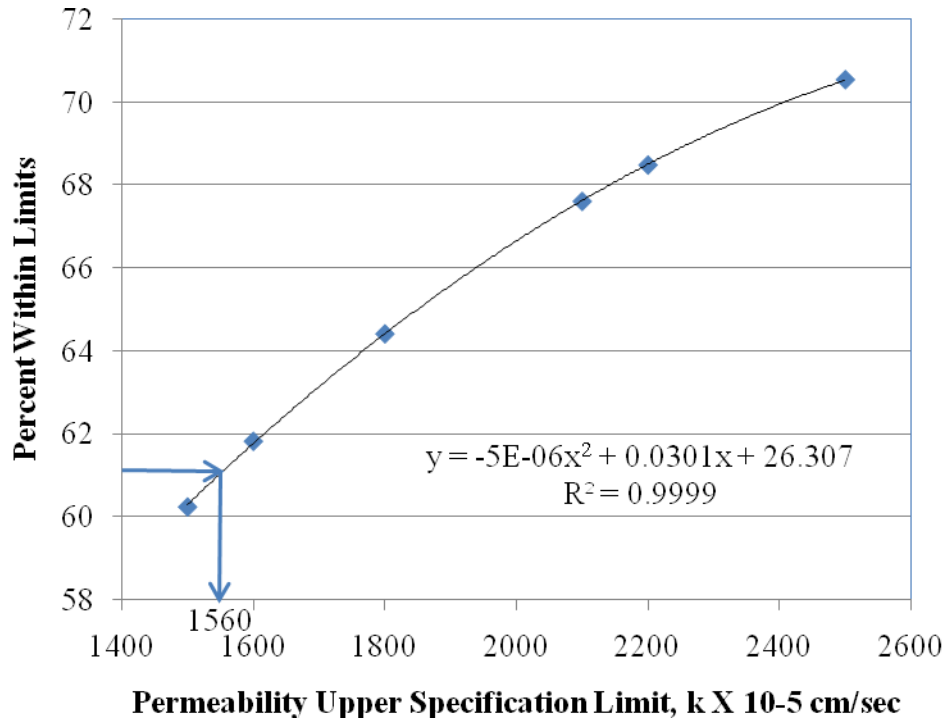


Figure 4.15 The Influence of Permeability Upper Specification Limit for the NCAT Permeameter on Percent within Limit

4.8.3 Karol-Warner Permeameter Criteria

The same approach was again used for determining the upper specification limit for the Karol-Warner Permeameter. The varying values of permeability and the corresponding values of PWL are shown in Figure 4.16. Again, the R^2 value for the data is very good at 99.61 percent. The upper specification limit identified with a corresponding 61.09 PWL is 530×10^{-5} cm/sec for the Karol-Warner Permeameter.

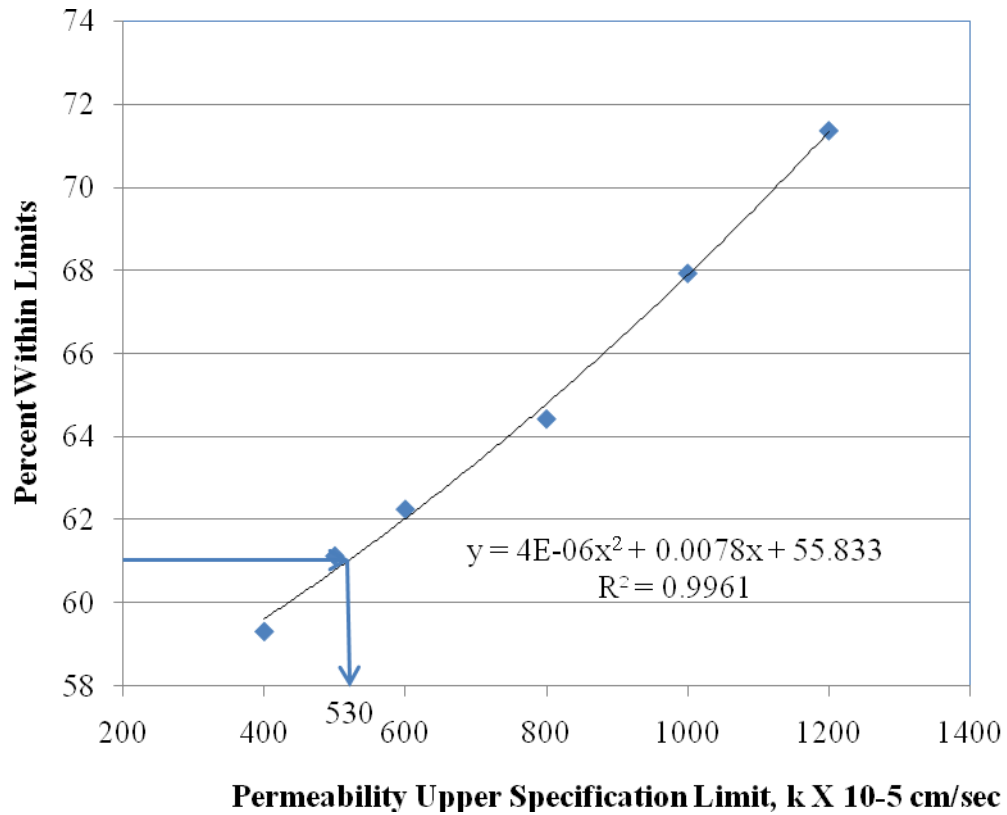


Figure 4.16 The Influence of Permeability Upper Specification Limit for the Karol-Warner Permeameter on Percent Within Limit

CHAPTER 5 FINDINGS AND RECOMMENDATIONS

5.1 Introduction

A design assumption used in developing a flexible (hot mix asphalt) structural pavement design is that it is essentially impermeable and that the water will drain across the pavement surface.

The literature review portion of this study clearly established the impetus for measuring density and/or air voids in assessing the quality of a hot mix asphalt pavement as it indirectly relates to the level of permeability of a pavement. However, current test methods such as AASHTO T166 for making density measurements and corresponding air void calculations identified limitations with regard to high permeable mixtures including open-graded mixtures and/or mixtures with a connected air void system. Recent developments in test equipment for measuring permeability of pavements has made it viable to consider measuring permeability and including it as a quality characteristic in assessing the quality of an HMA pavement.

5.2 Findings

The study identified the nominal maximum aggregate size (NMAS), the theoretical maximum specific gravity of the mixture (G_{mm}), and thickness of the pavement or core as statistically important factors influencing permeability and air voids. Generally, larger NMAS mixtures have an influence of lower permeability and lower air voids than smaller NMAS mixtures. Higher G_{mm} mixtures generally produced mixtures with higher permeability and higher air void values. Although statistically significant, the influence of thickness varied from one method/technology to another.

Beneficial findings from this research study identified the CoreLok as a viable method for determining the density and corresponding air voids of field samples and was comparable to

AASHTO T166. The CoreLok method did in general yield lower density values and thus higher air void values than AASHTO T166. The research study also found the PaveTracker did not have a strong relationship to neither AASHTO T166 nor the CoreLok methods for measuring density as well as the four methods of permeability testing conducted in this study.

5.3 Recommendations

This permeability study has identified three viable methods/devices for measuring permeability of hot mix asphalt. Two of the devices, a Kentucky Air Permeameter and an NCAT Permeameter, are field test devices that can be used on in-situ pavements. The third device, a Karol-Warner Permeameter, can be used to test field cores or laboratory prepared samples. The Kentucky and NCAT Permeameters are preferred for implementation over the Karol-Warner Permeameter as test results can be obtained on in-situ pavements and the results known in the same day the pavement is placed. Since the NCAT Permeameter is readily available commercially and is simpler in its operation, it is recommended over the Kentucky Air Permeameter. Thus, balancing availability of equipment and ease of use and timeliness of test results, the use of an NCAT Permeameter is recommended. The proposed test method for the NCAT Permeameter is contained in Appendix C which was used in this research study. Although the Karol-Warner Permeameter is not recommended for use in quality control/quality assurance testing, the strong relationship between the Karol-Warner and NCAT Permeameters illustrates that the Karol-Warner could be successfully used to identify mixtures during the laboratory mix design development that would meet construction specifications. The proposed test method for the Karol-Warner Permeameter is provided in Appendix D.

The specific criteria for using an NCAT Permeameter as part of a percent within limit specification is 1560×10^{-5} cm/sec for the upper specification limit and 0 cm/sec for the lower specification limit as identified in Chapter 4. Although the literature did not identify criteria for the NCAT Permeameter, 125×10^{-5} cm/sec average permeability criteria for the Karol-Warner device has been identified by Maupin at the Virginia Transportation Research Council (2001) as a criteria. A corresponding Karol-Warner Permeability criteria identified in this study is an upper specification limit of 530×10^{-5} cm/sec and 0 cm/sec for the lower specification criteria and results in an average permeability value of 265×10^{-5} cm/sec.

Supplemental training material for implementing the use of NCAT Permeameters in percent within limit specifications has been developed and is contained in Appendix E. Appendix E also contains training materials for using Karol-Warner Permeameters to test laboratory mixtures. It is important to point out that this study did not establish a relationship between permeability of laboratory compacted samples and field measurements.

5.4 Deliverables

The deliverables for the project are as follows:

1. A draft specification for permeability testing using an NCAT Permeameter as part of the Missouri Department of Transportation' construction quality control quality assurance testing utilizing percent within limit specifications;
2. A draft test criteria/method for permeability using a Karol-Warner Permeameter as part of the mix design evaluation process;
3. The test equipment for conducting permeability testing utilizing, namely an NCAT Permeameter, a Karol-Warner Permeameter, and a ROMUS Air Permeameter;

4. A database in an Excel spreadsheet that contains all of the data collected as part of the project, as well as majority of calculations and figures provided in this report; and
5. A draft training module for conducting permeability testing utilizing an NCAT and a Karol-Warner Permeameter.

LIST OF REFERENCES

- AASHTO T166 (2007). Standard Method of Test for Bulk Specific Gravity of Compacted Bituminous Mixes, Using Saturated Surface Dry Specimens. Standard Specifications for the Transportation Materials and Methods of Sampling and Testing, Part II Tests, Adopted by the American Association of State and Highway Transportation Officials.
- Allen, D. L., Schultz, D. B. Jr., and Willet, D. A. (2003). Evaluation of Non-Nuclear Density Gauges. Research Report KTC-03-24/FR115-01-1F. Kentucky Transportation Center, College of Engineering, University of Kentucky, Lexington, KY.
- Asphalt Contractor (1998). Pavement Quality Indicator is an Instant Success. Asphalt Contractor, Indianapolis, July, p. 78.
- ASTM, Standard D 6752, "Bulk Specific Gravity and Density of Compacted Asphalt Mixtures Using Automatic Vacuum Sealing Method," *Annual Book of ASTM Standards*, Vol. 4.03, ASTM International, West Conshohocken, PA, 2007.
- ASTM, Standard PS 129-01, "Standard Provisional Test Method for Measurement of Permeability of Bituminous Paving Mixtures Using a Flexible Wall Permeameter," *Annual Book of ASTM Standards*, Vol. 4.03, ASTM International, West Conshohocken, PA, 2004.
- Bhattacharjee, S., Mallick, R. B., and Mogawer, W. S. (2002). An Alternative Approach to Determination of Bulk Specific Gravity and Permeability of Hot Mix Asphalt (HMA). Unpublished Paper, Worcester Polytechnic Institute, Worcester, MA.
- Brown, E. R., Hainin, M. R., Cooley, A., and Hurley, G. (2004). Relationship of Air Voids, Lift Thickness, and Permeability in Hot Mix Asphalt Pavements. NCHRP Report 531 (NCHRP Project 9-27), TRB, National Research Council, Washington, D.C.
- Buchanan, M. S. and White, T. D. (2005). Hot Mix Asphalt Mix Design Evaluation Using the CoreLok Vacuum-Sealing Device. *Journal of Materials in Civil Engineering*, ASCE, Vol. 17, No. 2, pp. 137-142.
- Buchanan, M. S. (2000). An Evaluation of Selected Methods for Measuring the Bulk Specific Gravity of Compacted Hot Mix Asphalt (HMA) Mixes. Vol. 69, *Association of Asphalt Paving Technologist*, St. Paul, Minn., pp. 608-634.
- Burati, J. L., Jr. and Elzoghbi, G. B. (1987). Correlation of Nuclear Density Results with Core Densities. *Transportation Research Record* 1126, TRB, National Research Council, Washington, D.C., pp. 53-67.
- Choubane, B., Upsaw, P. B., Sholar, G. A., Page, G. C., and Musselman, J. A. (1999). Nuclear Density Readings and Core Densities. *Transportation Research Record* 1654, TRB, National Research Council, Washington, D.C., pp. 70-78.

- Cooley Jr., A. L., Prowell, B. D., Brown, E. R., Hall, K. D., Button, J., and Davis, R. (2002a). Issues Pertaining to the Permeability Characteristics of Coarse-Graded Superpave Mixes. *Asphalt Paving Technology: Association of Asphalt Paving Technologists-Proceedings of the Technical Sessions*, Vol. 71, pp. 1-29.
- Cooley, L. A., Powell, B. D., Hainin, M. R., Buchanan, M. S., and Harrington, J. (2002b). Bulk specific gravity round robin using the CoreLok vacuum sealing device. *National Center for Asphalt Technology (NCAT) Report 2002-11*, NCAT, Auburn, AL.
- Crouch, L. K., et al. (2002). Effect of Superpave gyratory compactor type on compacted hot mix asphalt HMA density. *Transportation Research Record 1813*, Transportation Research Board, National Research Council, Washington, D.C., pp. 39–46.
- Estakhri, C. K., Freeman, T. J., and Spiegelman, C. H. (2001). Density Evaluation of the Longitudinal Construction Joint of Hot Mix Asphalt Pavements. Report No. FHWA/TX-01/1757-1. Texas Transportation Institute, The Texas A&M University System, College Station, TX.
- Glagola, C. R. (2003). Pavement Quality Indicator: Investigator's Summary. Construction Innovation Forum, University of Florida, Gainesville, FL.
- Hall, K. D., Griffith, F. T., and Williams, S. G. (2001). Examination of Operator Variability for Selected Methods for Measuring Bulk Specific Gravity of Hot Mix Asphalt Concrete. *Transportation Research Record No. 1761*, TRB, Washington, D.C., pp. 81-85.
- Hausman, J. and Buttlar, W. (2002). Laboratory and Field Analysis of the TransTech Model 300 Pavement Quality Indicator (PQI) for Determining Asphalt Pavement Density. *Proceedings of the 2002 Transportation Research Board Annual Meeting*, Washington D.C.
- Henault, J. (2001). Field Evaluation of Non-nuclear Pavement Quality Indicator. Final Report. Report No. FHWA-CT-RD 2227-F-01-3. Connecticut Department of Transportation, Rocky Hill, CT.
- Hurley G.C., B. D. Prowell, and A. L. Cooley (2004). Evaluation of Non-Nuclear Density Measurement Devices for Determination of In-place Pavement Density. *Proceedings of the 2004 Transportation Research Board Annual Meeting*, Washington D.C.
- <http://www.in.gov/dot/div/testing/manuals/tests/aashto/166.pdf>, Indiana Department of Transportation, 2006.
- http://training.ce.washington.edu/WSDOT/Modules/05_mix_design/05-06.body.html, University of Washington, 2005.

- InstroTek (2001). Importance of Accurate Specific Gravity Measurements on Coarse SuperPave and SMA Asphalt Mixes. CoreLok Application Brief. InstroTek, Inc, Raleigh, NC.
- InstroTek (2003). CoreLok[®] Operator's Guide. Version 20. InstroTek, Inc., Raleigh, NC.
- Jaselskis, E. J., Han, H., Tan, L., and Grigas, J. (1998). Roller Mountable Asphalt Pavement Quality Indicator. Proceedings of Crossroads 2000: A Research Conference. Iowa State University, Ames, Iowa, pp. 192-194.
- Kanitpong, K., Benson, C. H., and Bahia, H. U., "Hydraulic Conductivity and Permeability of Laboratory Compacted Asphalt Mixtures," *Transp. Res. Rec.*, No. 1767, 2001, Paper No. 01-2997, pp. 25-32.
- Karlsson, T. (2002). Evaluation of the PQI: Pavement Quality Indicator. Swedish Roads Report. An SSIF-Financed Development Project. Project No. 1040. Skanska Asphalt and Technology Region, Rockneby, Sweden.
- Killingsworth, B. M. (2004). Quality Characteristics for Use with Performance Related Specifications for Hot Mix Asphalt. Research Results Digest 291, NCHRP Project 9-15, TRB, National Research Council, Washington, D.C.
- Landers, K. (2003). Pavement Testing Equipment. Better Roads. February.
- Malpass, G. and Khosla, P. N. (2002). Evaluation of Gamma Ray Technology for the Measurement of Bulk Specific Gravity of Compacted Asphalt Concrete Specimens. Asphalt Paving Technology: Association of Asphalt Paving Technologists-Proceedings of the Technical Sessions, Vol. 70, pp. 352-367.
- Maupin, G. W. (2000), Jr., "Asphalt Permeability Testing in Virginia," Transportation Research Board, *Transp. Res. Rec.*, No. 1723, Paper No. 1206, pp. 83-91.
- Maupin, G. W., Jr. (2001), "Asphalt Permeability Testing Specimen Preparation and Testing Variability," Transportation Research Board, *Transp. Res. Rec.*, No. 1767, Paper No. 2076, pp. 83-91.
- Maupin, G. W., Jr. (2005), "Asphalt Mix Design Method for Permeability," Transportation Research Board, Annual Meeting CD-ROM, pp. 1-20.
- Mitchell, T. D. (1984). Density Monitoring on Asphalt pavement. Better Roads, 54(12): p. 22-25.
- Mohammad, L. N., Herath, A., and Huang, B. (2003), "Evaluation of Permeability of Superpave Asphalt Mixtures," *Transp. Res. Rec.*, No. 1832, Paper No. 03-4464, pp. 50-58.
- Mohammad, L. N., Herath, A., Wu, Z., and Cooper, S. (2005), "A Comparative Study of Factors Influencing the Permeability of Hot Mix Asphalt Mixtures," Association of Asphalt Paving Technologists, Vol. 74E, pp. 1-25.

- Muench, S. T., Mahoney, J. P., and Pierce, L. M. (2002). Pavement Guide Interactive.
- NCHRP (1999). Pavement Quality Indicator. NCHRP-IDEA Concept Digest. Innovations Deserving Exploratory Analysis (IDEA) Projects 32 and 47. National Cooperative Highway Research Program, Transportation Research Board, Washington, D.C.
- NCHRP (2004). Quality Characteristics for Use with Performance-Related Specifications for Hot Mix Asphalt. NCHRP Research Results Digest 291. National Cooperative Highway Research Program, Transportation Research Board, Washington, D.C.
- NYDOT (2003). Non-Nuclear Density Gauge Data Collection for Hot Mix Asphalt. Materials Procedure No. NY 03-001. Materials Bureau, New York State Department of Transportation, Albany, NY.
- Padlo, P. T., Mahoney, J., Aultman-Hall, L., and Zinke, S. (2005). Correlation of Nuclear Density Readings with Cores Cut from Compacted Roadways. Report No. CT-2242-F-05-5, Connecticut Transportation Institute, University of Connecticut, Storrs, CT.
- Parker, F. and Hossain M. S. (1995). An Analysis of Hot Mix Asphalt Mat Density Measurement. *Journal of Testing and Evaluation*, ASTM, Vol. 23, No. 6, pp. 415-423.
- PaveTracker (2003). PaveTracker™ Model 2701: Manual of Operation and Instruction. Troxler Electronics Laboratory.
- PQI 301 (2002). Pavement Quality Indicator™ Model 301. Operator's Handbook. TransTech Systems, Inc. Schenectady, NY.
- PQI (2002). Pavement Quality Indicator™ (PQI) Model 301 Operation Handbook. TransTech Systems, Inc. Schenectady, NY
- PQI (2003). TransTech Systems' Pavement Quality Indicator™ (PQI). Technical Application Brief. TransTech Systems, Inc. Schenectady, NY.
- Prowell, B. D. and Dudley, M. C. (2002), "Evaluation of Measurement Techniques for Asphalt Pavement Density and Permeability," *Transp. Res. Rec.*, No. 1789, Paper No. 02-3907, pp. 36-45.
- Romero, P. (2000). Laboratory Evaluation of the PQI Model 300. Project Report. Multiple State Pooled Fund Study, DTFH61-00-P-00549, 2000.
- Romero, P. (2001). Field Evaluation of the PQI Model 300. Project Report. Multiple State Pooled Fund Study, DTFH61-00-P-00549, 2001.

- Romero, P. (2002). Evaluation of Non-Nuclear Gauges to Measure Density of Hot Mix Asphalt Pavements. Final Report. Pooled Fund Study. Department of Civil and Environmental Engineering, The University of Utah.
- Romero, P. and Kuhnaw, F. (2002). Evaluation of New Non-Nuclear Pavement Density Gauges Using Field Projects. Proceedings of the 2002 Transportation Research Board Annual Meeting, Washington D.C.
- Russell, J.; Bahia, H.U.; Kanitpong, K.; Croveti, J.; and Schmitt, R., "Effect of Pavement Thickness on Superpave Mix Permeability and Density," Wisconsin Highway Research Program SPR #0092-02-14c, 2005.
- Sanders, S. R., Rath, D., and Parker, F. (1994). Comparison of Nuclear and Core Pavement Density Measurement. *Journal of Testing and Evaluation*, ASTM, Vol. 120, No. 6, pp. 953-966.
- Sargand, S. M., Kim, S.-S., and Farrington, S. P. (2005). A Working Review of Available Non-Nuclear Equipment for Determining In-Place Density of Asphalt. Report No: FHWA/OH-2005/18. Executive Summary Report, Ohio Department of Transportation, Columbus, OH.
- Schmitt, R. (2004). Non-Nuclear Devices for Asphalt Pavement Density. Project ID: 0092-05-10. Research Progress Report for the Quarter Ending December 31, 2004. Wisconsin Department of Transportation, Madison, WI.
- Schmitt, R. (2005). Non-Nuclear Devices for Asphalt Pavement Density. Project ID: 0092-05-10. Research Progress Report for the Quarter Ending June 30, 2005. Wisconsin Department of Transportation, Madison, WI.
- Sebesta, S., Zeig, M., and Scullion, T. (2003). Evaluation of Non-Nuclear Density Gauges for HMAC: Year 1 Report. Report No. FHWA/TX-04/0-4577-1. Texas Transportation Institute, The Texas A&M University System, College Station, Texas.
- Sebesta, S., Scullion, T., and Liu, W. (2005). New Technologies for Assessing Quality of HMA Overlays. Project Summary Report. Project 0-4577: Further Development of NDT Devices to Identify Segregation in HMAC. Texas Transportation Institute, The Texas A&M University System, College Station, Texas.
- Sholar, G. A., Musselman, J. A., Page, G. C., and Upshaw, P. (1999). An Evaluation of Field Density Measuring Devices. Research Report FL/DOT/SMO/99-437. Florida Department of Transportation, Gainesville, FL.
- Shuler, S. (2005). Density Profiling of Asphalt Pavements. Final Report. Report No. CDOT-DTD-R-2005-6. Colorado Department of Transportation, Denver, CO.

- Stroup-Gardiner, M. and Newcomb, D. (2000). Statistical Evaluation of Nuclear Density Gauges Under Field Conditions. Transportation Research Record 1178, TRB, National Research Council, Washington, D.C., pp. 38-46.
- Sully-Miller (2000). A Summary of Operational Differences between Nuclear and Non-Nuclear Density Measuring Instruments. Prepared by Sully-Miller Contracting Company, Quality Control Department.
- Tarefder, R. A., Musharraf, Z., and Kenneth, H. (2004). Evaluating the CoreLok™ Measurement of Bulk Specific Gravity for Hot Mix Asphalt Samples. Journal of Testing and Evaluation, Vol. 30, No. 4, pp. 274-282.
- TransTech (2004). Assessment of Field Asphalt Density Gauge Data When Compared With Cores Processed According to AASHTO T-166. Technical Note 0302, Prepared by TransTech Systems Inc., Schenectady, NY.
- Williams, Brett A., Williams, R. Christopher, and Bausano, Jason P (2007). “Permeability Criterion Test for Method Selection in Determining the Bulk Specific Gravity of Hot Mix Asphalt”, *Journal of ASTM International, Volume 1, Issue 1*(published online).
- Williams, R. C. (1996). Measurement and Effects of Segregated Hot Mix Asphalt Pavement. Ph.D. Dissertation. Department of Civil Engineering, Purdue University, West Lafayette, IN.
- Williams, R.C., Duncan, G. Jr., and White, T. D. (1996). Hot Mix Asphalt Segregation: Measurement and Effects. Transportation Research Record No. 1543, TRB, Washington, D.C., pp. 97-105.
- Wen, H. and Bahia, H. (2004). Non-Nuclear Density Testing Devices and System to Evaluate In-Place Asphalt Pavement Density. Proposal for a Research Work Plan. Submitted to the Wisconsin Department of Transportation, Madison, WI.
- Wu, Z. (2005). In Situ Measurement of Density and Strength/Stiffness of HMA Mixtures. Presented at the Louisiana Asphalt Technology Conference, Shreveport, LA.
- Zha, J. (2000). *Revisions of California Test Method 11 for Nuclear Gage Calibration*. California Department of Transportation, Sacramento, pp. 1-18.

APPENDIX A

1. AASHTO T 166 Whole Model

- **Summary of Fit**

RSquare	0.312433
RSquare Adj	0.269072
Root Mean Square Error	2.428026
Mean of Response	7.487395
Observations (or Sum Wgts)	119

- **F-Ratio = 7.2055**

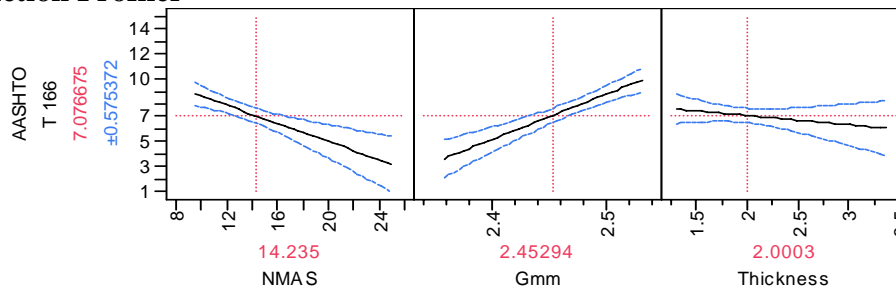
- **Parameter Estimates**

Term	Estimate	Std Error	t Ratio	Prob> t
<u>Intercept</u>	-75.49247	15.10219	-5.00	<.0001
<u>NMAS</u>	-0.362595	0.095157	-3.81	0.0002
<u>Gmm</u>	36.369706	6.354	5.72	<.0001
Thickness	-0.740898	0.76715	-0.97	0.3363
NMAS*Gmm	2.8387865	1.85929	1.53	0.1297
NMAS*Thickness	0.4234324	0.163873	2.58	0.0111
Gmm*Thickness	-47.87514	17.40914	-2.75	0.0070
NMAS*Gmm*Thickness	-0.108555	2.847875	-0.04	0.9697

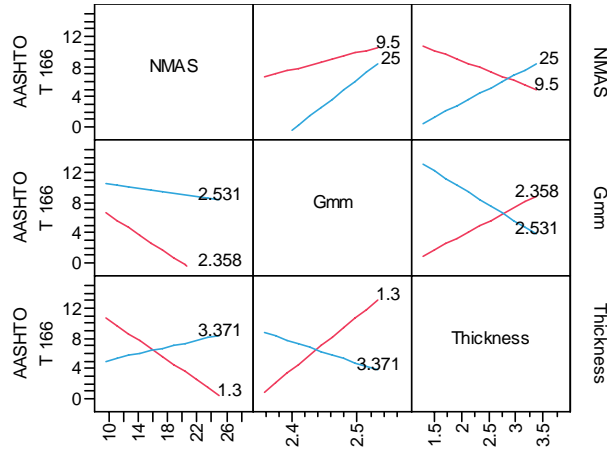
- **Prediction Expression**

$$\text{AASHTO T 166} = -75.4924 - 0.3625 \cdot \text{NMAS} + 36.3697 \cdot \text{Gmm} - 0.7409 \cdot \text{Thickness} + 2.8387 \cdot \text{NMAS} \cdot \text{Gmm} + 0.4234 \cdot \text{NMAS} \cdot \text{Thickness} - 47.8751 \cdot \text{Gmm} \cdot \text{Thickness} - 0.1085 \cdot \text{NMAS} \cdot \text{Gmm} \cdot \text{Thickness}$$

- **Prediction Profiler**



- **Interaction Profiles**



AASHTO T 166 Reduced Model

- **Summary of Fit**

RSquare	0.297958
RSquare Adj	0.266894
Root Mean Square Error	2.431641
Mean of Response	7.487395
Observations (or Sum Wgts)	119

- **F-Ratio = 9.5918**

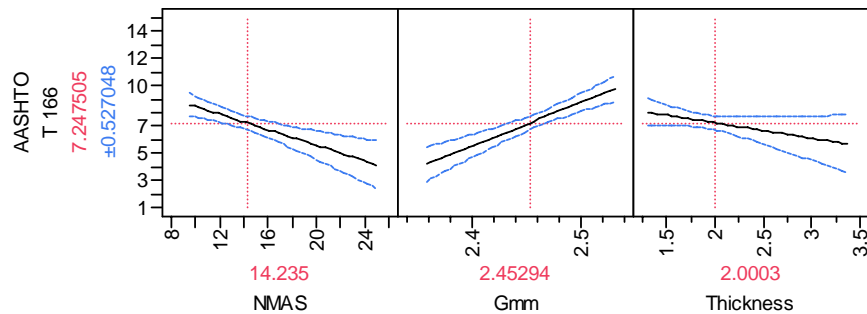
- **Parameter Estimates**

Term	Estimate	Std Error	t Ratio	Prob> t
<u>Intercept</u>	-64.96883	13.0655	-4.97	<.0001
<u>NMAAS</u>	-0.286715	0.075548	-3.80	0.0002
<u>Gmm</u>	32.032728	5.583369	5.74	<.0001
<u>Thickness</u>	-1.138147	0.722583	-1.58	0.1180
<u>NMAAS*Thickness</u>	0.4761477	0.135988	3.50	0.0007
<u>Gmm*Thickness</u>	-38.81741	16.24575	-2.39	0.0185

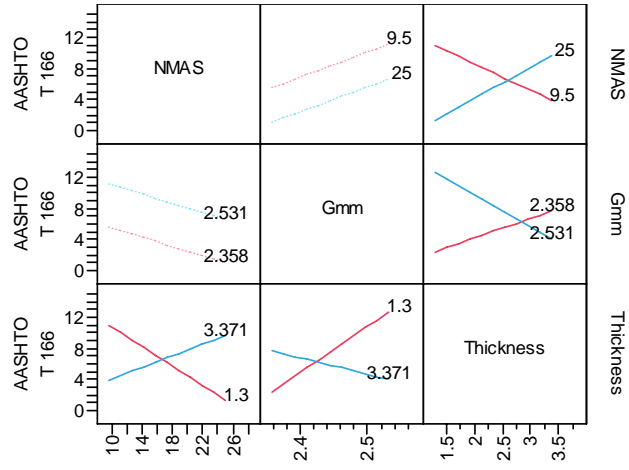
- **Prediction Expression**

$$\text{AASHTO T 166} = -64.9688 - 0.2867 \cdot \text{NMAAS} + 32.0327 \cdot \text{Gmm} - 1.1381 \cdot \text{Thickness} + 0.4761 \cdot \text{NMAAS} \cdot \text{Thickness} - 38.8174 \cdot \text{Gmm} \cdot \text{Thickness}$$

- **Prediction Profiler**



- Interaction Profiles



2. CoreLok Whole Model

- Summary of Fit

RSquare	0.340365
RSquare Adj	0.298767
Root Mean Square Error	2.521264
Mean of Response	8.114286
Observations (or Sum Wgts)	119

- F-Ratio = 8.1821

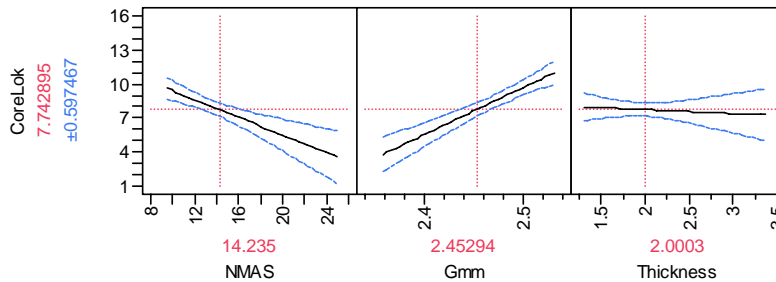
- Parameter Estimates

Term	Estimate	Std Error	t Ratio	Prob> t
Intercept	-87.79305	15.68212	-5.60	<.0001
NMAS	-0.390471	0.098811	-3.95	0.0001
Gmm	41.491211	6.597998	6.29	<.0001
Thickness	-0.340526	0.79661	-0.43	0.6699
NMAS*Gmm	3.9234807	1.930688	2.03	0.0445
NMAS*Thickness	0.3544815	0.170166	2.08	0.0395
Gmm*Thickness	-56.13152	18.07766	-3.11	0.0024
NMAS*Gmm*Thickness	-0.604853	2.957236	-0.20	0.8383

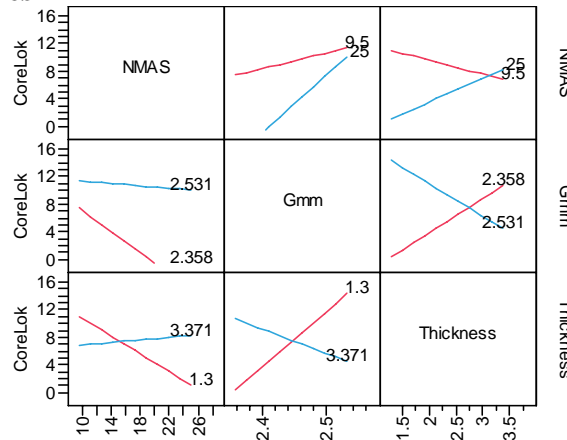
- Prediction Expression

$$\text{CoreLok} = -87.7930 - 0.3904 \cdot \text{NMAS} + 41.4912 \cdot \text{Gmm} - 0.3405 \cdot \text{Thickness} + 3.9234 \cdot \text{NMAS} \cdot \text{Gmm} + 0.3544 \cdot \text{NMAS} \cdot \text{Thickness} - 56.1315 \cdot \text{Gmm} \cdot \text{Thickness} - 0.6048 \cdot \text{NMAS} \cdot \text{Gmm} \cdot \text{Thickness}$$

- Prediction Profiler



- Interaction Profiles



CoreLok Reduced Model

- Summary of Fit**

RSquare	0.23573
RSquare Adj	0.208914
Root Mean Square Error	0.403637
Mean of Response	2.006292
Observations (or Sum Wgts)	119

- F-Ratio = 8.7905**

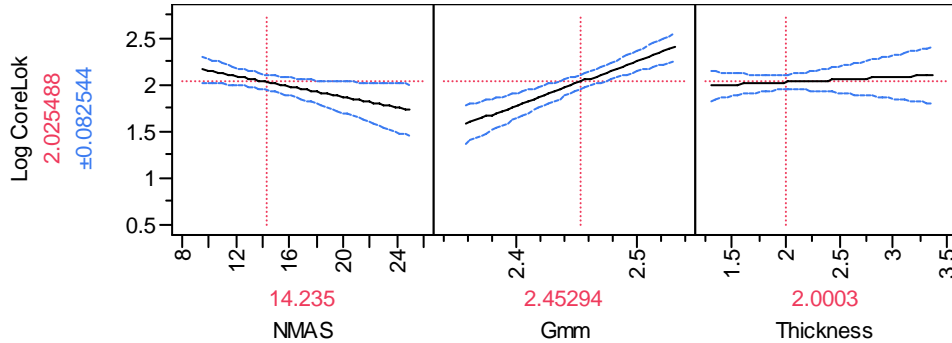
- Parameter Estimates**

Term	Estimate	Std Error	t Ratio	Prob> t
Intercept	-9.312326	2.164691	-4.30	<.0001
NMAS	-0.028036	0.012257	-2.29	0.0240
Gmm	4.7401947	0.920048	5.15	<.0001
Thickness	0.0547364	0.104543	0.52	0.6016
Gmm*Thickness	-2.274	2.270127	-1.00	0.3186

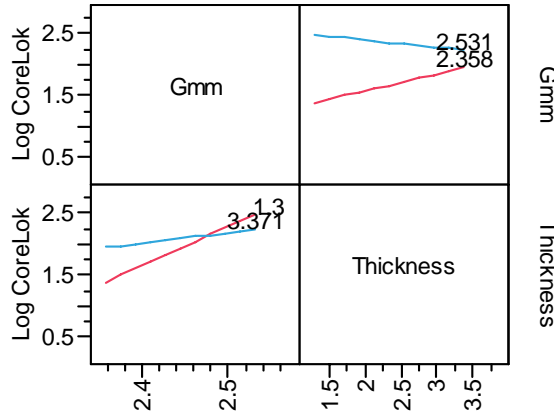
- Prediction Expression**

$$\text{CoreLok} = -9.3123 - 0.0280 \cdot \text{NMAS} + 4.7412 \cdot \text{Gmm} + 0.0547 \cdot \text{Thickness} - 2.2740 \cdot \text{Gmm} \cdot \text{Thickness}$$

- Prediction Profiler**



- Interaction Profiles**



3. Karol-Warner Whole Model

- Summary of Fit

RSquare	0.154044
RSquare Adj	0.081828
Root Mean Square Error	0.018846
Mean of Response	0.010055
Observations (or Sum Wgts)	90

- F-Ratio = 2.1331

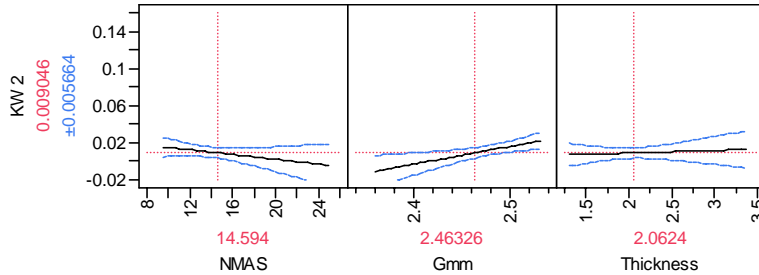
- Parameter Estimates

Term	Estimate	Std Error	t Ratio	Prob> t
Intercept	-0.446079	0.166563	-2.68	0.0089
NMAS	-0.001261	0.00101	-1.25	0.2152
Gmm	0.1899444	0.068796	2.76	0.0071
Thickness	0.002739	0.007304	0.37	0.7086
NMAS*Gmm	0.0445388	0.021844	2.04	0.0447
NMAS*Thickness	-0.000931	0.001381	-0.67	0.5021
Gmm*Thickness	-0.257429	0.190742	-1.35	0.1809
NMAS*Gmm*Thickness	-0.012916	0.031103	-0.42	0.6790

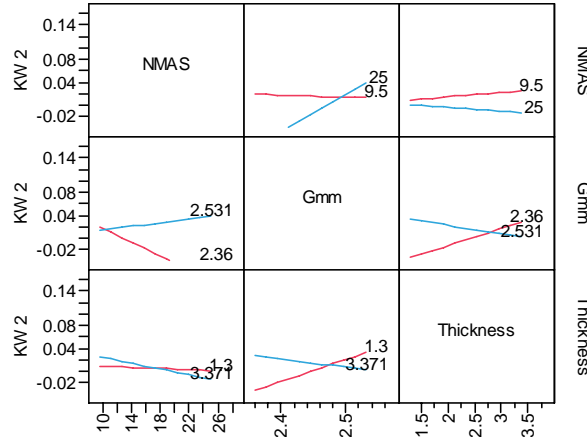
- Prediction Expression

$$\text{Karol-Warner} = -0.4460 - 0.0012 \cdot \text{NMAS} + 0.1899 \cdot \text{Gmm} + 0.0027 \cdot \text{Thickness} + 0.0445 \cdot \text{NMAS} \cdot \text{Gmm} - 0.0009 \cdot \text{NMAS} \cdot \text{Thickness} - 0.2574 \cdot \text{Gmm} \cdot \text{Thickness} - 0.0129 \cdot \text{NMAS} \cdot \text{Gmm} \cdot \text{Thickness}$$

- Prediction Profiler



- Interaction Profiles



Karol-Warner Reduced Model

- Summary of Fit**

RSquare	0.102716
RSquare Adj	0.06049
Root Mean Square Error	0.019064
Mean of Response	0.010055
Observations (or Sum Wgts)	90

- F-Ratio = 2.4326**

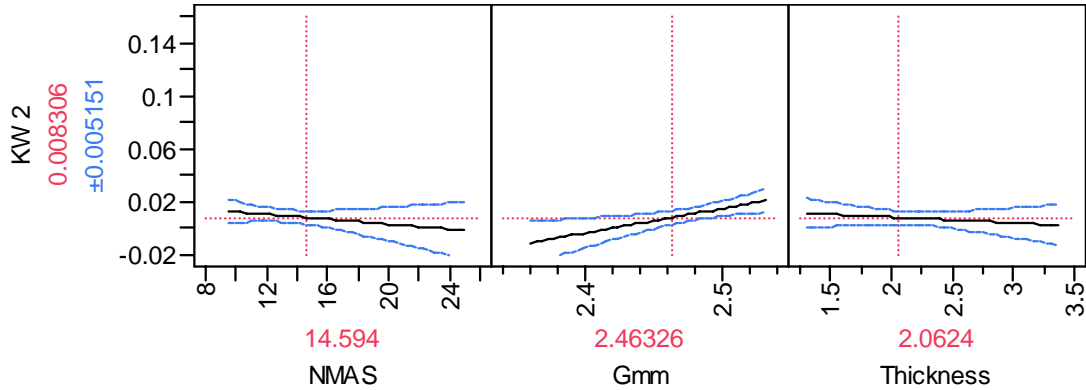
- Parameter Estimates**

Term	Estimate	Std Error	t Ratio	Prob> t
Intercept	-0.422737	0.159351	-2.65	0.0095
NMAS	-0.000929	0.000914	-1.02	0.3123
Gmm	0.1840848	0.066431	2.77	0.0069
Thickness	-0.004292	0.006007	-0.71	0.4769
Gmm*NMAS	0.0182458	0.017055	1.07	0.2877

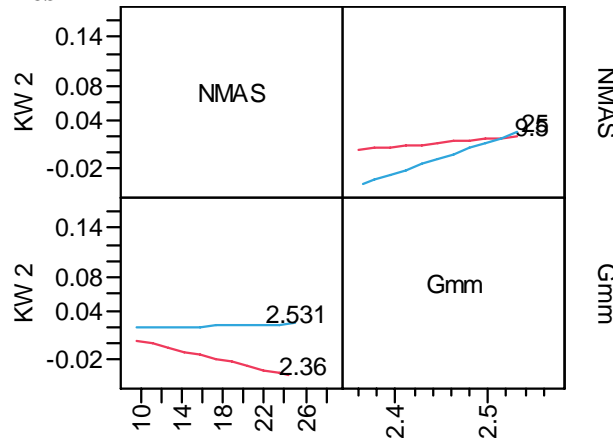
- Prediction Expression**

$$\text{Karol-Warner} = -0.4227 - 0.0009 \cdot \text{NMAS} + 0.1840 \cdot \text{Gmm} - 0.0043 \cdot \text{Thickness} + 0.0182 \cdot \text{NMAS} \cdot \text{Gmm}$$

- Prediction Profiler**



- Interaction Profiles**



4. KY Whole Model

- **Summary of Fit**

RSquare	0.102572
RSquare Adj	0.045978
Root Mean Square Error	0.017422
Mean of Response	0.006062
Observations (or Sum Wgts)	119

- **F-Ratio = 1.8124**

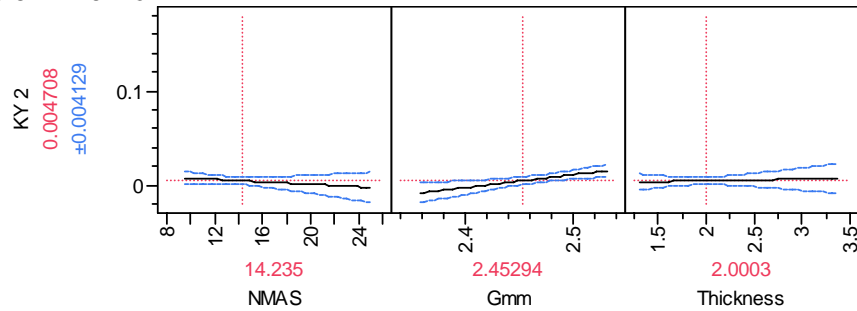
- **Parameter Estimates**

Term	Estimate	Std Error	t Ratio	Prob> t
<u>Intercept</u>	-0.325114	0.108365	-3.00	0.0033
<u>NMAS</u>	-0.000651	0.000683	-0.95	0.3422
<u>Gmm</u>	0.1368028	0.045593	3.00	0.0033
<u>Thickness</u>	0.0017615	0.005505	0.32	0.7496
<u>NMAS*Gmm</u>	0.0275907	0.013341	2.07	0.0410
<u>NMAS*Thickness</u>	-0.000315	0.001176	-0.27	0.7890
<u>Gmm*Thickness</u>	-0.138659	0.124918	-1.11	0.2694
<u>NMAS*Gmm*Thickness</u>	-0.009725	0.020435	-0.48	0.6351

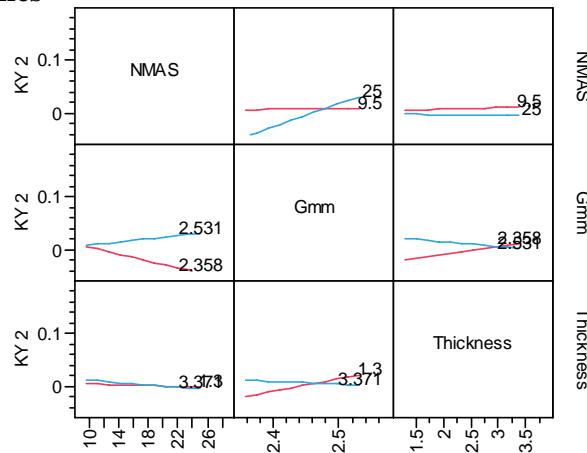
- **Prediction Expression**

$$\begin{aligned}
 \text{KY} = & -0.3251 - 0.0006 \cdot \text{NMAS} + 0.1368 \cdot \text{Gmm} + 0.0017 \cdot \text{Thickness} + \\
 & 0.0275 \cdot \text{NMAS} \cdot \text{Gmm} - 0.0003 \cdot \text{NMAS} \cdot \text{Thickness} - 0.1386 \cdot \text{Gmm} \cdot \text{Thickness} - \\
 & 0.0097 \cdot \text{NMAS} \cdot \text{Gmm} \cdot \text{Thickness}
 \end{aligned}$$

- **Prediction Profiler**



- **Interaction Profiles**



KY Reduced Model

- Summary of Fit**

RSquare	0.081681
RSquare Adj	0.04946
Root Mean Square Error	0.01739
Mean of Response	0.006062
Observations (or Sum Wgts)	119

- F-Ratio = 2.5350**

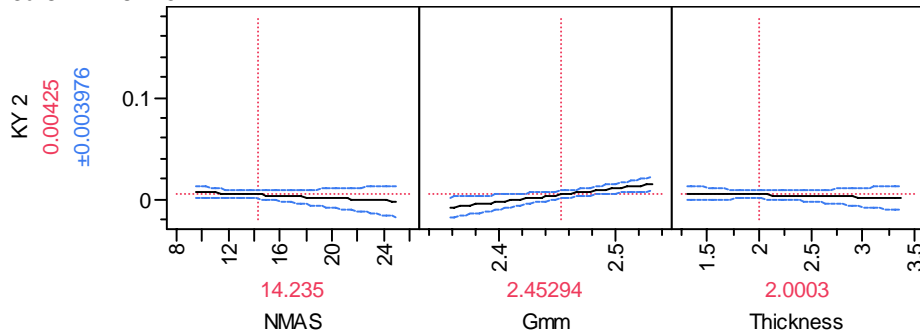
- Parameter Estimates**

Term	Estimate	Std Error	t Ratio	Prob> t
Intercept	-0.310264	0.105132	-2.95	0.0038
NMAS	-0.000578	0.000637	-0.91	0.3662
Gmm	0.1334952	0.0447	2.99	0.0035
Thickness	-0.002358	0.004358	-0.54	0.5895
NMAS*Gmm	0.0165114	0.011111	1.49	0.1400

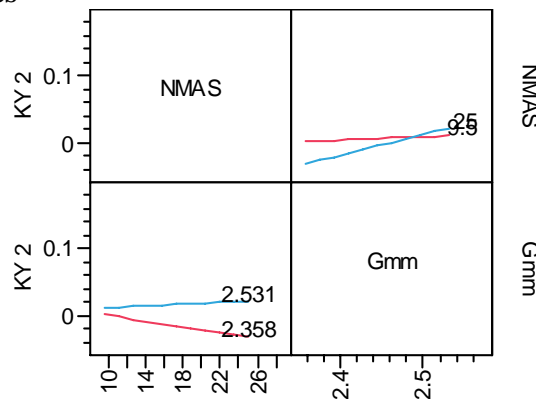
- Prediction Expression**

$$\text{KY} = -0.3102 - 0.0005 \cdot \text{NMAS} + 0.1334 \cdot \text{Gmm} - 0.0023 \cdot \text{Thickness} + 0.0165 \cdot \text{NMAS} \cdot \text{Gmm}$$

- Prediction Profiler**



- Interaction Profiles**



5. NCAT Whole Model

- Summary of Fit**

RSquare	0.18445
RSquare Adj	0.133019
Root Mean Square Error	0.016643
Mean of Response	0.010715
Observations (or Sum Wgts)	119

- F-Ratio = 3.5863**

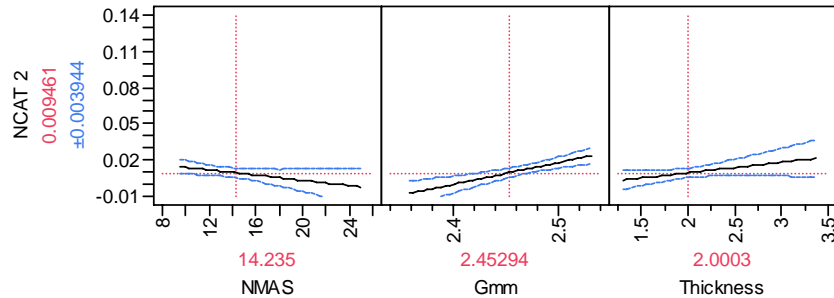
- Parameter Estimates**

Term	Estimate	Std Error	t Ratio	Prob> t
Intercept	-0.436108	0.103516	-4.21	<.0001
NMAS	-0.001091	0.000652	-1.67	0.0972
Gmm	0.1808937	0.043553	4.15	<.0001
Thickness	0.0086872	0.005258	1.65	0.1013
NMAS*Gmm	0.032087	0.012744	2.52	0.0132
NMAS*Thickness	-0.000405	0.001123	-0.36	0.7192
Gmm*Thickness	-0.179694	0.119329	-1.51	0.1349
NMAS*Gmm*Thickness	-0.020513	0.01952	-1.05	0.2956

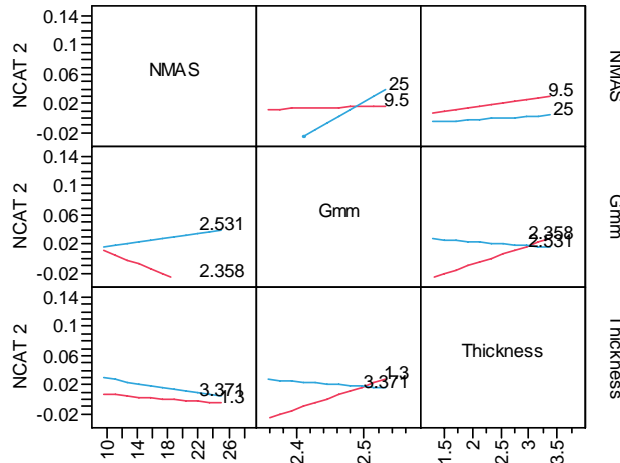
- Prediction Expression**

$$\text{NCAT} = -0.4361 - 0.0010 \cdot \text{NMAS} + 0.1809 \cdot \text{Gmm} + 0.0086 \cdot \text{Thickness} + 0.0321 \cdot \text{NMAS} \cdot \text{Gmm} - 0.0004 \cdot \text{NMAS} \cdot \text{Thickness} - 0.1797 \cdot \text{Gmm} \cdot \text{Thickness} - 0.0205 \cdot \text{NMAS} \cdot \text{Gmm} \cdot \text{Thickness}$$

- Prediction Profiler**



- Interaction Profiles**



NCAT Reduced Model

- **Summary of Fit**

RSquare	0.139939
RSquare Adj	0.109761
Root Mean Square Error	0.016864
Mean of Response	0.010715
Observations (or Sum Wgts)	119

- **F-Ratio = 4.6372**

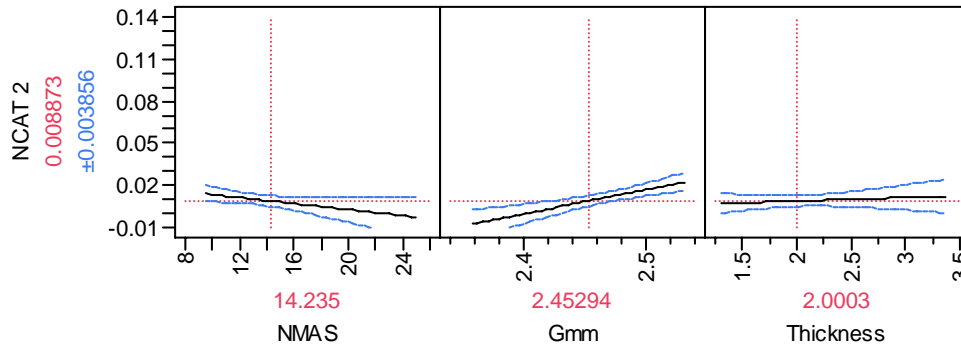
- **Parameter Estimates**

Term	Estimate	Std Error	t Ratio	Prob> t
Intercept	-0.405803	0.101952	-3.98	0.0001
NMAS	-0.001074	0.000617	-1.74	0.0847
Gmm	0.1732142	0.043348	4.00	0.0001
Thickness	0.0025375	0.004226	0.60	0.5494
Gmm*NMAS	0.0167896	0.010775	1.56	0.1219

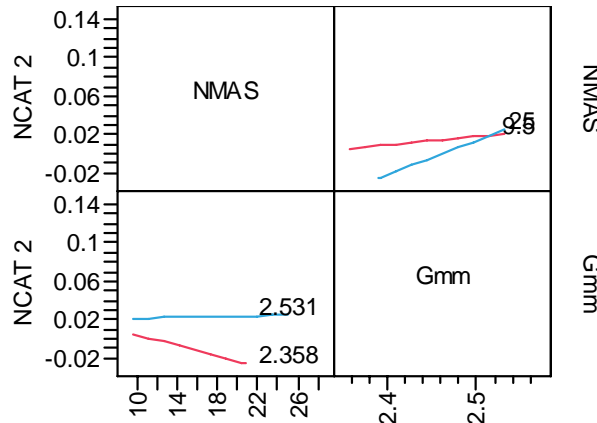
- **Prediction Expression**

$$\text{NCAT} = -0.4058 - 0.0010 \cdot \text{NMAS} + 0.1732 \cdot \text{Gmm} + 0.0025 \cdot \text{Thickness} + 0.0167 \cdot \text{NMAS} \cdot \text{Gmm}$$

- **Prediction Profiler**



- **Interaction Profiles**



6. PaveTracker Whole Model

- **Summary of Fit**

RSquare	0.451625
RSquare Adj	0.417043
Root Mean Square Error	3.359661
Mean of Response	8.078992
Observations (or Sum Wgts)	119

- **F-Ratio = 13.0595**

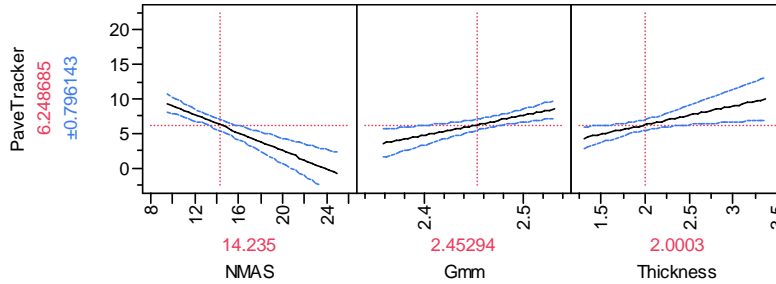
- **Parameter Estimates**

Term	Estimate	Std Error	t Ratio	Prob> t
<u>Intercept</u>	-59.94488	20.8969	-2.87	0.0049
<u>NMAS</u>	-0.658386	0.131669	-5.00	<.0001
<u>Gmm</u>	28.574133	8.792034	3.25	0.0015
<u>Thickness</u>	2.7371137	1.061507	2.58	0.0112
<u>NMAS*Gmm</u>	16.352122	2.572701	6.36	<.0001
<u>NMAS*Thickness</u>	-0.541555	0.226752	-2.39	0.0186
<u>Gmm*Thickness</u>	64.196878	24.08904	2.66	0.0088
<u>NMAS*Gmm*Thickness</u>	10.659184	3.940607	2.70	0.0079

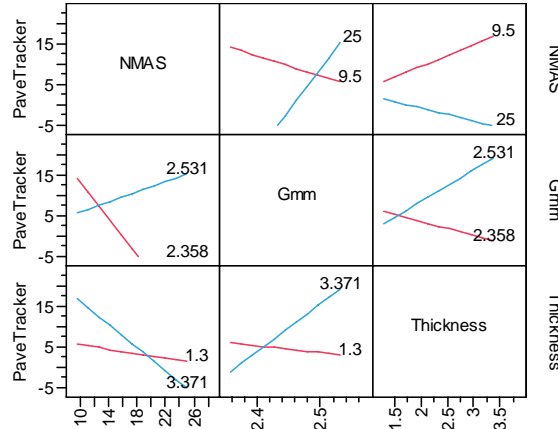
- **Prediction Expression**

$$\text{PaveTracker} = -59.9448 - 0.6583 \cdot \text{NMAS} + 28.5741 \cdot \text{Gmm} + 2.7371 \cdot \text{Thickness} + 16.3521 \cdot \text{NMAS} \cdot \text{Gmm} - 0.5415 \cdot \text{NMAS} \cdot \text{Thickness} + 64.1968 \cdot \text{Gmm} \cdot \text{Thickness} + 10.6592 \cdot \text{NMAS} \cdot \text{Gmm} \cdot \text{Thickness}$$

- **Prediction Profiler**



- **Interaction Profiles**



7. Romus Whole Model

- Summary of Fit

RSquare	0.634275
RSquare Adj	0.582028
Root Mean Square Error	0.000916
Mean of Response	0.002427
Observations (or Sum Wgts)	57

- F-Ratio = 12.1401

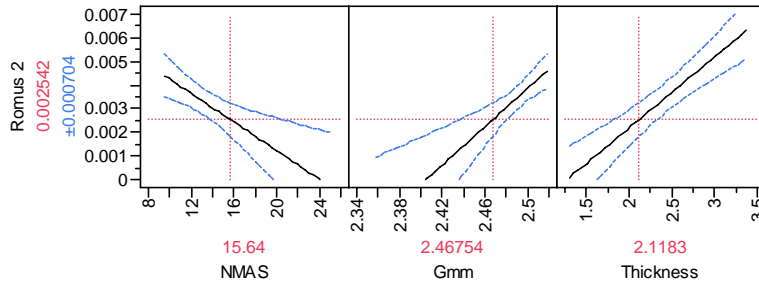
- Parameter Estimates

Term	Estimate	Std Error	t Ratio	Prob> t
Intercept	-0.09938	0.025726	-3.86	0.0003
NMAS	-0.000303	9.479e-5	-3.19	0.0025
Gmm	0.0406421	0.010509	3.87	0.0003
Thickness	0.003007	0.000536	5.61	<.0001
NMAS*Gmm	0.0017746	0.00145	1.22	0.2269
NMAS*Thickness	-0.000323	0.0001	-3.22	0.0023
Gmm*Thickness	0.0530934	0.013346	3.98	0.0002
NMAS*Gmm*Thickness	-0.00054	0.001779	-0.30	0.7627

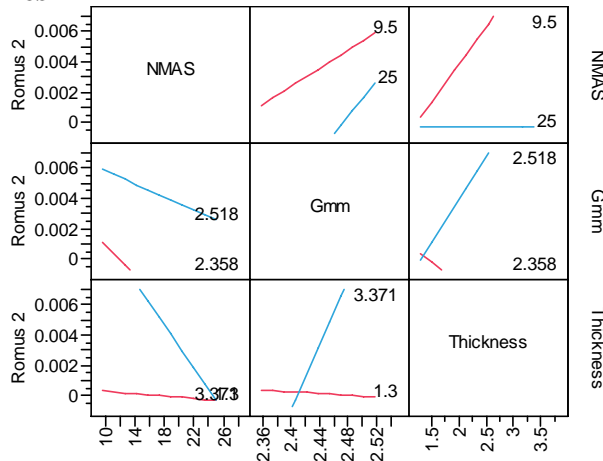
- Prediction Expression

$$\text{Romus} = -0.0994 - 0.0003 \cdot \text{NMAS} + 0.0406 \cdot \text{Gmm} + 0.0030 \cdot \text{Thickness} + 0.0017 \cdot \text{NMAS} \cdot \text{Gmm} - 0.0003 \cdot \text{NMAS} \cdot \text{Thickness} + 0.0531 \cdot \text{Gmm} \cdot \text{Thickness} - 0.0005 \cdot \text{NMAS} \cdot \text{Gmm} \cdot \text{Thickness}$$

- Prediction Profiler



- Interaction Profiles



Romus Reduced Model

- Summary of Fit**

RSquare	0.622967
RSquare Adj	0.586003
Root Mean Square Error	0.000912
Mean of Response	0.002427
Observations (or Sum Wgts)	57

- F-Ratio = 16.8533**

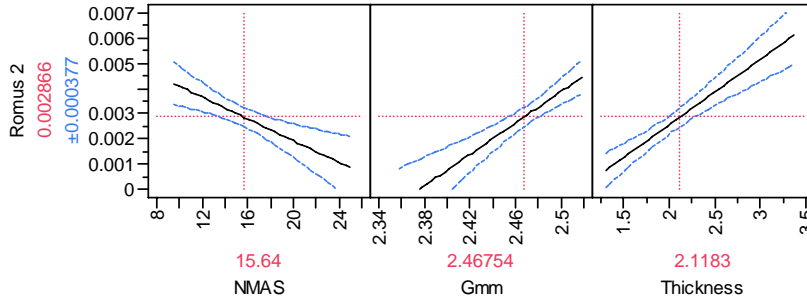
- Parameter Estimates**

Term	Estimate	Std Error	t Ratio	Prob> t
Intercept	-0.076467	0.014412	-5.31	<.0001
NMAS	-0.000216	0.000062	-3.48	0.0010
Gmm	0.0312754	0.005961	5.25	<.0001
Thickness	0.0026139	0.000413	6.33	<.0001
NMAS*Thickness	-0.000375	7.743e-5	-4.85	<.0001
Thickness*Gmm	0.0635884	0.010108	6.29	<.0001

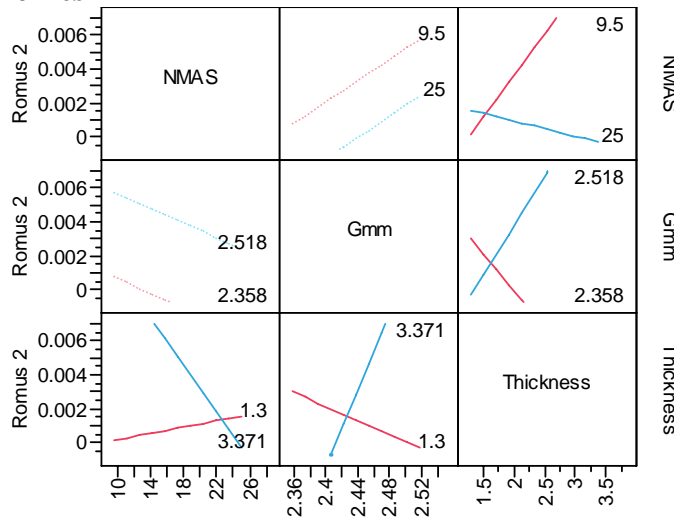
- Prediction Expression**

$$\text{Romus} = -0.0764 - 0.0002 \cdot \text{NMAS} + 0.0312 \cdot \text{Gmm} + 0.0026 \cdot \text{Thickness} - 0.0003 \cdot \text{NMAS} \cdot \text{Thickness} + 0.0635 \cdot \text{Gmm} \cdot \text{Thickness}$$

- Prediction Profiler**

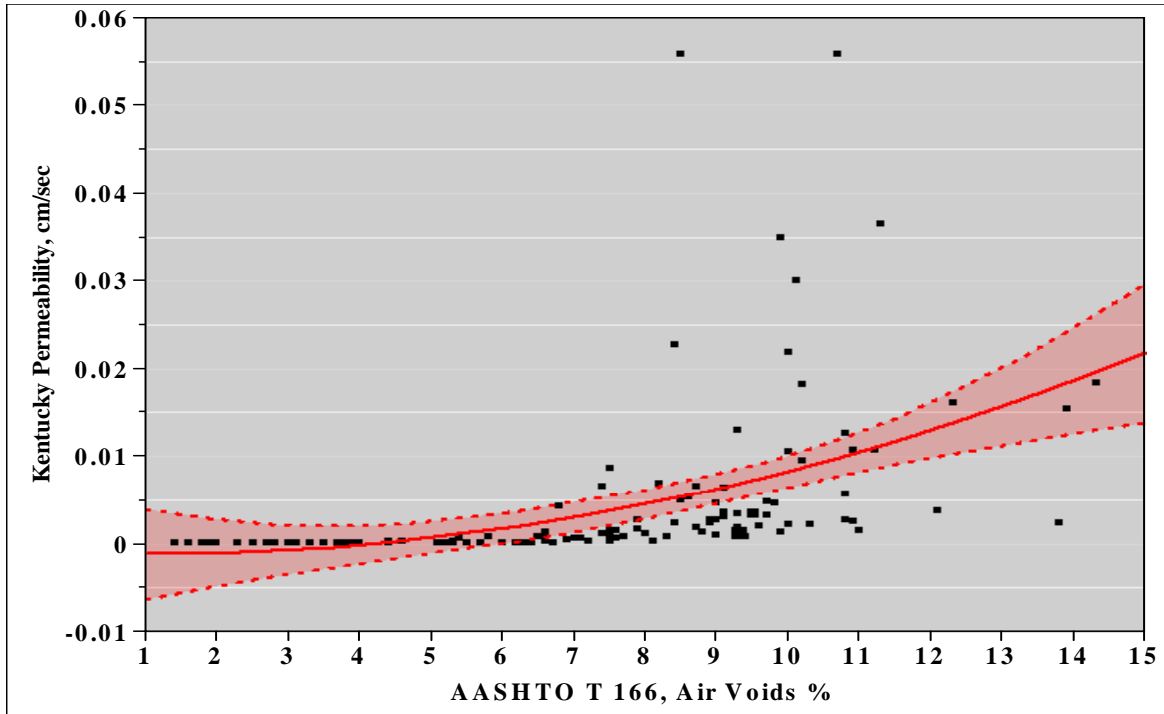


- Interaction Profiles**



APPENDIX B

1. Bivariate Fit of Kentucky Permeability By AASHTO T 166



- **Polynomial Fit**

$$KY = -0.007572 + 0.0015142 * \text{AASHTO T 166} + 0.0001176 * (\text{AASHTO T 166})^2$$

- **Summary of Fit**

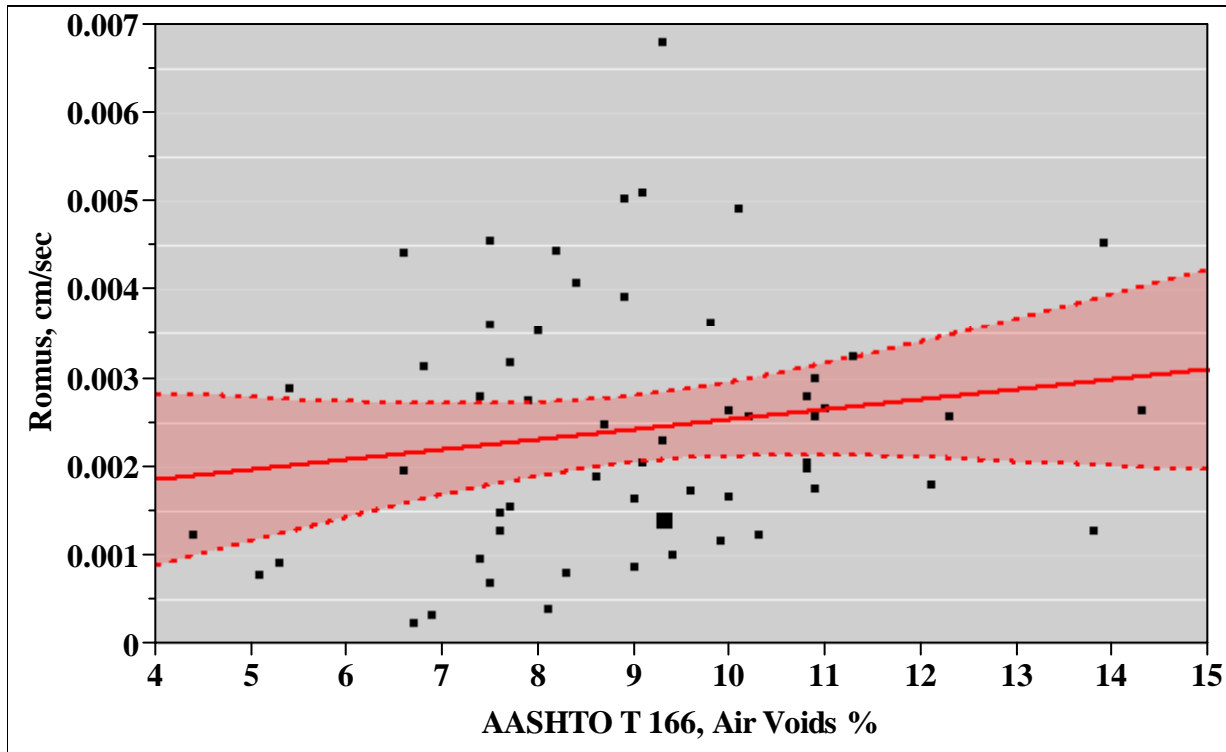
RSquare	0.201874
RSquare Adj	0.187994
Root Mean Square Error	0.008594
Mean of Response	0.004678
Observations (or Sum Wgts)	118

- **F-value = 14.5438**

- **Parameter Estimates**

Term	Estimate	Std Error	t Ratio	Prob> t
Intercept	-0.007572	0.002431	-3.11	0.0023
AASHTO T 166	0.0015142	0.000283	5.35	<.0001
(AASHTO T 166)²	0.0001176	7.936e-5	1.48	0.1412

2. Bivariate Fit of Romus By AASHTO T 166



- **Linear Fit**

$$\text{Romus} = 0.0014105 + 0.000113 * \text{AASHTO T 166}$$

- **Summary of Fit**

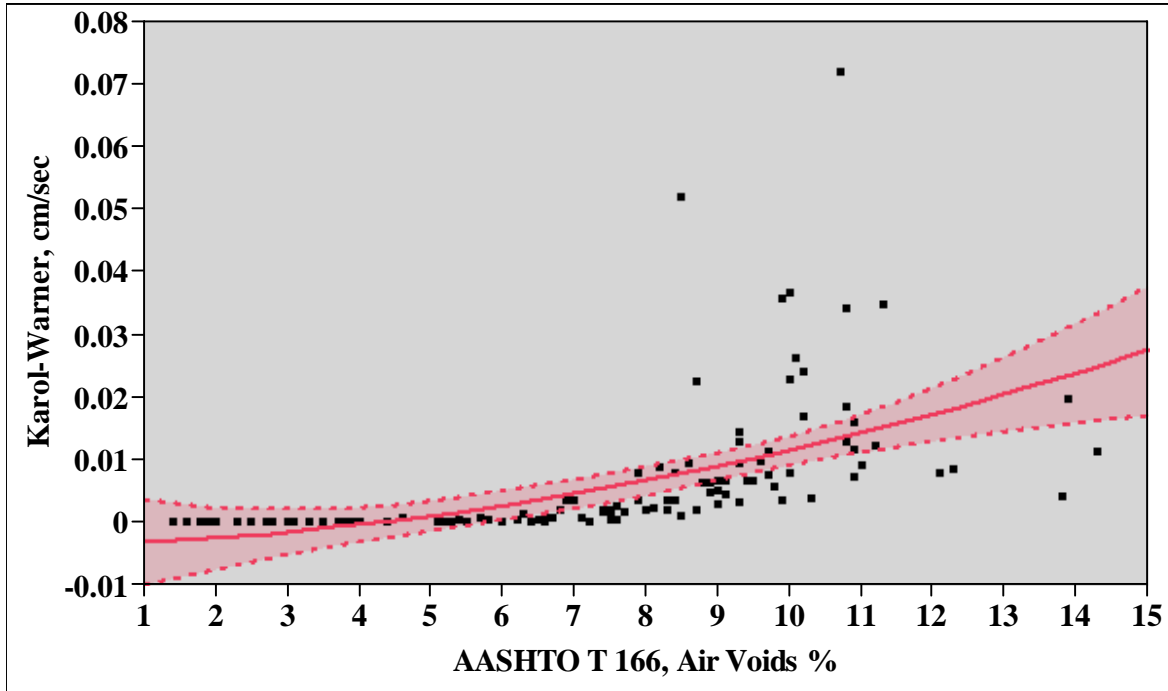
RSquare	0.028033
RSquare Adj	0.010361
Root Mean Square Error	0.00141
Mean of Response	0.002427
Observations (or Sum Wgts)	57

- **F-value = 1.5863**

- **Parameter Estimates**

Term	Estimate	Std Error	t Ratio	Prob> t
Intercept	0.0014105	0.000828	1.70	0.0943
AASHTO T 166	0.000113	8.97e-5	1.26	0.2132

3. Bivariate Fit of Karol-Warner By AASHTO T 166



- **Polynomial Fit**

$$\text{Karol-Warner} = -0.010001 + 0.0020792 * \text{AASHTO T 166} + 0.0001129 * (\text{AASHTO T 166})^2$$

- **Summary of Fit**

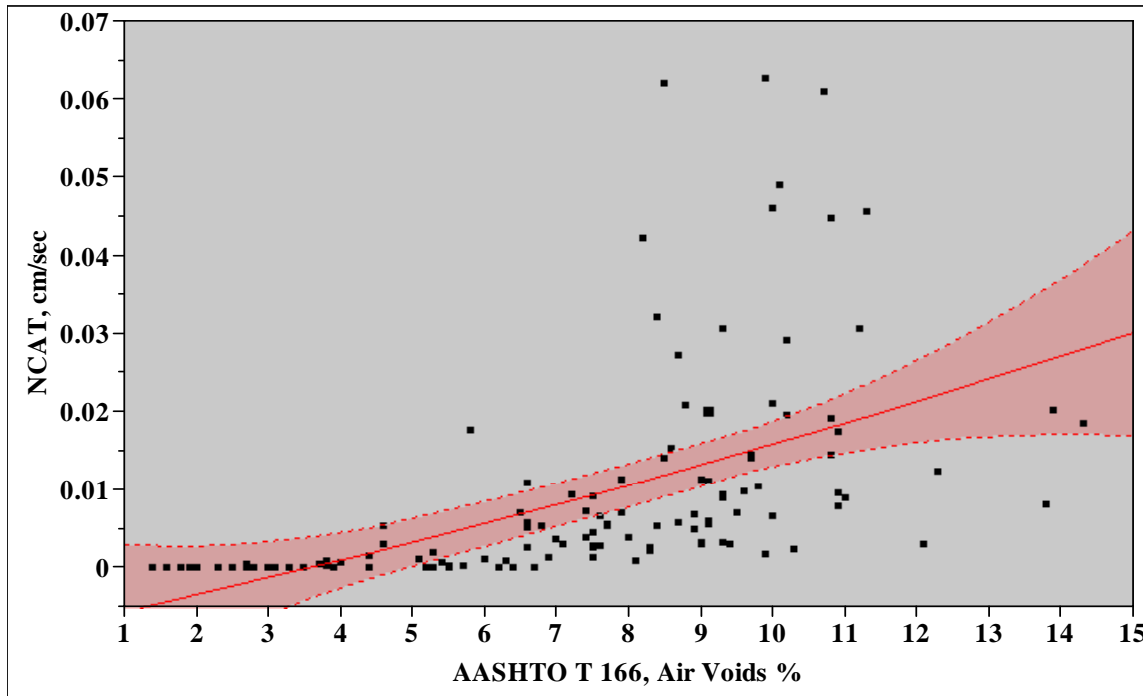
RSquare	0.282539
RSquare Adj	0.26984
Root Mean Square Error	0.00944
Mean of Response	0.006447
Observations (or Sum Wgts)	116

- **F-value = 22.2499**

- **Parameter Estimates**

Term	Estimate	Std Error	t Ratio	Prob> t
Intercept	-0.010001	0.002687	-3.72	0.0003
AASHTO T 166	0.0020792	0.000312	6.67	<.0001
(AASHTO T 166)²	0.0001129	8.736e-5	1.29	0.1987

4. Bivariate Fit of NCAT By AASHTO T 166



- **Polynomial Fit**

$$\text{NCAT} = -0.009336 + 0.0025087 * \text{AASHTO T 166} + 0.000033 * (\text{AASHTO T 166})^2$$

- **Summary of Fit**

RSquare	0.265619
RSquare Adj	0.252847
Root Mean Square Error	0.011891
Mean of Response	0.009663
Observations (or Sum Wgts)	118

- **F-value = 20.7972**

- **Parameter Estimates**

Term	Estimate	Std Error	t Ratio	Prob> t
Intercept	-0.009336	0.003364	-2.77	0.0064
AASHTO T 166	0.0025087	0.000391	6.41	<.0001
(AASHTO T 166)²	0.000033	0.00011	0.30	0.7643

APPENDIX C

NCAT Permeameter Test Method

	GILSON COMPANY, INC. <i>Your Source for Testing Solutions Since 1939</i>	AP-1B Asphalt Field Permeameter
Operating Instructions		

The preliminary instrument design and test protocol for in-situ testing of asphalt permeability was developed by the National Center for Asphalt Technology (NCAT). The Gilson AP-1B Permeameter is based upon the NCAT design.

Theory of operation:

The test is based on the falling head principle of permeability. The coefficient of permeability is calculated as follows:

$$K = (a L / At) \ln (h_1/h_2)$$

Where:

- k = coefficient of permeability.
- a = inside cross-sectional area of standpipe, cm²
(Varies depending on tier used for testing; see listed values in Calculation section.)
- L = length of the sample, cm (thickness of the asphalt mat).
- A = cross-sectional area of permeameter through which water can penetrate the pavement (test area), cm².
- t = Elapsed time between h₁ and h₂.
- h₁ = Initial head, cm.
- h₂ = Final head, cm.

Principle of operation:

The Gilson AP-1B Asphalt Permeameter apparatus is used to conduct the test.

The Permeameter assembly consists of up to 4 segments, or "tiers" of clear plastic in 2 sections. Two different top sections are included and are designed to increase the versatility and measurable permeability range of the unit. The standard top section consists of one nominal 3/4" (19mm) id tube and one nominal 1-3/4" (44.5mm) id tube. The alternate top section is comprised of one long 1-3/4" (44.5mm) id tube to allow extended test times in moderately permeable pavements. Using this section also allows faster filling of the permeameter with water when testing open-graded pavements, which may be very permeable.

In use, the apparatus is seated on the selected test site using the Moldable Sealant, filled with water to a beginning mark and the start time is recorded. Rate of outflow may be observed as water level drops past graduated marks on the side of the tiers. To keep equation parameter "a" constant, the operator must select one of the four different diameter tiers to track the falling head over a period of time. The choice of which tier to use depends upon the rate at which the head is falling after the apparatus is filled with water. Very permeable pavements will necessitate selection of one of the larger diameter tiers because the head will fall too quickly for accurate observation in the smaller diameter tiers.

Test sequence:

Select an area approximately one foot square of unsealed asphalt mat of known thickness (equation value "L"). Brush the selected test area clean of loose stone, dust and debris to enable a watertight seal between the AP-1 base, Moldable Sealant and asphalt surface.

Invert and secure the Permeameter vessel for placement of the APA-22 Moldable Sealant. The bottom of the base plate must be clean and free of residue to promote a watertight seal. An adhesive-backed rubber gasket has been placed on the bottom of the base plate to insure a well-defined test area for the permeability test. Replacements may be ordered as APA-19 Permeability Vessel Gaskets. The Moldable Sealant is intended to be formed around the outside diameter of this gasket.

When properly prepared for a test, the finished dimensions of the Moldable Sealant on the base plate of the Permeameter vessel should be approximately 3" (75mm) around the outside circumference of the Rubber Gasket and about 3/8" to 1/2" (9.5 to 12.5mm) uniform thickness. This takes approximately 1-1/4 lb (0.6kg) of sealant to form. The sealant is easily worked with the hands and will conform to the asphalt surface when seated. There is no need to have it exceptionally smooth, although some care should be taken in forming it uniformly against the outside edge of the Rubber

Gasket. Extra Moldable sealant may be added, if needed, by simply molding it into place with the fingers.

Once the Moldable Sealant is properly installed, turn the Permeameter right side up and place on the clean, prepared test area. Use gentle, uniform foot pressure around the perimeter of the base to seat the Permeameter Vessel. Gently step on opposite corners of the base plate, repeat on the remaining corners. Slowly and gently, step around the perimeter of the base without twisting it to force the sealant into the asphalt mat. Observe the area inside the Rubber Gasket to see that sealant material has not been forced into the test area. Place a 5 lb (2.3kg) weight on each side of the Permeameter base. This compensates for the head pressure exerted by the water column. Without these weights, the water pressure can break the seal.

After the Permeameter is sealed to the pavement surface, place a thin layer of Moldable Sealant material on the bottom rim of either the Standard or Alternate Top Section, and seat it onto the Base Section. Insert the filling tube assembly into the assembled vessel all the way to the bottom. Fill the Vessel completely with water at a steady rate. As the water level nears the top, continue filling while the tube is being withdrawn. Careful filling insures a minimum of bubbles and entrapped air in the water column. The Permeameter Vessel holds about a gallon (3.9L) of water in the standard configuration.

Observe the rate at which the water level in the Permeameter Vessel drops. Select a tier for recording rate of flow where the rate of fall is slow enough for accurate observation, but fast enough for timely completion of the test. Test times vary greatly depending on mix gradation and density, but should generally not exceed about five minutes. Make note of a starting time and a starting height for the falling head. The elapsed time is the value of "t" in the equation. The starting and ending head height are the equation values "h₁" and "h₂" respectively.

Upon completion of the test, gently lift one corner of the base plate to break the seal and allow the water to drain away.

Caution: Do not apply force to the side of the Vessel to break the seal. The Permeameter Vessel will break.

The Moldable Sealant can be reused, but its sealing effectiveness may be diminished over time. Debris must

be carefully cleaned out and excess water removed from the material before reuse.

Calculation:

Use the test values obtained to calculate the equation for coefficient of permeability as shown previously.

Area Values of "a" for each tier:

Tier 1 (Top)= area "a" = 2.85 cm²

Tier 2* = area "a" = 15.52 cm²

Tier 3 = area "a" = 38.32 cm²

Tier 4 (Bottom)= area "a" = 167.53 cm²

Pavement Test Area (value "A" in equation) = 214 cm²

* This value also applies to the 1-3/4" (44.5mm) id alternate top section.

NOTE: Values given are typical tier areas and are suitable for most determinations. If desired, the inside diameter of the tiers can be individually measured and the areas calculated.

General Notes

Cleaning:

The Permeameter Vessel may be gently cleaned with water and conventional dish-washing detergents. Over time, the Vessel material may become scratched or clouded, but should remain viable for use as long as the water level can be accurately observed.

Temperature:

At low temperatures, the Moldable Sealant will become less pliable and may not form a watertight seal. This should be taken into account for air and test surface temperatures below room temperature. Warming of the test surface or sealant may allow sealing at lower temperatures.

Water Leaks:

In most cases, it is fairly easy to obtain a good seal for the Permeameter Vessel on finished surfaces of asphalt pavement. Problems can occur if there is insufficient area or thickness of the Moldable Sealant, if the asphalt surface is unusually rough, or if the test time is

unusually long. Some open-graded mixes can be particularly difficult to seal. Selecting a different test site and using extra care in the seating process often overcomes these problems, although there is no guarantee that every attempted test will be successful.

A stream of water coming from the base is a leak, which affects the permeability test results. The test should be redone if a leak occurs. During unusually long test periods, condensate has been observed to form on the bottom of the base plate. This condensate comes from water vapor permeating outward through the asphalt and is not a sealant leak.

Accessories:

The following accessories are available from Gilson for your Asphalt Permeameter Kit:

APA-11B: Permeameter Vessel, complete. Includes Base and Standard Top Sections.

APA-16: Base Section only.

APA-17: Standard Top Section only.

APA-18: Alternate Top Section only.

APA-22: Moldable Sealant in 5 lb (2.3kg) plastic tubs. Enough for about 4 seals.

APA-19: Permeameter Vessel Gaskets. Adhesive-backed rubber gaskets for the bottom of the Permeameter Vessel.

APA-5: Whisk Broom for preparation of test site.

APA-7B: Carrying Case. Protects the Permeameter from damage during transport.

APA-9: Base Weights. Four 5 lb Weights. Required to counter the water head displacement force.

APPENDIX D

Karol-Warner Permeameter Test Method



Designation: PS 129 – 01

Standard Provisional Test Method for Measurement of Permeability of Bituminous Paving Mixtures Using a Flexible Wall Permeameter¹

This provisional standard is issued under the fixed designation PS 129; the number immediately following the designation indicates the year of original adoption.

1. Scope

1.1 This provisional test method covers procedures for determining the relative permeability (also referred to as *coefficient of permeability*) of water saturated laboratory compacted specimens or field cores of compacted bituminous paving mixtures using a flexible wall permeameter.

1.2 The values stated in SI units are to be regarded as the standard. The values given in parentheses are for information only.

1.3 Provisional standards² achieve limited consensus through approval of the sponsoring subcommittee.

1.4 This standard is being developed as a provisional standard because the subcommittee feels that the issuance and subsequent usage of this standard method will be critical in the refinement of the standard in the future.

1.5 *This provisional standard does not purport to address all of the safety concerns, if any, associated with its use. It is the responsibility of the user of this standard to establish appropriate safety and health practices and determine the applicability of regulatory requirements prior to use.*

2. Referenced Documents

2.1 ASTM Standards:

D 8 Terminology Relating to Materials for Roads and Pavements³

D 1188 Test Method for Bulk Specific Gravity and Density of Compacted Bituminous Mixtures Using Coated Samples³

D 2041 Test Method for Theoretical Maximum Specific Gravity and Density of Bituminous Paving Mixtures³

D 2726 Test Method for Bulk Specific Gravity and Density of Non-Absorptive Compacted Bituminous Mixtures³

D 4867/D 4867M Test Method for Effect of Moisture on Asphalt Concrete Paving Mixtures³

2.2 AASHTO Standards:

TP 4 Preparing and Determining the Density of Hot-Mix Asphalt (HMA) Specimens by Means of the Superpave

Gyratory Compactor⁴

T 283 Resistance of Compacted Bituminous Mixture to Moisture Induced Damage⁴

3. Terminology

3.1 Definitions:

3.1.1 Refer to Terminology D 8 for definitions of terms used in this provisional test method.

4. Summary of Test Method

4.1 A falling head permeability test is used to determine the rate of flow of water through a saturated specimen. Water from a graduated standpipe is allowed to flow through the saturated bituminous paving mixture specimen and the time interval to reach a known change in head is recorded. The coefficient of water permeability of the compacted paving mixture is then determined based on Darcy's Law.

5. Significance and Use

5.1 This provisional test method provides an indication of the water permeability of water-saturated samples. It applies to one-dimensional, laminar flow of water.

5.2 It is assumed that Darcy's Law is valid and that the permeability is essentially unaffected by hydraulic gradient. The validity of Darcy's Law may be evaluated by measuring the hydraulic conductivity of the specimen at three hydraulic gradients. If all measured values are similar (that is, within approximately 25 %), then Darcy's Law may be taken as valid.

6. Apparatus

6.1 *Permeameter*—See Fig. 1. The device shall meet the following requirements:

6.1.1 A graduated cylinder, having an inner diameter of 31.75 ± 0.50 mm (1.25 ± 0.02 in.), graduated in millimeters and capable of dispensing 500 ml of water.

6.1.2 A sealing tube using a flexible latex membrane 0.635 mm (0.025 in.) thick and capable of confining asphalt concrete specimens up to 152.4 mm (6.000 in.) in diameter and 80.0 mm (3.15 in.) in height.

6.1.3 A cap assembly for supporting the graduated cylinder and expanding an o-ring against the sealing tube. The opening in the cap shall be of the same diameter as the outer diameter

¹ This provisional test method is under the jurisdiction of ASTM Committee D04 on Road and Paving Materials and is the direct responsibility of Subcommittee D04.23 on Plant-Mixed Bituminous Surfaces and Bases.

Current edition approved April 27, 2001. Published September 2001. Originally published as PS 129 – 01. Last previous edition PS 129 – 01.

² Provisional standards exist for two years subsequent to the approval date.

³ Annual Book of ASTM Standards, Vol 04.03.

⁴ Available from American Association of State Highway and Transportation Officials, 444 N. Capitol St., NW, Washington, DC 20001.

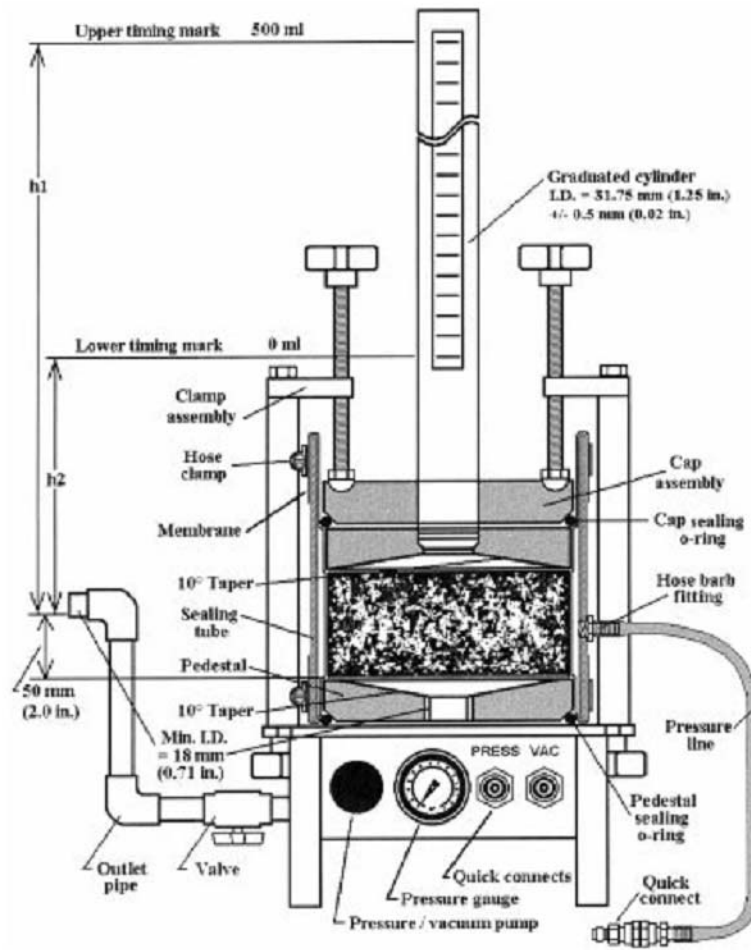


FIG. 1 Water Permeability Testing Apparatus (not to scale)

of the graduated cylinder mentioned previously in 6.1.1. The underside of the cap assembly should be tapered at an angle of $10 \pm 1^\circ$ (see Fig. 1).

6.1.4 A pedestal plate for supporting the asphalt concrete specimen and expanding an o-ring against the sealing tube. The opening in the pedestal plate should have a minimum diameter of 18 mm (0.71 in.). The top side of the lower cap should be tapered at an angle of $10 \pm 1^\circ$ (see Fig. 1).

6.1.5 O-rings of sufficient diameter and thickness for maintaining a seal against the sealing tube.

6.1.6 A frame and clamp assembly for supplying a compressive force to the cap assembly and pedestal plate necessary to expand the o-rings.

6.1.7 An air pump capable of applying 103 kPa (15 psi) pressure to the specimen as well as vacuum to evacuate the air from the sealing tube/membrane cavity.

6.1.8 A pressure gage with range 0 to 103 kPa (15 psi) with $\pm 2\%$ accuracy.

6.1.9 Quick connects for both vacuum and pressure lines.

6.1.10 An outlet pipe, 50.8 mm (2.0 in.) long with an inside diameter of 18 mm (0.71 in.).

6.1.11 Valve positioned upstream of the outlet pipe.

NOTE 1—A device manufactured by the Karol-Warner Company has been found to meet the above specifications.

6.2 *Vacuum Container, Type E*, described in Test Method D 2041.

6.3 *Vacuum Pump*, specified in Test Method D 2041.

6.4 *Manometer or Pressure Regulator*, specified in Test Method D 4867/D 4867M.

6.5 *Spacer*, described in AASHTO T 283.

6.6 *Balance*, meeting the requirements specified in Test Method D 2726.

6.7 *Water Bath*, meeting the requirements specified in Test Method D 2726.

6.8 *Stopwatch*, or other timing device capable of measurements to at least the nearest 0.1 s and accurate to within 0.05 % when tested over intervals of not less than 15 min.

6.9 *Meterstick*, capable of measuring to the nearest 0.1 mm.

6.10 *Caliper*, capable of measuring to the nearest 0.01 mm for measuring specimen thickness.

6.11 *Thermometer*, calibrated liquid-in-glass type capable of measuring the temperature of water to the nearest 0.1°C (0.2°F).

6.12 *Graduated Cylinder*, 100 ml minimum capacity with 1 ml or smaller graduations.

6.13 *Saw*, with diamond impregnated blade for wet cutting of specimens to the desired thickness. Dry cut type saws shall not be used.

6.14 *Sealing Agent (Petroleum Jelly)*, to produce a water-tight seal between the specimen and the flexible wall membrane of the permeameter.

6.15 *Spatula*, for applying the petroleum jelly sealant to the sides of the specimen.

6.16 *Electric Fan*, for drying the wet cut specimens.

7. Reagents

7.1 Supply of clean, non-aerated tap water.

8. Preparation of Test Specimens

8.1 Laboratory Prepared Specimens:

8.1.1 Specimens shall be compacted in accordance with AASHTO TP 4.

8.1.2 After compaction, specimens shall be allowed to cool to room temperature.

8.1.3 Specimens shall then be sawed on one side to the desired test sample thickness (for example, the anticipated in-place lift thickness).

8.1.4 The air void level of the specimen is user defined, however, it is recommended that the air void level represent the anticipated in-place density of the bituminous paving mixture.

8.2 Roadway Cores:

8.2.1 Layers of compacted bituminous paving mixture field cores shall be separated by sawing. Sawing shall also be required to remove any tack coat that would otherwise affect the test results.

8.3 Wash the test specimen thoroughly with water to remove any loose, fine material produced by the sawing and then dry the specimen to a constant mass by means of the electric fan.

8.4 Determine the bulk specific gravity of the specimen in accordance with Test Method D 2726 or Test Method D 1188 as appropriate.

8.5 Using the caliper, measure and record the height and diameter of the specimen to the nearest 0.5 mm (0.02 in.) or better. Individual height and diameter measurements shall be taken at three different locations. The three individual measurements shall not vary by more than 5 mm (0.2 in.). The diameter of the specimen shall not be less than 150.0 mm (5.910 in.) nor greater than 152.4 mm (6.000 in.).

NOTE 2—The measured permeability has been shown to vary as a function of the specimen thickness.

9. Saturation of Test Specimens

9.1 Place the specimen in a horizontal position in the vacuum container supported above the container bottom by the spacer. Fill the container with water at room temperature so that the specimens have at least 25 mm of water above their surface.

9.2 Remove trapped air and saturate the specimen by applying increased vacuum gradually until the residual pressure manometer reads 525 ± 2 mm of Hg. Maintain this residual pressure for 5 ± 1 min.

9.3 At the end of the vacuum period, release the vacuum by slowly increasing the pressure.

9.4 Allow the specimen to stand undisturbed for a minimum of 5 minutes. The specimen may be tested after this time or quickly transferred to another container where it will remain submerged until ready for testing.

10. Permeameter Setup

10.1 With the permeameter completely assembled (with a specimen of the size to be tested), use the meterstick to measure a distance of 10 cm from the cap assembly of the permeameter and place a mark onto the standpipe. This mark will be designated as the lower timing mark.

NOTE 3—Complete assembly is important since the springs of the cap assembly must be fully compressed in order to ensure an accurate distance measurement.

10.2 Using the meterstick, establish a mark on the graduated cylinder at a distance of 63.1 cm from the lower timing mark. This shall be designated as the upper timing mark. Additional "upper" timing marks may be established (for example, at 10.0 cm intervals) in order to facilitate the testing of mixtures having a wide range of permeability values.

NOTE 4—If the permeameter's graduated cylinder has manufacturer established timing marks, then steps 10.1 and 10.2 should be done to verify that the timing marks have been properly positioned.

NOTE 5—The permeameter setup described will produce a hydraulic gradient of approximately 8 to 12 (depending on specimen thickness). Tests using other hydraulic gradients may be conducted to verify the validity of Darcy's Law.

11. Testing Procedure

11.1 Disassemble the permeameter specimen cylinder from the permeameter base.

11.2 Connect the pressure line of the permeameter to the vacuum side of the pump. Using the pump, apply a vacuum to the flexible wall to remove entrapped air and collapse the membrane to the inside diameter of the cylinder. This will facilitate loading of the specimen.

11.3 With the flow control valve open, fill the outlet pipe with water until the taper in the base plate pedestal overflows.

11.4 For laboratory compacted specimens, it is necessary to apply a thin layer of petroleum jelly to the sides of the specimen to achieve a satisfactory seal between the membrane and the specimen. This shall be accomplished using a spatula or similar instrument. Sealant shall be applied ONLY to the sides of the specimen. Remove the specimen from the vacuum

container filled with water, dry to SSD, apply the petroleum jelly sealant to the sides, and then quickly place the specimen on the pedestal of the permeameter. For core specimens, remove the specimen from the vacuum container filled with water, dry to SSD, and then quickly place the specimen on the pedestal of the permeameter.

11.5 Expediently reassemble the permeameter making sure that all connections and clamps are tightened.

11.6 Disconnect the pressure line from the vacuum side of the pump and connect it to the pressure side.

11.7 Apply a confining pressure of 96.5 ± 7.0 kPa (14 ± 1 psi).

Note 6—Watch for fluctuations in confining pressure since these may be the result of insufficient seal or a hole in the flexible membrane. Care should be exercised to ensure that the confining pressure remains constant throughout the test.

11.8 Fill the permeameter graduated cylinder until water begins to flow from the outlet tube. Exercise care when filling to minimize the incorporation of air bubbles.

11.9 Close the flow control valve.

11.10 Carefully lean the permeameter from side to side to allow the escape of any entrapped air. Continue this operation until all entrapped air has been removed.

11.11 Fill the graduated cylinder above the upper timing mark (h1).

11.12 Refill the outlet pipe until it overflows.

11.13 Commence the water flow by opening the flow control valve of the permeameter. Start the timing device when the bottom of the meniscus of the water reaches the upper timing mark. Allow water to flow until the water level reaches the lower timing mark (h2). Once the water level reaches the lower timing mark, stop the timing device and close the valve. Record the elapsed time to the nearest second.

11.14 Saturation of the specimen may require many test runs. Therefore, steps 11.11-11.13 must be repeated. The specimen is considered sufficiently saturated when four consecutive measurements do not differ by more than ten percent (10 %) of the mean of the four consecutive test results. Once saturation has been verified, the final time measured shall be recorded as the test time and subsequently used in the calculations.

Note 7—If the test time is approaching thirty minutes during the first test run without the water reaching the lower timing mark, then the test may be terminated at the thirty minute mark and the water level at this time recorded. In this case, the test should be conducted one additional time by allowing water to flow for thirty minutes and recording the water mark at this time with the average of the two elapsed time measurements being recorded for use in calculating the permeability.

11.15 Measure and record the temperature of the permeate water in the system to the nearest 0.5°C.

11.16 After saturation has been achieved and verified and the final time and/or mark recorded, release the pressure from the permeameter, remove the clamp assemblies, upper platen and specimen. Wipe clean any excess sealant off of the latex membrane.

12. Calculation

12.1 The coefficient of water permeability, k , is determined using the following equation:

$$k = \frac{al}{At} \ln \left(\frac{h_1}{h_2} \right)$$

where:

- k = coefficient of water permeability, cm/s,
- a = inside cross-sectional area of inlet standpipe, cm²,
- l = thickness of test specimen, cm,
- A = cross-sectional area of test specimen, cm²,
- t = average elapsed time of water flow between timing marks, s,
- h_1 = hydraulic head on specimen at time t_1 , cm, and
- h_2 = hydraulic head on specimen at time t_2 , cm.

12.2 Correct the calculated permeability to that for 20°C (68°F), k_{20} , by multiplying k by the ratio of the viscosity of water at the test temperature to the temperature of water at 20°C (68°F), R_T , from Table 1, as follows:

$$k_{20} = R_T k$$

13. Report

13.1 Report the following information:

- 13.1.1 Specimen identification,
- 13.1.2 Mixture type/description,
- 13.1.3 Specimen type (that is, lab prepared or roadway core),
- 13.1.4 Specimen air voids,
- 13.1.5 Water temperature, and
- 13.1.6 Coefficient of water permeability is reported to the nearest whole unit $\times 10^{-3}$ cm/s.

14. Precision and Bias

14.1 *Precision*—Work is underway to develop a precision statement for this provisional test method. This method should not be used to accept or reject materials until the precision statement is available.

14.2 *Bias*—No information can be presented on the bias of the procedure in this provisional test method because no material having an accepted reference value is available.

15. Keywords

15.1 bituminous paving mixture; coefficient of permeability; permeability

TABLE 1 Correction Factor, R_T , for Viscosity of Water at Various Temperatures

Temperature, °C	R_T	Temperature, °C	R_T
15.0	1.125	25.0	0.889
15.5	1.121	25.5	0.879
16.0	1.106	26.0	0.869
16.5	1.092	26.5	0.860
17.0	1.077	27.0	0.850
17.5	1.064	27.5	0.841
18.0	1.051	28.0	0.832
18.5	1.038	28.5	0.823
19.0	1.025	29.0	0.814
19.5	1.013	29.5	0.805
20.0	1.000	30.0	0.797
20.5	0.988	30.5	0.789
21.0	0.976	31.0	0.780
21.5	0.965	31.5	0.772
22.0	0.953	32.0	0.764
22.5	0.942	32.5	0.757
23.0	0.931	33.0	0.749
23.5	0.921	33.5	0.741
24.0	0.910	34.0	0.733
24.5	0.900	34.5	0.725

APPENDIX E

Slide 1

MODULE X
Permeability Testing of Hot Mix Asphalt Methods

01-31-09

Slide 2

Permeability Testing- Why Test

- High permeability of asphalt mixtures leads to moisture infiltration
- Moisture infiltration makes the HMA more moisture susceptible
- Infiltration of moisture below the bound materials and into the unbound materials results in reduced pavement structural support and reduced service life

Slide 3

Two Methods for Permeability Testing

- Karol-Warner Permeameter Test Method, ASTM PS129-01
 - This is a laboratory device
 - Can be used to test gyratory samples during mix design or of QC/QA samples
 - Can be used to test field cores
- NCAT Permeameter Test Method
 - This is a field device
 - Can be used to test in-place pavements
 - This is a non-destructive test method

Slide 4

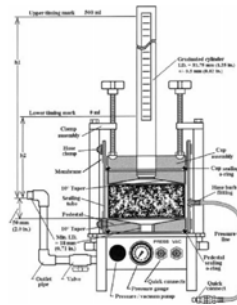
Karol-Warner Permeameter



- This is a falling head permeameter
- Device comes in two different sizes
 - 4-inch diameter
 - 6-inch diameter
- Assumes one-dimensional, laminar flow of water
- The coefficient of water permeability is based upon Darcy's Law

Slide 5

Detailed Schematic of Karol-Warner Permeameter



Slide 6

Preparation of Lab Compacted Test Specimens

- Test is conducted on compacted specimens that have cooled to room temperature
- Specimens should be compacted to the air void level anticipated in the field
- Specimens have to be sawed on one side (preferably to the pavement lift thickness if a laboratory compacted sample)

Slide 7

Preparation of Field Compacted Test Specimens

- Layers of compacted mixture should be separated by sawing including tack coated surfaces
- Wash the specimen after sawing to remove loose, fine material produced by sawing
- Dry the sample to a constant weight using an electric fan
- Measure and record the height and diameter of the specimen at three different locations each to the nearest 0.5mm (0.02 in.) using a caliper

Slide 8

Saturation Test of Specimens

- Place the specimen in a horizontal position in on top of a spacer in a vacuum container
- Fill the container with water at room temperature with at least 25mm (1 in.) of water above the tope of the specimen
- Removed trapped air by applying increased vacuum gradually until the residual pressure manometer is 525 +/- 2 mm of Hg.
- Maintain the pressure for 5 +/- 1 minute
- At the end of the vacuum period, slowly release the vacuum and thus increasing the pressure
- Allow the specimen to stand undisturbed for a minimum of 5 minutes.
- The specimen is ready for testing or can be transferred quickly to another water bath until ready for testing

Slide 9

Karol-Warner Permeameter Testing Procedure

- Disassemble the permeameter specimen cylinder from the permeameter base
- Connect the pressure line of the permeameter to the vacuum side of the pump
- Apply a vacuum to the flexible wall to remove entrapped air and collapse the membrane to the inside diameter of the cylinder
- Open the flow control valve.
- Fill the outlet pipe with water until the taper in the base pedestal overflows
- For lab compacted specimens, use a spatula to apply a thin layer of petroleum jelly to the sides to the specimen to achieve a satisfactory seal between the membrane and sides of the specimen in a saturated surface dry state

Slide 10

Karol-Warner Permeameter Testing Procedure

- Quickly reassemble the permeameter making sure all of the connections and clamps are tightened
- Disconnect the pressure line from the vacuum side of the pump and connect it to the pressure side
- Apply a confining pressure of 96.5 +/- 7.0kPa (14 +/- 1 psi)
- Fill the permeameter graduated cylinder until the water begins to flow from the outlet tube
- Close the flow control valve
- Carefully lean the permeameter from side to side to allow the escape of any entrapped air
- Fill the graduated cylinder above the upper timing mark (h1)

Slide 11

Karol-Warner Permeameter Testing Procedure

- Refill the outlet pipe until it overflows
- Commence the water flow by opening the flow control valve of the permeameter
- Start the timing device when the meniscus of the water reaches the upper timing mark
- Allow the water to flow until the water level reaches the lower timing mark (h2) and stop the timing device
- Record the time to the nearest 1 second
- Measure and record the temperature of the water to the nearest 0.5°C
- After saturation has been achieved and verified and the final time and/or mark recorded, release the pressure from the permeameter. Remove the specimen and clean the permeameter

Slide 12

Karol-Warner Permeameter Calculations

$$k = \frac{a^2}{4t} \ln \left(\frac{h_1}{h_2} \right)$$

where:
 k = coefficient of water permeability, cm/s.
 a = inside cross-sectional area of inlet standpipe, cm².
 l = thickness of test specimen, cm.
 A = cross-sectional area of test specimen, cm².
 t = average elapsed time of water flow between timing marks, s.
 h_1 = hydraulic head on specimen at time t_1 , cm, and
 h_2 = hydraulic head on specimen at time t_2 , cm.

- Correct the calculated permeability (k) to that for 20°C, k_{20} , by multiplying the ratio of the viscosity of water at the test temperature to the temperature of water at 20°C
- $k_{20} = R_T k$, where R_T is given in the Table on the next slide

Slide 13

R_T Values

TABLE 1 Correction Factor, R_T, for Viscosity of Water at Various Temperatures


Temperature, °C	R _T	Temperature, °C	R _T
14.0	1.128	26.0	0.989
15.0	1.121	26.5	0.978
16.0	1.106	26.8	0.969
16.5	1.092	26.9	0.965
17.0	1.077	27.0	0.960
17.5	1.064	27.5	0.951
18.0	1.051	28.0	0.942
18.5	1.038	28.5	0.933
19.0	1.026	28.8	0.924
19.5	1.013	28.9	0.920
20.0	1.000	29.0	0.917
20.5	0.988	29.5	0.908
21.0	0.976	31.0	0.899
21.5	0.965	31.5	0.892
22.0	0.953	32.0	0.884
22.5	0.942	32.5	0.877
23.0	0.931	33.0	0.869
23.5	0.921	33.5	0.861
24.0	0.910	34.0	0.853
24.5	0.900	34.5	0.845

Slide 14

- ### Karol-Warner Report
- Specimen identification
 - Mix type/description
 - Specimen type (lab compacted or roadway core)
 - Specimen air voids
 - Water test temperature
 - Coefficient of water permeability to the nearest whole unit X 10⁻⁵ cm/s

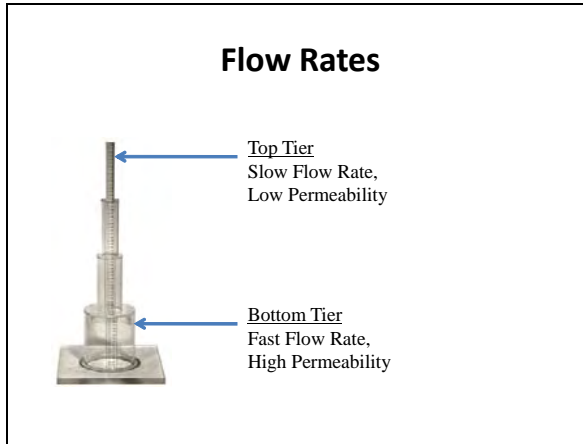
Slide 15

NCAT Permeameter



- Falling head permeameter
- Graduated cylinders represent different flow rates or levels of permeability
- Will need to use a timer to the nearest 0.1 second
- Timing marks on the cylinders represents measurement markings for determining the amount of water that has left the device

Slide 16



Slide 17

- ### NCAT Test Steps
1. Identify test location of 1 square foot
 2. Clean surface of pavement
 3. Invert permeameter to clean device surface and apply sealant uniformly outside of rubber gasket
 4. Install the permeameter right side up by gently applying foot pressure to seal
 5. Apply a thin amount of sealant between the two layers of the permeameter
 6. Carefully fill the permeameter with water, minimizing air bubbles collecting in the permeameter
 7. Time the rate of drop in the water level between timing marks within the same cylinder
 8. Record the time and the beginning and ending timing marks
 9. Determine the coefficient of permeability

Slide 18

NCAT Permeameter Calculations

$K = (a L / At) \ln (h_1/h_2)$

Where:

- k = coefficient of permeability,
- a = inside cross-sectional area of standpipe, cm²
(Varies depending on tier used for testing; see listed values in Calculation section.)
- L = length of the sample, cm (thickness of the asphalt mat).
- A = cross-sectional area of permeameter through which water can penetrate the pavement (test area), cm².
- t = Elapsed time between h₁ and h₂
- h₁ = Initial head, cm.
- h₂ = Final head, cm.

Area Values of "a" for each tier:

- Tier 1 (Top) = area "a" = 2.85 cm²
- Tier 2 = area "a" = 15.52 cm²
- Tier 3 = area "a" = 38.32 cm²
- Tier 4 (Bottom) = area "a" = 167.53 cm²
- Pavement Test Area (value "A" in equation) = 214 cm²

* This value also applies to the 1-3/4" (44.5mm) id alternate top section.

NCAT Report

- Project identification
- Mix type/description
- Test location including station location and paving lane offset
- Coefficient of water permeability to the nearest whole unit X 10^{-5} cm/s



Missouri Department of Transportation
Organizational Results
P. O. Box 270
Jefferson City, MO 65102

573.526.4335
1 888 ASK MODOT
innovation@modot.mo.gov